

of processes that transfers organic carbon from the surface to the deep ocean, is at the heart of the ocean carbon cycle. Monitoring the OBCP is critical to understanding how the Earth's carbon cycle is changing. At present, satellite remote sensing is the only tool available for viewing the entire surface ocean at high temporal and spatial scales. In this paper, we review methods for monitoring the OBCP with a focus on satellites. We begin by providing an overview of the OBCP, defining and describing the pools of carbon in the ocean, and the processes controlling fluxes of carbon between the pools, from the surface to the deep ocean, and among ocean, land and atmosphere. We then examine how field measurements, from ship and autonomous platforms, complement satellite observations, provide validation points for satellite products and lead to a more complete view of OBCP than would be possible from satellite observations alone. A thorough analysis is then provided on methods used for monitoring the OBCP from satellite platforms, covering current capabilities, concepts and gaps, and the requirement for uncertainties in satellite products. We finish by discussing the potential for producing a satellite-based carbon budget for the oceans, the advantages of integrating satellite-based observations with ecosystems models and field measurements, and future opportunities in space, all with a view towards bringing satellite observations into the limelight of ocean carbon research.

29 *Keywords:* Ocean, Carbon cycle, Satellite

30 **1. Introduction**

31 The ocean biological carbon pump (OBCP) can be defined as a suite of
32 biological, physical, and chemical processes that contributes to, and controls, the
33 transfer of organic carbon (in dissolved and particulate forms) from the surface
34 layer to the deep ocean (Volk and Hoffert, 1985). The magnitude of this pump
35 has been estimated to be between 4 and 12 Pg C yr⁻¹ (Laws et al., 2000; Henson

*Corresponding author: Robert J. W. Brewin, College of Life and Environmental Sciences, University of Exeter, Penryn Campus, Penryn, Cornwall, TR10 9EZ, United Kingdom

Email address: r.brewin@exeter.ac.uk (Robert J. W. Brewin)

Preprint submitted to Earth-Science Reviews

February 16, 2021

36 et al., 2011; DeVries and Weber, 2017). The OBCP has a profound impact on the
37 functioning of the ocean and the planet. It helps modulate the CO₂ concentration
38 and pH of the ocean, which together with physical processes, impacts the transfer
39 of CO₂ between the ocean and atmosphere. If the OBCP were to be switched off,
40 it has been estimated that atmospheric CO₂ concentration would be 50 % higher
41 than it is today (Parekh et al., 2006), and consequently, we would be living in a
42 very different world. The carbon exported to the deep ocean through the OBCP
43 supports meso-, bathy- and abysso-pelagic food webs, and controls the vertical
44 and horizontal distribution of elements in the ocean. Studying and monitoring
45 the OBCP is thus of paramount importance for understanding and predicting
46 environmental and ecological changes at the planetary scale.

47 There are a variety of techniques we use to monitor the OBCP, which can
48 be deployed from various platforms such as ships, autonomous vehicles, and
49 satellites. In this paper, we review these tools with a focus on satellite-based
50 methods. We highlight current capabilities in space-based OBCP monitoring,
51 identifying the components of the OBCP not amenable to observations from space,
52 and how we can fill these gaps. We discuss the future of satellite-based OBCP
53 monitoring, and how satellites, monitoring electromagnetic radiation at different
54 frequencies and resolutions, can be used in synergy with other monitoring tools
55 (e.g. ships-based and autonomous-based) and ecosystem models, to advance our
56 understanding of the OBCP and ultimately the global carbon cycle.

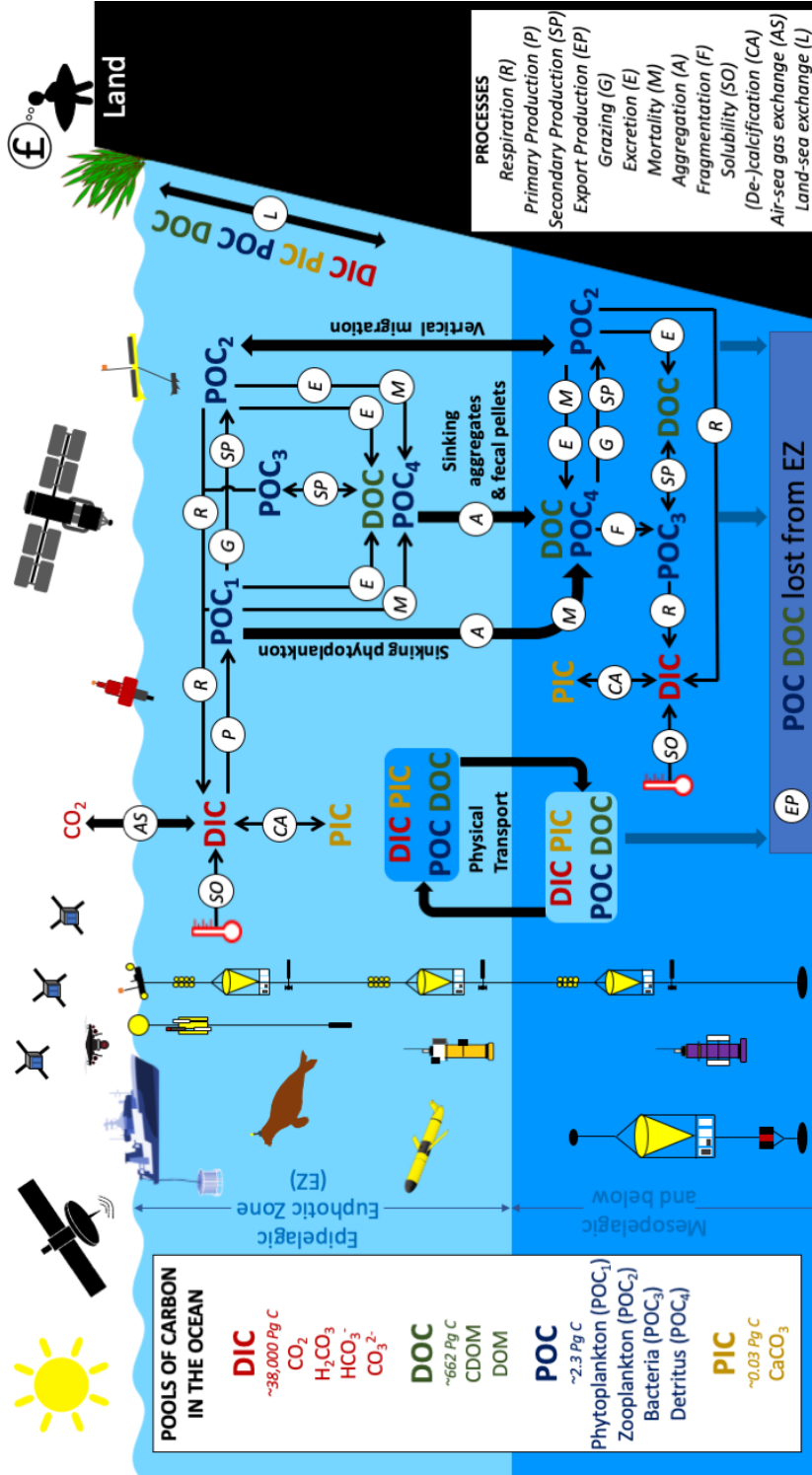


Figure 1: Pools, fluxes and processes that form the ocean biological carbon pump (OBCP), and current methods used to monitor them. Bold black text and thick black arrows represent the key export pathways and interactions with other domains (land and atmosphere). Global stocks of the different carbon pools in the ocean are given in the box on the left; the four major kinds of pools – DIC, DOC, POC and PIC – are given in different colours. This figure has been inspired by, and builds on, two earlier figures, one from the CEOS carbon from space report (CEOS, 2014) and the other from the NASA EXPORTS plan (Siegel et al., 2016).

57 2. Overview of the Ocean Carbon Cycle

58 2.1. The Ocean Biological Carbon Pump (OBCP)

59 The OBCP depends on a number of key pools, components and processes that
60 influence its functioning (Figure 1). There are four main pools of carbon in the
61 ocean.

- 62 • **Dissolved Inorganic Carbon (DIC)** is the largest pool. It constitutes
63 around 38,000 Pg C (Hedges, 1992) and includes: dissolved carbon dioxide
64 (CO_2); bicarbonate (HCO_3^-); carbonate (CO_3^{2-}); and carbonic acid
65 (H_2CO_3). The equilibrium between carbonic acid and carbonate determines
66 the pH of the seawater. Carbon dioxide dissolves easily in water and its
67 solubility is inversely related to temperature. Dissolved CO_2 is taken up in
68 the process of photosynthesis, and can reduce the partial pressure of CO_2
69 in the seawater, favouring drawdown from the atmosphere. The reverse
70 process respiration, releases CO_2 back into the water, can increase partial
71 pressure of CO_2 in the seawater, favouring release back to the atmosphere.
72 The formation of calcium carbonate by organisms such as coccolithophores
73 has the effect of releasing CO_2 into the water (Zeebe and Wolf-Gladrow,
74 2001; Rost and Riebesell, 2004; Zeebe, 2012)

- 75 • **Dissolved Organic Carbon (DOC)** is the next largest pool at around
76 662 Pg C (Hansell and Carlson, 2013). DOC can be classified accord-
77 ing to its reactivity as refractory, semi-labile or labile. The labile pool
78 constitutes around 0.2 Pg C, is bioavailable, and has a high production rate
79 ($\sim 15\text{-}25 \text{ Pg C y}^{-1}$; Hansell, 2013). The refractory component is the biggest
80 pool ($\sim 642 \text{ Pg} \pm 32$; Hansell and Carlson, 2013), but has a very low turnover
81 rate ($0.043 \text{ Pg C y}^{-1}$; Hansell, 2013). The turnover time for refractory DOC
82 is though to be greater than 1,000 years (Williams and Druel, 1987; Druffel
83 et al., 2016).

- 84 • **Particulate Organic Carbon (POC)** constitutes around 2.3 Pg C (Stram-
85 ska and Cieszyńska, 2015; CEOS, 2014) and is relatively small compared

86 with DIC and DOC. Though small in size, this pool is highly dynamic,
87 having the highest turnover rate of any organic carbon pool on the planet
88 (Sarmiento and Gruber, 2006). Driven by primary production, it produces
89 around 50 Pg C y⁻¹ globally (Longhurst et al., 1995; Sathyendranath et al.,
90 2019b; Kulk et al., 2020). It can be separated into living (e.g. phytoplank-
91 ton, zooplankton, bacteria) and non-living (e.g. detritus) material. Of these,
92 the phytoplankton carbon is particularly important, because of its role in
93 marine primary production, and also because it serves as the food resource
94 for all the larger organisms in the pelagic ecosystem.

95 • **Particulate Inorganic Carbon (PIC)** is the smallest of the pools at around
96 0.03 Pg C (Hopkins et al., 2019). It is present in the form of calcium
97 carbonate (CaCO₃) in particulate form, and impacts the carbonate system
98 and pH of the seawater. Estimates for PIC production are in the region
99 of 0.8-1.4 Pg C y⁻¹, with at least 65 % of it being dissolved in the upper
100 water column, the rest contributing to deep sediments (Feely et al., 2004).
101 Coccolithophores and foraminifera are estimated to be the dominant sources
102 of PIC in the open ocean (Schiebel, 2002; Feely et al., 2004). The PIC pool
103 is of particular importance due to its role in the ocean carbonate system, and
104 in facilitating the export of carbon to the deep ocean through the carbonate
105 pump, whereby PIC is exported out of the photic zone and deposited in the
106 bottom sediments (Riebesell et al., 2000).

107 There are a series of key processes that determine the fluxes of carbon between
108 these pools (Figure 1).

109 • **Primary production** converts DIC, in the form of CO₂, to POC, in the form
110 of phytoplankton tissue, through the processes of photosynthesis. Light
111 and nutrients are required for photosynthesis by autotrophic phytoplankton.
112 Primary production is the engine behind the OBCP and it occurs within
113 the euphotic zone (the region of the surface ocean where 99 % of light
114 penetrates). Gross primary production represents total organic carbon
115 production irrespective of respiration. Net primary production is defined

116 as gross primary production minus autotrophic respiration. In the ocean
117 net primary production is equivalent to that in the terrestrial environment
118 ($\sim 50 \text{ Pg C yr}^{-1}$; Field et al., 1998).

119 • **Grazing** by heterotrophic organisms. The carbon produced by primary
120 production can be transferred from phytoplankton to other POC components
121 (heterotrophic organisms, such as zooplankton and nekton), through the
122 process of grazing. This can occur on various time scales, for example,
123 in the surface ocean soon after primary production, or at deeper depths
124 long after primary production, following the sinking of phytoplankton. For
125 simplicity, in this review we consider consumption (which occurs when
126 all organisms take up carbon) under the same category as grazing. The
127 fraction of organic carbon from primary production consumed by organisms
128 becomes smaller as you move up the food chain, from herbivores (secondary
129 production) through to carnivorous organisms (tertiary production), such as
130 fish and even humans.

131 • **Secondary production** refers to the growth rate of herbivores. Only a very
132 small fraction of the carbon grazed by herbivores is used for growth. The
133 ratio of secondary production to primary production is used as an index of
134 the efficiency with which organic carbon is transferred up the marine food
135 chain (Sigman and Hain, 2012).

136 • **Respiration** is the conversion of POC, in the form of bacteria, phytoplank-
137 ton, zooplankton and other higher trophic levels (or labile DOC), to DIC,
138 in the form of CO_2 . It is the principal mechanism of remineralisation in
139 the ocean. This process is the reverse of photosynthesis, results in the
140 consumption of oxygen and can occur at various depths.

141 • **Excretion** is the release of metabolic waste by marine organisms (Wiebe
142 and Smith, 1977). The majority of carbon released by excretion is in the
143 form of DOC.

- 144 • **Aggregation** is the joining together of different components into a cluster.
145 It is controlled in part by coagulation and flocculation and influences the
146 sinking rate of particles, which is critical to the export of material from
147 surface to deep waters (Riley, 1963; Burd and Jackson, 2009).
- 148 • **Fragmentation** is the breaking apart of larger particles (or aggregates) into
149 smaller components. This can occur through physical (e.g. shear stress)
150 or biological (e.g. grazing, sloppy feeding) processes. It has recently been
151 demonstrated that fragmentation is the primary process controlling the
152 downward flux of POC through the mesopelagic zone (Briggs et al., 2020).
- 153 • **Non-predatory mortality** is death of phytoplankton and zooplankton
154 through non-predatory means. This can be caused, for example, by cell lysis
155 or viral infection (Kirchman, 1999). Other causes include senescence, tem-
156 perature change, light exposure, physical and chemical stresses, parasitism
157 and food-related death (Tang et al., 2014).
- 158 • **Solubility.** The solubility of CO₂ in the ocean is dependent on seawater
159 temperature (Takahashi et al., 2002). Cooler, deeper water can store larger
160 amounts of dissolved CO₂ in the form of DIC than warmer surface water.
- 161 • **Calcification.** Marine organisms, notably coccolithophores, and to a lesser
162 extent foraminifera and pteropods, produce calcium-carbonate particles,
163 which can sink out the upper ocean and settle at the bottom of the sea. The
164 chemical processes involved in the formation of calcium carbonate release
165 CO₂ into the water (Zeebe, 2012).

166 The OBCP by definition is concerned with the transfer of organic carbon
167 (DOC and POC) from the surface layer of the ocean (epipelagic or euphotic zone)
168 to the deep ocean (mesopelagic and below). This can be achieved through three
169 main routes, or pathways (Figure 1, also see Boyd et al. (2019) and Le Moigne
170 (2019) for recent reviews on the topic).

- 171 • **Physical transport.** POC and DOC can be transported vertically through
172 physical processes. These may include: subduction by large-scale ocean

173 circulation (e.g. see Lévy et al., 2013); eddy-driven subduction (Lévy et al.,
174 2001; Omand et al., 2015; Llort et al., 2018; Resplandy et al., 2019); and
175 the detrainment of organic matter due to fluctuations in the mixed-layer
176 depth (Stramska, 2010; Dall’Olmo et al., 2016; Lacour et al., 2019).

177 • **Sinking of POC** (gravitational pump). Particles can sink from the
178 epipelagic to the mesopelagic zone (Sanders et al., 2014; Cael and Bisson,
179 2018; Bisson et al., 2020). The gravitational sinking of POC has been
180 closely related to the spring phytoplankton bloom at high latitudes (Martin
181 et al., 2011). The particles can sink in the form of dead phytoplankton cells,
182 in the form of aggregates of particles, and in the form of faecal pellets.
183 The sinking rates of the particles are dependent on their size, density and
184 morphology.

185 • **Migration of POC**. Organisms capable of vertical migration (e.g. zoo-
186 plankton and carnivorous organisms) can transfer carbon from the epipelagic
187 to the mesopelagic (Longhurst et al., 1990; Steinberg and Landry, 2017).
188 Diel zooplankton migration is believed to be a large component of this
189 flux. During the night, zooplankton migrate from the mesopelagic to the
190 epipelagic to graze on phytoplankton. During the day, they return back
191 to the mesopelagic (partly to avoid predation) and synthesise this carbon,
192 resulting in a net downward flux of organic carbon. The vertical transport
193 of carbon from migration can also occur on longer time-scales, for example,
194 through the hibernation of copepods (and in some cases mortality at the
195 hibernation depth) in winter in the mesopelagic zone, referred to as the
196 seasonal-lipid pump (Jónasdóttir et al., 2015).

197 Once the carbon reaches the mesopelagic zone, its fate is dependent on which
198 pool it belongs to, and on the extent to which the various processes control it
199 (Figure 1). Part of the POC exported to the mesopelagic zone continues to sink
200 and can contribute to sequestration, where the carbon is consequently stored in
201 the deep ocean for long timescales. There are three production terms that often
202 feature in descriptions of the OBCP:

- 203 • **New production** is defined as the rate of primary production supported by
204 exogenously supplied nutrients (Dugdale and Goering, 1967).
- 205 • **Net community production** is gross primary production minus total (all
206 organisms) community respiration.
- 207 • **Export production** is the amount of organic matter produced by primary
208 production that is lost from the surface ocean. The definition of what
209 constitutes the surface ocean varies between studies, with some using the
210 euphotic depth (1 % light level), some the mixed-layer depth, and others
211 using an arbitrary horizon at 100 m (Buesseler et al., 2020). It is often used
212 as a measure of the net amount of carbon removed from the atmosphere
213 through the OBCP. Note that, at certain time scales at which steady state
214 may be assumed to prevail, and for appropriate depth scales, new production
215 and export production may be equivalent to each other.

216 2.2. *Interactions with the atmosphere and land*

217 The ocean surface is constantly exchanging carbon dioxide (CO₂) with the
218 atmosphere. It has been estimated that, since the start of the industrial revolution,
219 approximately a quarter of anthropogenically emitted CO₂ has been taken up
220 by the surface ocean (Friedlingstein et al., 2019). This uptake varies spatially,
221 seasonally, and on interannual scales (Watson et al., 2009; Wanninkhof et al.,
222 2013; Landschützer et al., 2016; Gruber et al., 2019). The exchange of carbon
223 between the atmosphere and ocean is dependent on concentrations in the atmo-
224 sphere and ocean and turbulent exchange between the two (Woolf et al., 2016).
225 The concentrations (combination of temperature and partial pressure of CO₂)
226 in the water and atmosphere dictate the gradient of transfer, and any CO₂ gas
227 transfer across the interface varies with environmental conditions and surface
228 water constituents. The in-water CO₂ concentration can then be modulated by
229 biological uptake or respiration. Once within the surface ocean, the gaseous CO₂
230 reacts with the seawater and becomes part of the buffered inorganic carbonate
231 system comprised of aqueous CO₂, carbonic acid, bicarbonate and carbonate, and

232 the sum of these different species is the total inorganic carbon, often called the
233 dissolved inorganic carbon (DIC). The combination of species that determine the
234 capacity of the water to resist changes in pH is referred to as the total alkalinity
235 (AT). Satellite data are critical for quantifying synoptic-scale ocean gas fluxes,
236 and for a recent review of these capabilities along with the use of satellite data
237 for studying the surface inorganic carbonate system, the reader is referred to the
238 work of Shutler et al. (2019).

239 There are also exchanges in carbon between the ocean and the land. Riverine
240 outflow can transfer carbon (DIC, DOC, POC and PIC) produced or stored on
241 land to the ocean (Tranvik et al., 2009). This outflow also contains nutrients that
242 can support new production in coastal and open ocean waters (Seitzinger et al.,
243 2010). Current estimates suggest that 0.455 to 0.78 Pg C enters the ocean each
244 year due to rivers (Jacobson et al., 2007; Resplandy et al., 2018). Many of the
245 processes controlling the exchange of carbon between the ocean and the land are
246 highly sensitive to human activities (e.g. land-use change). It has been estimated
247 that since the start of the industrial revolution, there has been an increase in the
248 flux of carbon from the land to inland waters ($\sim 1.0 \text{ Pg C yr}^{-1}$), with an estimated
249 10 % of that carbon entering the ocean (Regnier et al., 2013). Other process
250 can moderate the exchanges of carbon between the land and ocean, for example,
251 precipitation changes (Sinha et al., 2017), tides (Wei et al., 2019) and storms (Call
252 et al., 2019). In polar regions, changes in ice sheets (e.g. glacial melting) also
253 influence land-ocean carbon exchange (Wadham et al., 2019).

254 **3. Field observations of carbon pools and fluxes in the ocean**

255 While this review focuses primarily on satellite-based techniques for moni-
256 toring the OBCP, their development is highly dependent on data collected in the
257 ocean. Satellite products depend heavily on precise *in-situ* measurements to test
258 algorithms and validate products. Field measurements are required to fill gaps
259 in satellite products, whether it be through observations of pools and fluxes that
260 are not currently accessible to remote sensing, or through observations at depth.
261 This section provides an overview of key tools and methods used in the ocean for

262 monitoring components of the OBCP.

263 *3.1. Ship and laboratory-based measurements*

264 A wide range of laboratory and field techniques have been developed to
265 measure pools and fluxes of carbon in the ocean. In the following section (see
266 also Table 1) we outline some of the key techniques and tools used in the field
267 and laboratory. Table 2 lists examples of *in-situ* databases, synthesis, data portals
268 and observational programmes available to the community.

Table 1: Key OBCP tools and techniques used in the laboratory and field. References are examples (see main text for a comprehensive list).

Pools and fluxes		Common techniques	References	
Pools	DIC	Using either ion-sensitive field effect transistors, infrared detection, and titrimetric, colourmetric, spectrophotometric, and potentiometric approaches.	Liu et al. (2013) & Zeebe (2012)	
	DOC	Samples separated from POC by 0.2 μ m filtration. DOC separated from DIC by acidification and sparging. DOC quantified through oxidation of organic compounds to CO ₂ , and measured using an infrared CO ₂ analyser or by colourmetric methods.	Sharp (2002)	
	POC	Total POC	Organic carbon retained on pre-combusted GF/F filter, dried then acidified to remove PIC. Filters combusted in an elemental analyser to convert the organic carbon in CO ₂ , which is then detected by thermal conductivity.	Sharp (1974) Chaves et al. (2020)
		Phytoplankton Carbon	Proposed techniques include: measuring chlorophyll-a concentration then converting to carbon; measuring cell counts then converting biovolume and carbon; calibrating flow cytometer scattering and video-based imaging; and flow cytometric sorted samples; and x-ray microanalysis.	Olson et al. (2003), Graff et al. (2015) & Martínez-Vicente et al. (2017)
		Zooplankton Carbon	Zooplankton cell counts (from nets, optical counters or video-based cameras) and biovolume and carbon conversions. Acoustic signals have also been related to zooplankton biomass.	Gallienne et al. (1996)
Bacterial Carbon		Techniques include: cell counts, biovolume estimates and carbon conversions; and separation of bacteria by tangential flow filtration and use of high-temperature catalytic oxidation.	Fukuda et al. (1998) & Martínez-Vicente et al. (2016)	

Continued on the next page.

Table 1: Key OBCP tools and techniques used in the laboratory and field. References are examples (see main text for a comprehensive list).

Pools and fluxes		Common techniques	References
	PIC	Inorganic carbon retained on pre-combusted GF/F filter, rinsed with 0.2 μm filtered seawater, extracted in a bath using 50 % HCl, and quantified by atomic absorption spectrometry.	Mitchell et al. (2017)
Fluxes	Primary, New, and Export production	Use of <i>in-vivo</i> techniques (e.g. ^{14}C assimilation and O_2 evolution), triple isotope methods, O_2/Ar measurements, measurements of bulk properties, optical methods and proxies, and quantifying upper and lower limits.	Sathyendranath et al. (2019b) and Church et al. (2019)
	Grazing	^{14}C method, dilution techniques, radioisotope methods, and measuring ingestion of [methyl- ^3H] methylamine hydrochloride ($^3\text{H-MeA}$) labelled particles. Consumption has been estimated from the composition of major bioelements and biochemicals in the ocean.	Haney (1971), Daro (1978), Landry and Hassett (1982), White and Roman (1991) & Kaiser and Benner (2012)
	Secondary production	Zooplankton production has been estimated from measurements of zooplankton biomass, hatching success and fecundity, and bacterial production from measurement of change in bacterial abundance in filtered seawater, and through bacterial deoxyribonucleic acid synthesis.	Fuhrman and Azam (1980) & Poulet et al. (1995)
	Respiration	Inverse modelling of the community composition and activity, measuring the rate of production and consumption of a product or a reactant, the assay of an appropriate respiratory enzyme or enzyme system, and biomass-based predictions.	Robinson and Williams (2005)

Continued on the next page.

Table 1: Key OBCP tools and techniques used in the laboratory and field. References are examples (see main text for a comprehensive list).

Pools and fluxes		Common techniques	References
	Excretion	Radiocarbon methods or kinetic-based methods.	Sharp (1979) and Lancelot (1979)
	Aggregation	Laboratory-based experiments using flocculators, photographic observations and high resolution video analysis (in mesocosm-based and field-based experiments).	Burd and Jackson (2009)
	Fragmentation	Monitoring abundances and size distributions of marine particles as a function of time, laboratory video-based analysis, and using optical measurements.	Dilling and Allredge (2000), Goldthwait et al. (2004) & Briggs et al. (2020)
	Non-predatory mortality	Microscopic-based methods for zooplankton, spectrofluorometric methods for phytoplankton cell lysis and pigment-based methods for phytoplankton senescence.	Tang et al. (2014), Agustí et al. (1998) & Bale et al. (2011)
	Solubility	Solubility of CO ₂ is dependent of temperature and salinity.	Murray and Riley (1971) & Weiss (1974)
	Calcification	Two techniques are commonly used. The first involves filtering ¹⁴ C-labelled samples through two filters, one is fumed with acid to remove Ca ¹⁴ CO ₃ giving an estimate of particulate organic production, the other left as an estimate of total particulate production, with calcification representing the difference between filters. The second uses the micro-diffusion technique, that captures ¹⁴ CO ₂ liberated from Ca ¹⁴ CO ₃ .	Daniels et al. (2018)
	Air-sea CO ₂ transfer	Tracer studies using ambient gases, deliberately introduced tracers, direct eddy-covariance flux measurements.	Landwehr et al. (2018)

Table 2: Some examples of *in-situ* datasets from data synthesis, general databases and portals, and observational programmes, for use in ocean carbon studies.

Name	Description	Reference
Global Data Syntheses		
OC-CCI <i>in-situ</i> data	Synthesis of <i>in-situ</i> bio-optical observations of: spectral remote-sensing reflectances, concentrations of chlorophyll-a, spectral inherent optical properties, spectral diffuse attenuation coefficients and total suspended matter.	Valente et al. (2019a,b)
POC data	Synthesis of POC measurements from the ESA POCO project, including data from: PANGAEA; NASA SeaBASS (Werdell and Bailey, 2005); data compiled by Martiny et al. (2014); data from BCO-DMO; data from AMT (Rasse et al., 2017); data from cruises in the Southern Ocean (Thomalla et al., 2017).	Evers-King et al. (2017)
POC flux data	Synthesis of POC flux estimates from POC concentration observations derived from sediment traps and ²³⁴ Th, compiled across the global ocean.	Mouw et al. (2016a,b)
Picoplankton carbon data	Synthesis of more than 12,000 global observations of picophytoplankton abundance converted into carbon concentrations from the ESA POCO project.	Martínez-Vicente et al. (2017)
PIC data	Synthesis of PIC concentration data stored in NASA-SeaBASS data archive (http://seabass.gsfc.nasa.gov/) and the BCO-DMO archive.	Balch et al. (2018)
Coccolithophore calcification rates	Synthesis of 2765 CaCO ₃ production measurements, the majority of which were measured using 12 to 24 h incorporation of radioactive carbon (¹⁴ C) into acid-labile inorganic carbon (CaCO ₃).	Daniels et al. (2018)
Photosynthesis Irradiance parameters	Global synthesis of photosynthesis–irradiance parameters from a range of oceanographic regimes as an aid to examining the basin-scale variability in the photophysiological response of marine phytoplankton.	Bouman et al. (2018)
Continued on the next page.		

Table 2: Some examples of *in-situ* datasets from data synthesis, general databases and portals, and observational programmes, for use in ocean carbon studies.

Name	Description	Reference
MAREDAT	Synthesis of carbon biomass for 11 plankton functional types (picophytoplankton, diazotrophs, coccolithophores, <i>Phaeocystis</i> , diatoms, picoheterotrophs, microzooplankton, foraminifers, mesozooplankton, pteropods and macrozooplankton) plus phytoplankton pigment data, compiled as part of the MARine Ecosystem biomass DATA (MAREDAT) initiative (http://www.pangaea.de/search?&q=maredat).	Buitenhuis et al. (2013)
GOCAD	The Global Ocean Carbon Algorithm Database (GOCAD) is a global, carbon-focused synthesis of optical (apparent and inherent optical properties, hyperspectral and extending to the UV), physical, biogeochemical and carbon data (e.g. DOC and POC), for use in satellite algorithm development.	Aurin et al. (2018)
LDEO pCO ₂ data	Synthesis of 13.5 million measurements of surface water pCO ₂ made over the global oceans during 1957-2018.	Takahashi et al. (2019)
SOCAT fCO ₂ data	Synthesis of surface ocean fCO ₂ (fugacity of carbon dioxide) observations. The latest SOCAT version (v2019) has 25.7 million global observations from 1957 to 2019 (https://www.socat.info).	Bakker et al. (2016)
General Databases and Portals		
Copernicus <i>In Situ</i> Component	Includes <i>in-situ</i> ocean data (ship, drifters, floats and buoys) for use in combination with space-based data. It includes contributions of the member states to the Copernicus programme, and benefits from international efforts to collect and share data.	https://insitu.copernicus.eu
EMODnet	The European Marine Observation and Data Network (EMODnet) has contributions from 150 organisations assembling marine data, products and metadata to integrate these resources and make them more publicly-available, using quality-assured, standardised and harmonised methods.	https://www.emodnet.eu
Continued on the next page.		

Table 2: Some examples of *in-situ* datasets from data synthesis, general databases and portals, and observational programmes, for use in ocean carbon studies.

Name	Description	Reference
OceanSITES	OceanSITES is a global network of long-term, reference stations measuring many variables and at the full depth of the water column.	http://www.oceansites.org
Argo programme	Profiles of physical variables (ocean temperature, salinity and pressure) from the global network array of Argo floats.	http://www.argo.ucsd.edu
Biogeochemical-Argo programme	An extension of the Argo float array containing profiles of biogeochemical variables (in addition to physical variables), including: pH, oxygen, nitrate, chlorophyll, suspended particles, and downwelling irradiance.	https://biogeochemical-argo.org
SeaBASS	The SeaWiFS Bio-optical Archive and Storage System (SeaBASS) is a publicly shared archive of <i>in-situ</i> oceanographic and atmospheric data maintained by the NASA Ocean Biology Processing Group.	https://seabass.gsfc.nasa.gov
BCO-DMO	The Biological and Chemical Oceanography Data Management Office (BCO-DMO) is a facility where marine biogeochemical and ecological data and information can easily be disseminated, protected, and stored on short and intermediate time-frames. Created to serve principal investigators funded by the US National Science Foundation (NSF).	https://www.bco-dmo.org
PANGAEA	Open Access library aimed at archiving, publishing and distributing georeferenced data from earth system research.	https://www.pangaea.de/
OCADS	The Ocean Carbon Data System (OCADS) is a data management project located within the NOAA National Centers for Environmental Information.	https://www.nodc.noaa.gov/ocads/
Simons CMAP	Simons Collaborative Marine Atlas Project (Simons CMAP) is an open-source data portal interconnecting data sets across oceanography disciplines.	https://simonscmap.com
Continued on the next page.		

Table 2: Some examples of *in-situ* datasets from data synthesis, general databases and portals, and observational programmes, for use in ocean carbon studies.

Name	Description	Reference
COPEPOD	Coastal and Oceanic Plankton Ecology, Production, and Observation Database (COPEPOD). A global plankton database that contains over 400,000 observations of copepods, along with other zooplankton, phytoplankton, and microbial plankton taxa.	https://www.st.nmfs.noaa.gov/copepod/
Observational programmes		
HOT	The Hawaii Ocean Time-series (HOT) program has been making repeated observations of the hydrography, chemistry and biology of the water column at a station north of Oahu, Hawaii since 1988.	http://hahana.soest.hawaii.edu/hot/
MOBY	The NOAA funded Marine Optical BuoY (MOBY) provides vicarious calibration of ocean colour satellites. It is an autonomous optical buoy which is moored off the island of Lanai in Hawaii.	https://www.mlml.calstate.edu/moby/
BATS	The Bermuda Atlantic Time-series Study (BATS) has been making repeated observations on the physical, biological, and chemical properties of the ocean every month since 1988 in an area of the western Atlantic Ocean (~ 32.17°N, 64.5°N). The programme is supplemented by biweekly Hydrostation-S cruises to a neighbouring location that began in 1954.	http://bats.bios.edu
BOUSSOLE	The Bouée pour l'acquisition de Séries Optiques à Long Terme (BOUSSOLE) is a time series of optical properties in western Mediterranean oceanic waters to support the calibration and validation of ocean colour satellite sensors. Phytoplankton pigments and oceanic particles are also measured.	http://www.obs-vlfr.fr/Boussole/html/project/introduction.php
CARIACO	The CARbon Retention In A Coloured Ocean (CARIACO) is an ocean time series program situated in the Cariaco Basin with the objective of studying the relationship between surface primary production, regional hydrography, physical forcing variables, and the settling flux of POC.	http://imars.marine.usf.edu/cariaco

Continued on the next page.

Table 2: Some examples of *in-situ* datasets from data synthesis, general databases and portals, and observational programmes, for use in ocean carbon studies.

Name	Description	Reference
WCO	The Western Channel Observatory (WCO) is an oceanographic time-series (dating back to 1903) and marine biodiversity reference site in the Western English Channel. <i>In-situ</i> measurements are undertaken weekly at coastal station L4 and fortnightly at open shelf station E1.	https://www.westernchannelobservatory.org.uk
AMT	The Atlantic Meridional Transect (AMT) is a multidisciplinary programme which undertakes biological, chemical and physical oceanographic research during an annual voyage between the UK and destinations in the South Atlantic.	https://www.amt-uk.org
CPR	The Continuous Plankton Recorder (CPR) Survey has been collecting data in the North Atlantic and the North Sea on the biogeography and ecology of plankton since 1931, and more recently expanded to other regions around the globe. The CPR is an instrument designed to capture plankton samples that is towed from the stern of volunteer ships.	https://www.cprsurvey.org
LTER	The Long-Term Ecological Research (LTER) programme, supported by the US National Science Foundation, consists of 28 sites throughout the United States, Puerto Rico and Tahiti. Key marine sites include the Palmer LTER, California Current Ecosystem LTER, and Northeast U.S. Shelf LTER.	https://lternet.edu
Station Stončica	Located in the central Adriatic Sea, near the island of Vis, monthly phytoplankton primary production measurements have been collected at Station Stončica since April 1962, providing one of the longest time-series of primary production measurements to date.	Kovač et al. (2018a)
EXPORTS	EXport Processes in the Ocean from Remote Sensing (EXPORTS) is a NASA funded programme aiming to develop a predictive understanding of the export and fate of global ocean net primary production and its implications for present and future climates	https://oceanexports.org

Continued on the next page.

Table 2: Some examples of *in-situ* datasets from data synthesis, general databases and portals, and observational programmes, for use in ocean carbon studies.

Name	Description	Reference
NAAMES	The North Atlantic Aerosols and Marine Ecosystems Study (NAAMES) is a NASA funded programme designed to improve understanding of Earth's ocean ecosystem-aerosol-cloud system	Behrenfeld et al. (2019b)
Plumes and Blooms	Since 1996, monthly research cruises in the Santa Barbara Channel, US, have been collecting <i>in-situ</i> measurements with relevance to the marine carbon cycle	Toole and Siegel (2001) & Catlett and Siegel (2018) http://www.oceancolor.ucsb.edu/plumes_and_blooms/

271 *3.1.1. DIC and components of the carbonate system*

272 The complete carbonate system can be quantified *in situ* by measurement
273 of two or more core variables within a water sample (see section "*Two Out*
274 *of Six*" in Zeebe, 2012, for details) along with temperature and pressure: pH,
275 carbon dioxide fugacity ($f\text{CO}_2$), total alkalinity (TA), and total dissolved inorganic
276 carbon (DIC). Shipboard and *in-situ* analyses of these components often rely on
277 dissimilar instrumentation and methodologies, including: ion-sensitive field effect
278 transistors; infrared detection; and titrimetric, colourmetric, spectrophotometric,
279 and potentiometric approaches (Liu et al., 2013; Byrne, 2014; Martz et al., 2015).

280 *3.1.2. DOC*

281 DOC is typically separated from POC by filtration through a $0.2\ \mu\text{m}$ filter.
282 The DOC is then separated from DIC by acidification and sparging with CO_2 -free
283 gas (Sharp, 2002). This is typically based on the oxidation of organic compounds
284 to CO_2 (typically by high-temperature combustion or UV, historically using
285 persulfate methods) and is determined using either a non-dispersive infrared CO_2
286 analyser or through colourmetric measurements of CO_2 (Sharp, 2002). Coloured
287 Dissolved Organic Matter (CDOM), that can be used as a tracer for DOC in
288 coastal regions (see Section 4.1.2), is typically measured from discrete samples
289 using long-pathlength capillary waveguides with single-beam spectrophotometers
290 (Bricaud et al., 2010; Nelson et al., 2007), though higher-frequency ship-based
291 measurements are possible using underway spectrophotometry (see Dall'Olmo
292 et al., 2017).

293 *3.1.3. POC*

294 Particulate organic carbon is typically defined as all the organic carbon that
295 is retained by GF/F filters (nominal pore size of $0.7\ \mu\text{m}$). Samples are typically
296 collected on pre-combusted ($450\ ^\circ\text{C}$) GF/F filters and dried overnight at $65\ ^\circ\text{C}$
297 before analysis. To remove particulate inorganic carbon, filters are acidified either
298 by adding low-carbon HCl directly or by overnight exposure to the fumes of
299 a concentrated HCl solution in a desiccator. Filters are then dried, packed in
300 pre-combusted tin capsules, combusted in an elemental analyser to convert the

301 organic carbon in CO₂ (Sharp, 1974). The liberated CO₂ is finally detected by
302 thermal conductivity. Acetanilide is used as a standard. For further details on
303 measuring POC, the reader is referred to protocols recently published by the
304 IOCCG (Chaves et al., 2020).

305 *3.1.4. Phytoplankton Carbon*

306 Phytoplankton carbon is notoriously difficult to quantify and no standard
307 method exists. Current techniques include: measuring chlorophyll-a concentration
308 then converting to carbon by making assumptions on the carbon to chlorophyll-a
309 ratio (e.g. Sathyendranath et al., 2009); measuring cell counts (e.g. from light
310 microscopy and flow cytometry) for different communities of phytoplankton,
311 then making assumption on per-cell biovolume and carbon (e.g. Llewellyn et al.,
312 2005; Martínez-Vicente et al., 2013, 2017); calibrating flow cytometer forward
313 and side scattering (for small phytoplankton) and video-based analysis (for large
314 phytoplankton) (e.g. Veldhuis and Kraay, 2002; Olson et al., 2003; Casey et al.,
315 2013); and elemental analysis of flow cytometrically-sorted samples (Graff et al.,
316 2015); and x-ray microanalysis (Heldal et al., 2003).

317 *3.1.5. Zooplankton and Bacterial Carbon*

318 Techniques used to estimate zooplankton carbon typically involve counting
319 microzooplankton (e.g. using nets, optical counters or video-based cameras), and
320 using biovolume estimates (or length-weight relationships) and carbon conver-
321 sions (Gallienne et al., 1996; Alcaraz et al., 2003). Efforts have also been made
322 to relate acoustic signals to zooplankton biomass (Powell and Ohman, 2012).
323 Techniques used to estimate bacterial carbon typically involve cell counts, biovol-
324 ume estimates and carbon conversions. Other techniques include separation of
325 bacteria from phytoplankton and detritus by tangential flow filtration, then use of
326 high-temperature catalytic oxidation (HTCO) to determine carbon and nitrogen
327 content (Fukuda et al., 1998; Martínez-Vicente et al., 2012, 2016).

328 *3.1.6. PIC*

329 Particulate inorganic carbon is typically defined as the inorganic carbon that
330 is retained on a GF/F filter following filtration. Samples are collected on pre-
331 combusted GF/F filters, rinsed with 0.2 μm filtered seawater, and extracted in
332 a 40 °C bath by means of 50 % HCl. Particulate calcium is then quantified by
333 atomic absorption spectrometry and converted to PIC (Mitchell et al., 2017). It
334 can also be estimated through the acid-labile backscattering technique and through
335 inductively coupled plasma optical emission spectrometry (Balch et al., 2005).

336 *3.1.7. Primary Production, New production and Export production*

337 There are a wide range of methods used to measure primary production in the
338 ocean. For a full review on the topic, the reader is referred to the recent works of
339 Regaudie-de Gioux et al. (2014), Sathyendranath et al. (2019b) and Church et al.
340 (2019). Common methods used include: *in-vivo* techniques (^{14}C and ^{13}C assim-
341 ilation; O_2 evolution; $^{15}\text{NO}_3$ assimilation; $^{15}\text{NH}_4$ assimilation; $^{18}\text{O}_2$ evolution);
342 triple isotope methods; O_2/Ar measurements; bulk properties (NO_3 flux to the
343 photic zone, O_2 utilisation rate, net O_2 accumulation in photic zone, $^{238}\text{U}/^{234}\text{Th}$;
344 $^3\text{H}/^3\text{He}$); optical methods (double-flash fluorescence; passive fluorescence); and
345 monitoring upper and lower limits (sedimentation rate below the photic zone,
346 optimal energy conversion of photons absorbed, depletion of winter accumulation
347 of NO_3), typically through the use of sediment traps (Buesseler et al., 2007).

348 *3.1.8. Grazing and Secondary production*

349 Common methods for estimating grazing rates include: the ^{14}C method (Daro,
350 1978); dilution techniques (Landry and Hassett, 1982); the radioisotope method
351 using ^{32}P -labeled yeast (*Rhodotorula*) (Haney, 1971); and measuring ingestion of
352 [methyl- ^3H] methylamine hydrochloride (^3H -MeA) labelled particles (White and
353 Roman, 1991). Consumption has been estimated from vertical measurements of
354 the composition of major bioelements and biochemicals in the ocean (Kaiser and
355 Benner, 2012). Secondary production by zooplankton has been estimated using
356 information on zooplankton biomass, hatching success and fecundity, derived
357 from laboratory mesocosm experiments or ship-based incubations (Poulet et al.,

358 1995). Secondary production by bacteria has been estimated from measurements
359 of increasing bacterial abundance with time in filtered seawater, and through
360 bacterial deoxyribonucleic acid synthesis by tritiated thymidine incorporation in
361 seawater (Fuhrman and Azam, 1980).

362 *3.1.9. Respiration and Excretion*

363 Planktonic respiration rates can be derived through various means (see Robin-
364 son and Williams, 2005, for a review on the topic). Common methods include:
365 inverse modelling of the community composition and activity; measuring the
366 rate of production and consumption of a product or a reactant; the assay of an
367 appropriate respiratory enzyme or enzyme system; and biomass-based predictions
368 (Robinson and Williams, 2005). Excretion rates are typically determined using
369 either the radiocarbon method indirectly (Fogg, 1952; Watt and Fogg, 1966; Sharp,
370 1979) or directly using kinetic-based methods (Lancelot, 1979).

371 *3.1.10. Aggregation and Fragmentation*

372 Aggregation has been measured in laboratory-based experiments using floc-
373 culators (Waite et al., 1997), and using mesocosm based experiments (Passow
374 and Alldredge, 1995), or in the field using photographic observations (Suzuki
375 and Kato, 1953) and high resolution video analysis (Gorsky et al., 2000). For a
376 full review on the topic of aggregation the reader is referred to the work of Burd
377 and Jackson (2009). Fragmentation has been measured through comparisons
378 of abundances and size distributions of marine particles in time (Dilling and
379 Alldredge, 2000), laboratory video-based analysis (Goldthwait et al., 2004), and
380 using optical measurements to track changes in small and large particles (Briggs
381 et al., 2020).

382 *3.1.11. Non-predatory mortality*

383 Non-predatory plankton mortality has been estimated using microscopic meth-
384 ods. These typically involve differentiating between living and dead plankton
385 using staining based methods or morphological characteristics (Tang et al., 2014).
386 Phytoplankton cell lysis rates have been estimated by using spectrofluorometric

387 methods to quantify dissolved esterase activity (Agustí et al., 1998), flow cytomet-
388 ric staining has been used for monitoring phytoplankton vitality (Peperzak and
389 Brussaard, 2011), and algal senescence has been estimated through pigment-based
390 methods (Bale et al., 2011).

391 3.1.12. Solubility

392 The solubility of CO₂ is dependent on temperature and salinity and various
393 equations have been proposed relating CO₂ solubility to these physical variables
394 (Murray and Riley, 1971; Weiss, 1974).

395 3.1.13. Calcification

396 Rates of calcification, or CaCO₃ production, are typically measured using
397 ¹⁴C. This was first proposed by Paasche (1962, 1963), who demonstrated in the
398 laboratory that radioactive ¹⁴C could be used to infer the production of both
399 organic (photosynthesis) and inorganic carbon (calcification) by coccolithophores
400 (Daniels et al., 2018). At present two techniques are commonly used: 1) following
401 incubation, ¹⁴C-labelled samples are filtered through two filters, one is used to
402 give an estimate of total particulate production, the other is fumed with acid to
403 remove Ca¹⁴CO₃ giving an estimate of particulate organic production, with calci-
404 fication representing the difference between filters; 2) using the micro-diffusion
405 technique, that captures ¹⁴CO₂ liberated from Ca¹⁴CO₃, which gives a measure
406 of calcification. Additional techniques have been developed, for example, using
407 ⁴⁵Ca as a tracer (Van der Wal et al., 1995). For further details on these techniques,
408 and data on calcification rates, the reader is referred to Daniels et al. (2018).

409 3.1.14. Air-sea CO₂ transfer

410 *In-situ* methods used to measure or determine the exchange of CO₂ between
411 the ocean and atmosphere include: tracer studies using ambient gases (¹⁴CO₂) that
412 integrate the flux over years; deliberately introduced tracers that integrate the flux
413 over days; and direct eddy-covariance flux measurements on hourly timescales
414 (Landwehr et al., 2018). A recent review of the history and current capabilities of
415 these approaches can be found in Shutler et al. (2019).

416 3.2. *Autonomous platforms*

417 Over the past few decades there has been a rapid increase in the use of
418 autonomous platforms for ocean sampling (Bushinsky et al., 2019; Chai et al.,
419 2020). While not the main focus of this review, this section discusses the types
420 of autonomous platforms currently in use for monitoring the OBCP and directs
421 the reader to additional reviews on the topic. Autonomous platforms have the
422 advantage over ship-based methods in that they are capable of operating in hostile
423 environments, at temporal and spatial scales that challenge research ship operation,
424 and operating below the eyes of the satellite. They are also cheap to operate once
425 deployed, without generally needing at-sea personnel. Examples of autonomous
426 ocean platforms include:

- 427 • **Argo and biogeochemical Argo (BGC-Argo) floats.** These are floating
428 devices that profile the vertical structure of the water column, measuring
429 key physical (temperature, salinity and pressure) and biogeochemical and
430 related variables (pH, oxygen, nitrate, chlorophyll, backscattering and irra-
431 diance) usually down to 1000 or 2000 m, transmitting the data via satellite
432 communication. The network of Argo and BGC-Argo floats is transforming
433 our understanding of OBCP processes and fluxes (e.g. Johnson et al., 2009;
434 Boss and Behrenfeld, 2010; Dall’Olmo and Mork, 2014; Dall’Olmo et al.,
435 2016; Bishop et al., 2016; Lacour et al., 2017; Mignot et al., 2018; Ardyna
436 et al., 2019; Estapa et al., 2019; Gittings et al., 2019; Briggs et al., 2020),
437 and there is huge potential for integrating vertical data from BGC-Argo
438 floats with surface satellite observations, for improving the monitoring of
439 carbon pools and fluxes like primary production (Richardson and Bendtsen,
440 2019). For a recent review of the topic the reader is referred to the work of
441 Claustre et al. (2020).
- 442 • **Underwater gliders** are autonomous underwater vehicles that, unlike
443 floats, which float passively as a preprogrammed pressure level and prede-
444 termined time (Bork et al., 2008), can profile vertically (typically down to
445 around 1000 m, depending on design) and move horizontally by changing

446 their buoyancy and using wings (Stommel, 1989; Rudnick, 2016). Equipped
447 with physical, biological and chemical sensors, they can be programmed
448 to operate in hostile or inaccessible environments (e.g. under sea ice), can
449 track physical, chemical and biological features, and can operate for long
450 durations, measuring key components of the OBCP (e.g. Hemsley et al.,
451 2015). They are particularly useful for complementing ship-cruises, for
452 instance, by putting discrete observations collected by ship in the context
453 of larger-scale oceanic processes. Towed undulated gliders, equipped with
454 sensors, have also been used to monitor at depth (Rudnick and Cole, 2011).
455 Similar to BGC-Argo floats, they have been transforming our understanding
456 of the OBCP (e.g. Alkire et al., 2014; Omand et al., 2015; Bol et al., 2018).
457 For a recent review of the topic the reader is referred to the work of Rudnick
458 (2016).

- 459 • **Unmanned surface vehicles**, including wave gliders (Daniel et al., 2011),
460 sea gliders (Eriksen et al., 2001) and sail drones (Gentemann et al., 2020),
461 are small (typically 2-7 m long) surface platforms powered by wind, wave
462 and solar energy. These platforms are capable of operating for long dura-
463 tion, covering vast distances (100 km per day), and when equipped with
464 environmental sensors, can sample the biological, chemical and physical
465 properties of the surface ocean, as well as the air-sea interface and lower
466 atmosphere (e.g. wind and surface irradiance), and transmit the data via
467 satellite communication. They are increasingly being used to complement
468 satellite observations (Villareal and Wilson, 2014; Vazquez-Cuervo et al.,
469 2019; Scott et al., 2020), and reveal ocean and atmosphere dynamics in
470 remote regions (Mitarai and McWilliams, 2016; Thomson and Girton, 2017)
471 that are relevant to ocean carbon cycling.
- 472 • **Next generation autonomous buoys and drifters.** New autonomous
473 buoys (stationary platforms) and drifters (Lagrangian platforms) are being
474 developed, with satellite tracking and transmission, that are capable of host-
475 ing physical, biological and chemical sensors for monitoring the surface

476 ocean, and for use in satellite-algorithm validation (e.g. Brown et al., 2019;
477 Le Menn et al., 2019). These systems have the capability of being produced
478 at low cost and deployed *en masse*, and consequently, increasing surface
479 ocean observations.

480 • **Unmanned aerial vehicles.** Unmanned aerial vehicles (UAVs) – in par-
481 ticular portable and affordable, aerial drones – are now being used in
482 physical and biological oceanography. Systems have been developed
483 for measuring: SST and surface salinity (Lee et al., 2016; McIntyre and
484 Gasiewski, 2007); for collecting water samples (Ore et al., 2015; Terada
485 et al., 2018); measuring aerosols over the ocean (Corrigan et al., 2008,
486 useful for atmospherically-correcting ocean-colour data); for measuring
487 chlorophyll, macroalgae and harmful algal blooms (Su, 2017; Xu et al.,
488 2018; Lyu et al., 2017); and monitoring the ecology of large ocean animals
489 (Durban et al., 2016). For a recent review of the topic the reader is referred
490 to the work of Johnston (2019).

491 • **Ship-based autonomy.** There is a long history of marine scientists using
492 ships of opportunity for autonomous ocean sampling. The Continuous
493 Plankton Recorder (CPR) survey uses an instrument towed from the stern
494 of volunteer ships designed to capture plankton samples, that has been
495 successfully operating since 1931. In more recent years, autonomous
496 systems have been integrated into commercial ships for monitoring sea-
497 surface and atmospheric properties relevant to the marine carbon cycle,
498 including: partial pressure of CO₂ (pCO₂), phytoplankton concentration,
499 biogeochemical properties, above-water and in water marine optical and
500 thermal properties, ocean physics and atmospheric gases (e.g. Donlon et al.,
501 2008; Pierrot et al., 2009; Slade et al., 2010; Gülzow et al., 2013; Simis and
502 Olsson, 2013; Petersen, 2014).

503 • **Marine animal platforms.** Marine animals are used as platforms for
504 oceanographic sampling, particularly in the polar seas (Fedak, 2004, 2013;
505 Harcourt et al., 2019). Seals (Fedak, 2004; Meredith et al., 2011), turtles

506 (McMahon et al., 2005), whales (Lydersen et al., 2002), penguins (Xavier
507 et al., 2018), sea birds (Yoda et al., 2014; Yonehara et al., 2016), even
508 humans (Brewin et al., 2015a, 2017b; Bresnahan et al., 2016, 2017b; Wright
509 et al., 2016), have all been proposed as oceanographic platforms. Data from
510 such platforms have been used for evaluating satellite observations (Brewin
511 et al., 2017c; Keates et al., 2020) and integrated with other autonomous
512 observations to gain new insight into biological oceanography in remote
513 regions (Carranza et al., 2018).

514 The capacity of autonomous platforms for hosting physical, chemical and
515 biological sensors varies with each platform. Common physical sensors hosted on
516 in-water platforms are temperature, salinity and pressure sensors (CTDs), useful
517 for understanding physical controls on ocean carbon cycling, for example, the
518 retrieval of ocean surface currents from drifting buoys, which play a key role in
519 advecting carbon pools. The most common technology used to derive information
520 on carbon pools and fluxes are optical sensors. Frequently-used optical sensors
521 include fluorimeters and backscattering meters (single photodetectors), which
522 are typically used to estimate chlorophyll concentration and POC, respectively,
523 through establishing relationships between the optical signals and concentrations
524 of the biogeochemical variable of interest. These sensors are primarily used to
525 derive information on small particles, though analysis of optical spikes offer a way
526 to access information on larger particles, including aggregates and zooplankton
527 (Briggs et al., 2011, 2013, 2020; Burt and Tortell, 2018). Light sensors are also a
528 common feature on autonomous platforms, useful for quantifying light availability
529 for photosynthesis and light attenuation. Absorption and attenuation meters have
530 been deployed on larger autonomous platforms (e.g. Cunningham et al., 2003),
531 for measuring beam attenuation and absorption properties of water constituents.
532 Fluorimeters can also be tuned to measure fluorescence by CDOM, offering a
533 route into monitoring the DOC pool.

534 Advancement in microelectronics, battery technology and wireless commu-
535 nications have presented opportunities to integrate new optical sensors onto
536 autonomous platforms, including: transmissometers (Bishop et al., 2004; Bishop

537 and Wood, 2009); photodetector arrays (Miles et al., 2018); holographic systems
538 (Anderson et al., 2018), and photographic systems (Haëntjens et al., 2020). Data
539 from these sensors are capable of providing insight into pools and fluxes of car-
540 bon, for example, the particle size distribution, plankton composition, particle
541 biovolume, inorganic and organic content of particles, sinking velocities, particle
542 fluxes, sedimentation rates, and zooplankton migration. For a full review on the
543 topic see the recent work of Giering et al. (2020).

544 Oxygen and pH probes are increasingly being integrated into autonomous
545 platforms, with potential for estimating carbonate chemistry (Bresnahan et al.,
546 2016) and surface ocean pCO₂ (Williams et al., 2017), as are acoustic sensors,
547 for monitoring zooplankton, currents (ADCPs), bathymetry, marine mammals,
548 wind and rain (McCollum and Krajewski, 1997; Baumgartner et al., 2013; Guihen
549 et al., 2014; Todd et al., 2017; Cauchy et al., 2018). Nutrient sensors can be
550 used on BGC-Argo floats and underwater gliders (Johnson et al., 2013), and
551 there are increasing efforts to integrate miniature lab-on-a-chip style chemical
552 sensors (Beaton et al., 2011; Vincent et al., 2018) as well as water samplers (Bres-
553 nahan et al., 2017a) on autonomous platforms. As microelectronic and battery
554 technologies develop, there will be potential to miniaturise other oceanographic
555 technologies for use on autonomous platforms.

556 Despite the huge potential, there are challenges in the operation and main-
557 tenance of sensors (e.g. bio-fouling) on autonomous platforms, and at present
558 in maintaining their global distribution. It is critical that data quality assurances
559 are in place. This can be done through rigorous, community-assessed protocols,
560 sensor calibrations, monitoring of sensor drift and stability, cross-checking with
561 existing datasets, validation, database management, and data filtering (e.g. Xing
562 et al., 2011, 2012, 2018; Organelli et al., 2016; Claustre et al., 2020). Efforts
563 also need to be placed on quantifying uncertainties (Williams et al., 2017). For
564 sustained observations of the OBCP, an integrative approach has been suggested,
565 combining autonomous observations with other field data, models and satellite
566 remote sensing (Claustre et al., 2010).

567 **4. Monitoring carbon pools and fluxes from space**

568 Satellite remote sensing is the only method capable of viewing our entire
569 surface ocean synoptically, and at a relatively high temporal frequency (daily) and
570 spatial resolution (0.3 to 25 km). While providing powerful horizontal (global)
571 and temporal coverage, satellite ocean observations have limitations, for example:

- 572 • Satellite ocean observations are limited to the surface layer of the ocean.
573 The satellite signals in the visible portion of the electromagnetic spectrum
574 are representative of about one optical depth (Zaneveld et al., 2005, $1/K_d$,
575 where K_d (m^{-1}) represent the diffuse attenuation coefficient) of the water
576 column (up to 50 m depending on water clarity and the wavelength used).
577 Other parts of the electromagnetic spectrum utilised for ocean observations
578 from satellite (e.g., thermal and microwave regions) are representative of
579 less than a millimetre at the surface.
- 580 • Passive satellite visible and thermal remote sensing is limited to cloud-free
581 conditions, and for visible sensing, low to moderate sun-zenith angles.
- 582 • Satellite observations often have limitations and difficulties in coastal re-
583 gions. For example, for visible remote sensing, the optical complexity of
584 coastal waters makes it challenging to derive some pools and fluxes of
585 carbon (IOCCG, 2000; Kostadinov et al., 2007). Atmospheric-correction
586 of satellite data is often more complex in coastal regions (Hu et al., 2000).
- 587 • Satellite ocean observations are limited to information that can be com-
588 municated by electromagnetic radiation. The primary observables (e.g.,
589 remote-sensing reflectance, brightness temperature and backscatter) need to
590 be related to surrogate (geophysical/biogeochemical/ecological) variables
591 used to compute the carbon pools and fluxes. These relationships can be
592 complex and prone to large uncertainties.
- 593 • To resolve some very fine spatial and temporal scale physical oceanographic
594 processes at the surface, complementary information to satellite data is often
595 required.

596 Therefore, like other technologies, satellite data often needs to be integrated
597 with other observations and models, for algorithm development, for extrapolating
598 the surface signal down to depth, for filling gaps in the data, and for resolving fine
599 scale surface processes. Techniques used to monitor pools and fluxes of ocean
600 carbon using satellite data lie on a scale between direct and indirect techniques,
601 with some using aspects of both.

- 602 • **Direct techniques** (i.e. detection methods) are dependent on whether the
603 carbon pool in question modifies (absorbs and/or scatters) visible electro-
604 magnetic radiation to the extent its presence and its concentration leaves an
605 imprint on the signal that can be seen from space.
- 606 • **Indirect techniques** involve relating the pool or flux of interest to some
607 variable (or variables) that can be retrieved with confidence from space
608 (e.g. through ocean-colour, thermal radiometry, microwave radiometry and
609 satellite altimetry). This approach essentially uses satellite remote-sensing
610 as a method of extrapolation. Proposed relationships between satellite
611 variables and pools (or fluxes) can be mechanistic, empirical or statistical.

612 In this section, we provide an overview of the satellite techniques used to
613 derive information on pools and fluxes (see also Table 3).

Table 3: Techniques for monitoring the OBCP from satellites. (For Maturity, N = Not currently possible, I = In it's infancy; Y = Possible). References are examples (see main text for more).

Pools and fluxes		Maturity	Common techniques	References	
Pools	DIC		I	Indirect approaches that integrate space-based sea surface salinity, temperature and ocean colour observations.	Land et al. (2015) & Shutler et al. (2019)
	DOC		I	Using empirical relationships between CDOM absorption (retrievable from satellite ocean colour) and DOC. These have been found to work well in coastal waters and the Arctic Ocean, but not in the open ocean where the relationship breaks down. There is potential for developing indirect approaches in the open-ocean using multiple satellite products.	Mannino et al. (2008) & Matsuoka et al. (2017)
	POC	Total POC	Y	Methods include: empirical band ratio algorithms; empirical band-difference algorithms; backscattering-based algorithms; algorithms using satellite estimates of backscattering and chlorophyll; and algorithms using satellite estimates of diffuse attenuation, and a two-step relationship between diffuse attenuation and beam attenuation.	Stramski et al. (2008), Evers-King et al. (2017) & Le et al. (2018)
		Phytoplankton carbon	I	Methods include: relationships between phytoplankton carbon and chlorophyll; reflectance-based; absorption-based; and backscattering-based. Algorithms are available for partitioning phytoplankton carbon into different size classes.	Martínez-Vicente et al. (2017), Kostadinov et al. (2016), Roy et al. (2017) & Sathyendranath et al. (2020b)
Continued on the next page.					

Table 3: Techniques for monitoring the OBCP from satellites. (For Maturity, N = Not currently possible, I = In it's infancy; Y = Possible). References are examples (see main text for more).

Pools and fluxes		Maturity	Common techniques	References
	Zoo-plankton carbon	I	Methods include: indirect approaches, through estimates of the slope of the particle size spectrum, or bio-physical models driven by visible and thermal ocean remote sensing products; and some emerging direct approaches, for large congregations of certain species, or through active satellite ocean colour (lidar) methods.	Strömberg et al. (2009), Basedow et al. (2019) & Behrenfeld et al. (2019a)
	Bacteria carbon	I	Indirect methods have been proposed for mapping bacterial abundance for some species, typically using multiple satellite products.	Grimes et al. (2014), Racault et al. (2019) & Larsen et al. (2015)
	PIC	Y	All approaches relate elevated water-leaving radiance (or reflectance), a result of elevated backscattering due to the presence of coccolths, to PIC concentrations. Methods proposed include: band-ratio approaches; band-difference approaches; optical water type methods; and semi-analytical inversions and look-up-tables.	Gordon et al. (2001), Balch et al. (2005), Mitchell et al. (2017) & Kondrik et al. (2019)
Fluxes	Primary production	Y	Retrieval from space using products of light (PAR), chlorophyll-a, and appropriate assignment of photosynthesis irradiance parameters. Products partitioned into phytoplankton groups or size classes have also been proposed.	Platt and Sathyendranath (1993) & Uitz et al. (2010)
	Export production	Y	Previous attempts have focused on empirical relationships between export production, SST and primary production. Satellite-data driven food-web export flux models have also been proposed.	Laws et al. (2000, 2011) & Siegel et al. (2014)

Continued on the next page.

Table 3: Techniques for monitoring the OBCP from satellites. (For Maturity, N = Not currently possible, I = In it's infancy; Y = Possible). References are examples (see main text for more).

Pools and fluxes	Maturity	Common techniques	References
Grazing	N	Not currently retrievable from space (but see Section 4.2.3).	–
Secondary production	N	Not currently retrievable from space (but see Section 4.1.3).	–
Respiration	N	Not currently retrievable from space (but see Section 4.2.3).	–
Excretion	N	Not currently retrievable from space (but see Section 4.2.3).	–
Aggregation	N	Not currently retrievable from space.	–
Fragmentation	N	Not currently retrievable from space.	–
Non-predatory mortality	N	Not currently retrievable from space (but see Section 4.2.3).	–
Solubility	I	Feasible at the surface with estimates of SST and SSS.	Land et al. (2015) & Shutler et al. (2019)
Calcification	N	Not currently retrievable from space (but see Section 4.1.4).	–
Air-sea CO ₂ transfer	I	Regional, indirect approaches have been proposed. These involve forcing empirical equations and statistical models with satellite retrievals of SST, SSS and chlorophyll-a, individually or in combination	Land et al. (2015) & Shutler et al. (2019)

615 *4.1. Pools of carbon from space*

616 *4.1.1. DIC from space*

617 DIC cannot be directly observed from space. However, indirect approaches
618 have been proposed. Land et al. (2015) identified the potential of these indi-
619 rect approaches and Land et al. (2019) evaluated the precision and accuracy of
620 these approaches for regional and global waters. These approaches can use a
621 combination of satellite sea-surface temperature (SST), the major controller of
622 the solubility of CO₂, and satellite retrievals of sea surface salinity (SSS), and
623 sometimes use climatology nutrient data or satellite ocean-colour observations,
624 for interpreting the biological modulation of DIC. DIC has been estimated using
625 these indirect approaches in the Equatorial Pacific (Loukos et al., 2000), the Arctic
626 (Arrigo et al., 2010) and the Arabian Sea (Sarma, 2003), the Caribbean, the Bay
627 of Bengal, the Amazon outflow, and globally (Land et al., 2019). As discussed
628 by Land et al. (2015), such approaches require tuning for different regions of
629 the ocean, are based on *in-situ* data-derived empirical relationships between DIC
630 variables and the oceanic variables, and so may require tuning for a particular
631 region and season (e.g., Sarma, 2003; Sarma et al., 2006).

632 *4.1.2. DOC from space*

633 From a remote-sensing perspective, the ensemble of all DOC pools does not
634 have a strong optical signature that can be used to quantify its concentration in
635 surface waters. A small component (~10 %) of the DOC pool is chromophoric
636 (coloured), and thus can be directly monitored by ocean colour. Satellite retrievals
637 of spectral absorption by CDOM, and combined spectral absorption coefficient
638 by CDOM and coloured detrital matter (CDM), are routinely produced by space
639 agencies, and have been shown to perform with reasonable accuracy in satellite
640 validation exercises (Siegel et al., 2013; Mannino et al., 2014; Loisel et al., 2014;
641 Brewin et al., 2015c). Though representative of "matter" rather than "carbon", and
642 acknowledging difficulties in separating CDOM and detrital absorption owing to
643 their similar spectral signatures, there have been increasing efforts to use satellite
644 CDOM and CDM products as an avenue for monitoring DOC.

645 In coastal and shelf regions, strong correlations between CDOM absorption
646 (magnitude and spectral slope) and DOC have been observed (Ferrari et al., 1996;
647 Vodacek et al., 1997; Bowers et al., 2004; Fichot and Benner, 2012; Tehrani et al.,
648 2013). Mannino et al. (2008) analysed a large dataset of CDOM absorption (m^{-1})
649 and DOC concentration ($\mu\text{mol C L}^{-1}$) in the Mid Atlantic Bight and established
650 empirical relationships between the two variables that changed with season.
651 Application of these algorithms to satellite CDOM absorption estimates indicated
652 a capacity to retrieve DOC within 10 % uncertainty (mean absolute percentage
653 difference). Mannino et al. (2016) updated these relationships using a larger
654 dataset, and developed a neural network algorithm to model the vertical profile
655 of DOC from the surface concentrations (retrievable from satellite) and physical
656 model data. They then combined satellite estimates of water column DOC with
657 physical circulation model simulations to quantify the shelf boundary fluxes of
658 DOC in the Mid Atlantic Bight.

659 Relationships between CDOM absorption and DOC have also been established
660 for Arctic regions. Using the method of Fichot and Benner (2012), that relates
661 terrigenous DOC concentration in coastal waters to the exponential slope of the
662 absorption coefficient of CDOM in the 275 to 295 nm range ($S_{275-295}$), Fichot et al.
663 (2013) estimated the first pan-Arctic distribution of terrigenous dissolved organic
664 matter and continental runoff in the surface Arctic Ocean, by estimating $S_{275-295}$
665 from satellite remote-sensing reflectance data. In a further study, Matsuoka
666 et al. (2017) demonstrated that satellite estimates of CDOM absorption across
667 the Arctic region can be retrieved with an uncertainty of 12 %, and showed a
668 tight correlation between CDOM absorption and DOC (Matsuoka et al., 2012),
669 demonstrating that DOC in river-influenced coastal waters can be retrieved from
670 satellite ocean colour with an average uncertainty of 28 %. Le Fouest et al. (2018)
671 showed good agreement between the Matsuoka et al. (2017) satellite estimates
672 of DOC and modelled DOC, and used the data to assess the concentration of
673 terrestrial DOC in surface waters in the western Arctic Ocean.

674 Rivers are a major source of allochthonous DOC in the ocean. Assuming
675 DOC behaves as a conservative property, then it will change with salinity as

676 the freshwater gets mixed with seawater. It has in fact been shown that the
677 absorption by CDOM in coastal waters under the influence of freshwater influx
678 is closely related to salinity. For example, Bowers et al. (2000) have proposed
679 a remote-sensing algorithm for estimating the concentration of CDOM in the
680 Clyde Sea, which could then be used to estimate salinity in waters affected by
681 freshwater. Today, with the advent of salinity sensors in space, the potential
682 exists for using salinity as a tracer for DOC influx. But there is also emerging
683 evidence that terrigenous DOC may be susceptible to microbial degradation,
684 based on a study of DOC from the Congo River (Spencer et al., 2009). They
685 suggested that the CDOM absorption coefficient could potentially be used for
686 studying photochemical degradation of terrigenous DOC. It would therefore be
687 desirable to compare the timescales involved in the microbial degradation with
688 those of mixing between freshwater and seawater, to ensure the degradation did
689 not introduce significant errors into the calculation of DOC from salinity, or,
690 if necessary, to correct for such processes. The algorithms noted above have
691 been developed for coastal waters, and are regional in their implementation. The
692 question remains whether an algorithm that would be globally applicable in all
693 coastal waters might be established, for detection of riverine DOC inputs into the
694 ocean. Efforts towards establishing the data required to answer this question are
695 underway (Aurin et al., 2018). Many of these algorithms are designed to study the
696 dynamics of allochthonous DOC (e.g. from river runoff), as opposed to biogenic,
697 autochthonous DOC produced in the ocean through microbial cycling.

698 In the open ocean, Nelson and Siegel (2013), in a major study involving over
699 a thousand samples from a variety of locations and depths, concluded that no
700 relationship existed between CDOM absorption and DOC concentration, hence
701 demonstrating major challenges in using satellite CDOM absorption products
702 to quantify open-ocean DOC. Considering the different components of DOC
703 (labile and semi-labile), their timescales, vertical structure, processes such as
704 photobleaching, and the biotic and abiotic factors controlling DOC processes
705 (Hansell, 2013), indirect satellite methods for open ocean DOC estimation could
706 be developed, using conceptual, empirical or statistical models, driven by multi-

707 ple satellite products (e.g. chlorophyll, plankton type, light (PAR), salinity and
708 SST). In a recent study, Roshan and DeVries (2017) combined an artificial neural
709 network estimate of the global DOC distribution, developed using input data on
710 chemical (e.g. nutrients), physical (e.g. depth, salinity and temperature), and bio-
711 logical variables (depth of the euphotic zone and chlorophyll concentration), with
712 a data-constrained ocean circulation model, to produce the first observationally
713 based global-scale assessment of DOC production and export. Many of these
714 physical and biological products are available through satellite, suggesting the
715 potential to develop similar satellite-driven approaches.

716 *4.1.3. POC from space*

717

718 Total POC from space

719 POC is accessible through satellite remote-sensing of ocean colour because par-
720 ticles suspended in seawater that make up the POC influence the bulk seawater
721 inherent optical properties, namely the particle beam attenuation, scattering and
722 backscattering coefficients, which are all sensitive to particle abundance, to the
723 composition of particles (complex refractive index), their size distribution, shape
724 and their internal structure (e.g. Stramski and Kiefer, 1991; Organelli et al., 2018).
725 Empirical relationships between POC and particle beam attenuation measured
726 from optical instruments (transmissometers) have been quantified, and used to
727 monitor POC optically (Gardner et al., 1993; Bishop, 1999; Claustre et al., 1999;
728 Stramska and Stramski, 2005). In addition, relationships between POC and parti-
729 cle backscattering and absorption have also been quantified (e.g. Stramski et al.,
730 2008; Allison et al., 2010; Rasse et al., 2017), the latter two directly retriev-
731 able from satellite ocean colour inversion algorithms (acknowledging indirect
732 estimates of beam attenuation have also been attempted, see Roesler and Boss,
733 2003).

734 The first attempts to use satellite ocean colour to estimate POC synoptically
735 were made by Stramski et al. (1999). Using satellite remote sensing reflectance
736 data, and empirical relationships between reflectance and particle backscatter-
737 ing on the one hand, and POC and particle backscattering on the other hand,

738 basin-scale POC concentrations were quantified in the Southern Ocean. Global
739 and regional satellite POC estimates quickly followed (e.g. Loisel et al., 2001,
740 2002; Mishonov et al., 2003; Gardner et al., 2006). At present, there are var-
741 ious algorithms designed to estimate POC from satellite ocean-colour remote
742 sensing (Evers-King et al., 2017), including: empirical band ratio algorithms
743 (Stramski et al., 2008); empirical band-difference algorithms (Le et al., 2018);
744 backscattering-based algorithms (Stramski et al., 2008), using satellite estimates
745 of backscattering from inversion algorithms, and empirical relationships between
746 POC and backscattering (Stramski et al., 1999, 2008); algorithms using satellite
747 estimates of backscattering and chlorophyll (Loisel et al., 2002); algorithms using
748 satellite estimates of diffuse attenuation, and a two-step relationship between
749 diffuse attenuation and beam attenuation, and the beam attenuation and POC
750 (Gardner et al., 2006); and algorithms based on magnitude and spectral shape
751 of the backscattering coefficient, and their relationships with the particle size
752 distribution and POC (Kostadinov et al., 2009, 2016). Global validation has indi-
753 cated some satellite POC algorithms perform with similar precision and accuracy
754 to satellite ocean-colour chlorophyll algorithms (Świrgoń and Stramska, 2015),
755 highlighting POC as one of the carbon pools retrievable from satellite with high
756 confidence. Intercomparison and validation exercises have demonstrated good
757 performance by empirical band ratio algorithms, band-difference algorithms and
758 algorithms using satellite estimates of backscattering and chlorophyll (Evers-King
759 et al., 2017; Le et al., 2018; Tran et al., 2019), but that algorithm performance
760 varies regionally (Allison et al., 2010), and that blending of region-specific al-
761 gorithms may provide the best way forward for generating global POC products
762 (Evers-King et al., 2017).

763 In a study by Evers-King et al. (2017), uncertainties in POC products were
764 mapped globally for a range of POC algorithms, using fuzzy-logic optical water
765 type mapping (Moore et al., 2009; Jackson et al., 2017a). They found that for some
766 of the better performing algorithms, the majority of satellite pixels at global scale
767 fell within an error range that is widely accepted by the ocean colour community
768 (<30 %, Evers-King et al., 2017). Many of the approaches described above are

769 designed for surface open-ocean waters, that are less optically complex when
770 compared with surface coastal waters. However, increasing efforts are being made
771 to develop satellite POC algorithms for surface coastal waters (Le et al., 2017;
772 Tran et al., 2019). Approaches have been developed for extrapolating surface
773 POC estimates in the open-ocean vertically, to quantify depth-integrated POC
774 from space (Duforêt-Gaurier et al., 2010).

775

776 *Phytoplankton Carbon from space*

777 Owing to the central role of phytoplankton carbon in the OBCP, there are in-
778 creasing efforts to develop and refine algorithms for deriving phytoplankton
779 carbon from satellite data (Martínez-Vicente et al., 2017). Methods include those
780 based on backscattering at a single wavelength, empirical relationships based
781 on chlorophyll concentration, and methods based on allometric considerations
782 combined with either phytoplankton absorption characteristics or the spectral
783 slope of backscattering (Kostadinov et al., 2016; Roy et al., 2017). Behrenfeld
784 et al. (2005) produced estimates of phytoplankton carbon as a linear function of
785 satellite estimates of particle backscattering at 443 nm (Maritorena et al., 2002),
786 following subtraction of a fixed background contribution to backscattering from
787 non-algal particles. Further refinements to the approach, either to the linear rela-
788 tionship or by including a variable background contribution, have been proposed
789 (Martínez-Vicente et al., 2013; Bellacicco et al., 2016, 2018). Sathyendranath
790 et al. (2009) developed a simple conceptual model to infer phytoplankton carbon
791 as a function of chlorophyll-a concentration. The model was tuned to a large
792 dataset of POC and chlorophyll-a concentration using quantile regression. Similar
793 relationships have been proposed using other datasets (Buck et al., 1996; Marañón
794 et al., 2014), but this was the first application of the model to satellite observations,
795 for mapping phytoplankton carbon at large scales.

796 The last couple of decades have shown considerable progress and proliferation
797 in satellite algorithms developed to identify various aspects of phytoplankton
798 community structure (size structure, functional types, diversity, dominant phy-
799 toplankton types) from satellite data. The progress achieved and the prospects

800 for further developments are outlined in a number of recent reports, reviews
801 and scientific roadmaps (i.e. IOCCG, 2014; Bracher et al., 2017; Mouw et al.,
802 2017). Synergy between ocean-colour products and SCIAMACHY data have
803 been exploited (Losa et al., 2017), as well as synergy with other satellite products
804 (Raitos et al., 2008; Palacz et al., 2013; Ward, 2015; Brewin et al., 2017a; Lange
805 et al., 2018; Sun et al., 2019; Moore and Brown, 2020). An active grass-roots level
806 initiative of interested scientists has assembled validation data, and carried out
807 inter-comparison exercises (Brewin et al., 2011; Hirata et al., 2012; Kostadinov
808 et al., 2017; Mouw et al., 2017). However, much of the work carried out in
809 this domain, so far, has focussed on partitioning the phytoplankton community
810 according to their contributions to the total chlorophyll concentration, rather than
811 carbon concentration.

812 Only a small number of attempts have addressed the problem of partitioning
813 phytoplankton carbon into fractions residing in various size classes or functional
814 types. These include the work of Kostadinov et al. (2016) and of Roy et al. (2017),
815 both of which are based on allometric considerations. The method of Kostadinov
816 et al. (2016) uses the satellite-derived particle-backscattering signal as the starting
817 point, and makes assumptions about how the total particle pool in the pelagic
818 ocean is partitioned between phytoplankton and other particulate matter. The
819 method of Roy et al. (2017) is based on phytoplankton absorption coefficient
820 in the red part of the spectrum, and its modification by the size structure and
821 concentration of phytoplankton. Both methods assume that the size spectrum of
822 phytoplankton follows a power-law distribution, with cell numbers increasing
823 with decreasing cell size.

824 Recently, Sathyendranath et al. (2020b) proposed an alternative approach
825 to deriving phytoplankton carbon and size fractions. In their approach, they
826 estimate the chlorophyll-to-carbon ratio of a phytoplankton population using a
827 physiological model (Jackson et al., 2017b) driven by light (photosynthetically
828 available radiation, PAR), modified to account for spectral distribution of light
829 and spectral variations in light absorption by phytoplankton. The model then
830 estimates the maximum chlorophyll-to-carbon ratio of a phytoplankton population

831 attained as light approaches zero, which is allowed to vary as a function of the
832 phytoplankton community structure (Brewin et al., 2015b), and used estimates
833 of the photosynthesis-irradiance parameters (Mélin and Hoepffner, 2011). Once
834 the chlorophyll-to-carbon ratio is estimated, it becomes possible to transform a
835 chlorophyll-based size-class model to one that is based on carbon. The advantage
836 of this method is the consistency it shows between chlorophyll-based biomass
837 estimates and carbon-based biomass estimates as well as with primary production,
838 bringing us towards unification of photo-acclimation models of phytoplankton
839 (which deal with changes in chlorophyll-to-carbon ratio) and primary production
840 models. Such consistency is paramount in work towards closing the budget of
841 the biologically-mediated carbon cycle in the ocean. Key to implementing such
842 a model through remote sensing is a method to map photosynthesis-irradiance
843 parameters, especially the photo-adaptation parameter, at space and time scales
844 that are consistent with satellite-derived information on chlorophyll and PAR
845 (Kovač et al., 2018b; Kulk et al., 2020). The method is also useful for exploring the
846 physiological responses of phytoplankton to changes in the marine environment
847 in the context of climate change, and consequent changes in pools and fluxes of
848 carbon in the ocean.

849 To date, validation efforts of satellite phytoplankton carbon products (Martínez-
850 Vicente et al., 2017; Burt et al., 2018) suggest higher uncertainties (e.g. > 35,%)
851 than some standard ocean colour products (e.g. chlorophyll-a concentration)
852 and some other carbon pools (e.g. POC, Evers-King et al., 2017). Part of the
853 reason for this is that phytoplankton carbon is difficult to quantify *in situ* and
854 consequently *in-situ* phytoplankton carbon measurements have high uncertainties
855 (see section 3.1.4).

856

857 Zooplankton Carbon from space

858 It has traditionally been thought that surface-dwelling zooplankton cannot be ob-
859 served directly from space, considering they do not require pigments for capturing
860 light energy like phytoplankton do, owing to their preference for transparency,
861 as a means to avoid predation, and their smaller abundance when compared with

862 phytoplankton (less likely to influence bulk inherent optical properties). Until
863 recently, only indirect approaches have been suggested for mapping zooplankton
864 biomass from satellite. Strömberg et al. (2009) developed a model that related
865 the flow of energy from primary production (derived using satellite data) to
866 zooplankton biomass. The model was parameterised with primary production
867 estimated from the SeaWiFS sensor and a subset of a global dataset of zooplank-
868 ton biomass. The model was then validated with the remaining zooplankton
869 data and used to produce global maps of zooplankton biomass. Similar models,
870 based on the metabolic theory of ecology (Platt and Denman, 1977, 1978), driven
871 by remotely-sensing variables (e.g. primary production and SST), have also
872 been used for predicting biomass in higher trophic levels (e.g. Jennings et al.,
873 2008). Satellite products of phytoplankton community structure also have the
874 potential for predicting energy flow to higher trophic levels (Siegel et al., 2014).
875 For example, in the Benguela ecosystem, it has been suggested that flagellates
876 favour the growth of sardines, whereas diatoms favour the growth of anchovy
877 (Cury et al., 2008). Bio-physical models to estimate zooplankton biomass, using
878 satellite chlorophyll and SST as input, have been developed for regions of the
879 Indian Ocean (e.g. Solanki et al., 2015). Mahesh et al. (2018) developed a regional
880 model of mesozooplankton biomass in the Bay of Bengal, as a function of SST
881 and chlorophyll-a concentration, that was subsequently applied to MODIS data to
882 estimate mesozooplankton biomass. Other novel ways of deriving zooplankton
883 biomass using satellite observations are also being pursued, for example, the use
884 of productivity fronts (Druon et al., 2019).

885 It has recently been demonstrated that certain zooplankton species, such as
886 the red coloured copepod *Calanus finmarchicus*, that can congregate in large
887 surface patches, are capable of modifying the colour of the ocean such that it is
888 detectable directly from satellite (Basedow et al., 2019). Such direct methods of
889 zooplankton remote-sensing have the potential to provide new understanding of
890 the distribution and behaviour of the species, with implications for ocean carbon
891 cycling. Furthermore, it has recently been shown that satellite active ocean colour
892 (lidar) observations are capable of detecting zooplankton diel vertical migration

893 patterns (Behrenfeld et al., 2019a), through comparison of day-night particle
894 backscattering differences, with implications for monitoring zooplankton biomass.
895 Direct zooplankton monitoring from space appears to be an emerging field of
896 research.

897

898 Bacterial Carbon from space

899 Submicron photosynthetic cyanobacteria are typically treated as part of the phyto-
900 plankton pool. Whereas algorithms have been developed to detect cyanobacteria
901 from space exploiting their absorption characteristics or their ecological niches
902 (IOCCG, 2014), we are not aware of satellite algorithms developed to detect
903 other pigmented bacteria. Stomp et al. (2007) have provided information on
904 the absorption spectra and major pigments of some pigmented bacteria, such as
905 green sulphur bacteria, purple sulphur bacteria and purple non-sulphur bacteria,
906 and Grossart et al. (2009) have isolated a blue pigment Glaukothalin from two
907 strains of marine *Protobacteria*. No doubt algorithm development for such pig-
908 mented bacteria are hampered by low magnitude of the signal, the difficulty with
909 differentiating them from some phytoplankton groups, and moreover because
910 their habitats are not typically targeted through remote sensing. For example,
911 purple sulphur bacteria require anoxic, but illuminated locations where hydrogen
912 sulphide accumulates.

913 Potential exists for exploitation of the backscattering signal from bacteria.
914 Theoretical work based on homogeneous sphere models has indicated bacteria can
915 contribute significantly to particle backscattering in the open ocean (Ulloa et al.,
916 1994; Stramski et al., 2004), implying a route to direct detection. Bellacicco et al.
917 (2018) have estimated the backscattering coefficient for non-algal particles (inclu-
918 sive of heterotrophic bacteria, detritus and viruses) using satellite ocean colour
919 observations (see also Bellacicco et al., 2019, for application of a similar approach
920 to BGC-Argo float data), and observed large regional variations. However, the
921 contribution of bacteria to backscattering, predicted theoretically using homoge-
922 neous sphere models, may underestimate the contribution by larger particles as
923 indicated by coated sphere modeling (Meyer, 1979; Quirantes and Bernard, 2004;

924 Dall’Olmo et al., 2009; Organelli et al., 2018). Lack of comprehensive knowledge
925 of the particulate assemblage characteristics and size distribution for sub-micron
926 particles is a significant impediment to identifying the sources of backscattering in
927 the ocean (Stramski et al., 2004). To date, and with the exception of the night-time
928 detection of bioluminescent bacteria such as *Vibrio harveyi* (Lapota et al., 1988)
929 using satellite observations (Miller et al., 2005), there have not been attempts (to
930 our knowledge) to directly estimate heterotrophic bacteria from space.

931 Indirect methods have been suggested and Grimes et al. (2014) provide an
932 overview of some of these methods. Indirect methods typically focus on moni-
933 toring cyanobacteria (considered in this review under phytoplankton carbon) and
934 vibrios, the latter tied with health and water quality, for instance, associated with
935 outbreaks of cholera. Approaches have been proposed to map *Vibrio cholerae*
936 using satellite visible and thermal radiometry (chlorophyll-a and SST), altime-
937 try (sea surface height), and precipitation (e.g. Lobitz et al., 2000; Ford et al.,
938 2009; de Magny et al., 2011). For a recent review on the topic of *Vibrio cholerae*
939 detection using satellite data, the reader is referred to Racault et al. (2019) and
940 Sathyendranath et al. (2020a).

941 Driving advanced statistical tools with multiple satellite ocean products could
942 offer a route to mapping heterotrophic bacteria at global scale. For example,
943 in a regional study, Larsen et al. (2015) extrapolated marine surface microbial
944 community structure and metabolic potential observations using remotely-sensed
945 environmental data (visible and thermal radiometry), to create a system-scale
946 model of the marine microbial metabolism in the Western English Channel. They
947 found their model predicted relative abundance of the microbes with reasonable
948 accuracy.

949 Another indirect route to gather information on bacterial communities relies
950 on the large-scale structure in ecological provinces of the ocean (Longhurst,
951 2007) that can be detected from space. Gomez-Pereira et al. (2010) showed that
952 the composition of flavobacterial communities varied with ecological provinces
953 detected from space.

954 4.1.4. PIC from space

955 Detection of PIC using satellite ocean-colour data primarily exploits the
956 impact of calcium carbonate (CaCO_3) from coccolithophores (a group of phyto-
957 plankton in the nano-size range, typically around $5\ \mu\text{m}$ in diameter) on the visible
958 light field. Coccoliths are individual plates of CaCO_3 formed by coccolithophores
959 that aggregate to form a coccosphere surrounding the cell. Because coccoliths
960 are composed of inorganic CaCO_3 which has higher real index of refraction than
961 organic cellular material, they are characterized by strong backscattering. In large
962 densities, the coccoliths turn the colour of the water a pale turquoise, visible to
963 the naked eye (Birkenes and Braarud, 1952; Berge, 1962).

964 The first observations of the impact of coccolithophore blooms on satellite
965 ocean-colour imagery were made using Landsat MSS4 images (Le Fèvre et al.,
966 1983) and using Coastal Zone Colour Scanner (CZCS) images (Holligan et al.,
967 1983). In the seminal paper by Holligan et al. (1983), patches of strong re-
968 flectance in CZCS imagery thought to be caused by coccolithophore blooms were
969 confirmed with ship-based surveys. Similar combined satellite and ship-based
970 studies followed using satellite images from the Advanced Very High Resolu-
971 tion Radiometer (AVHRR) (GREMPA, 1988). The first global distribution of
972 coccolithophore blooms using CZCS satellite data were produced by Brown and
973 Yoder (1994), revealing coverage of around $1.4 \times 10^6\ \text{km}^2$, with 71 % of this area
974 located in subpolar waters. They identified blooms and classified these features
975 using normalised water leaving radiance at 440 nm and 550 nm and using ratios
976 between 440/520 nm, 440/550 nm and 520/550 nm. This work identified diffi-
977 culties associated with misclassification of bright waters affected by sediment
978 concentrations, and under-detection of CaCO_3 compared with *in-situ* measure-
979 ments. Follow-on algorithms were developed for the SeaWiFS sensor, either
980 adapting the Brown and Yoder (1994) technique (Iglesias-Rodríguez et al., 2002)
981 or making use of near infrared bands (Gordon et al., 2001). To bridge the gap
982 between the CZCS and more current ocean colour satellites, and building on work
983 of Groom and Holligan (1987), Smyth et al. (2004) used data from AVHRR and a
984 semi-analytical algorithm to detect coccolithophores, again based on their high

985 reflectances. Recently, Loveday and Smyth (2018) have produced a consistently
986 calibrated 40-year-long data set of coccolithophore bloom occurrence derived
987 from AVHRR.

988 Balch et al. (2005) developed a technique for use with MODIS sensors, us-
989 ing normalised water leaving radiance at 440 and 550 nm and a look-up table
990 generated to calculate coccolithophore concentrations. The look-up table was
991 based on the inversion of a semi-analytical model to separate and derive pigment
992 concentration and coccolithophore concentration. The underlying relationships in
993 this semi-analytical model capture the effects of coccolithophores on backscatter-
994 ing. This study highlighted the error in estimation of chlorophyll-a concentration
995 when signal in the 440 and 550 nm bands was attributed to pigment concentration
996 rather than backscattering by coccolithophores. Challenges in estimating of PIC
997 using the Balch et al. (2005) approach include the use of the absolute magnitude
998 of water-leaving radiance, which is subject to errors from atmospheric correction.
999 Similarly, elevated water-leaving radiance, a result of elevated backscattering,
1000 may be due to the presence of other constituents which increase scattering, such
1001 as diatom silica, or sediments. Because of the effect of sediments, these methods
1002 are difficult to employ in optically-complex (case 2) waters, where there are sub-
1003 stantial non-algal scattering components, or in cases of blooms of high biomass
1004 or of species with complex intracellular structure, where it may be inappropriate
1005 to characterise phytoplankton scattering with the formulations of Balch et al.
1006 (2005) (Chami et al., 2006; Robertson Lain et al., 2014). Further techniques have
1007 been developed to reduce these false positive classifications in coastal zones, for
1008 example, by subtraction of stationary (background) structures to allow improved
1009 spectral detection of the coccolithophores (Shutler et al., 2010). Recent work
1010 has also added coccolithophore bloom spectra to optical water type classifiers
1011 (Moore et al., 2012). Hyperspectral sensors have also been used to detect coccol-
1012 ithophores, for example, based on differential absorption spectroscopy, applied to
1013 SCIAMACHY data (Sadeghi et al., 2012). For examples of each approach and a
1014 detailed history the author is referred to IOCCG (2014).

1015 Many of these satellite-based methods for detecting coccolithophores from

1016 space have had the object of mapping the aerial extent of the blooms. Some
1017 others (e.g. Sadeghi et al., 2012) focus on estimating the chlorophyll associated
1018 with coccolithophores, which is not necessarily indicative of the coccoliths (PIC)
1019 produced by these organisms. Only a few (e.g. Gordon et al., 2001; Balch et al.,
1020 2005; Mitchell et al., 2017; Kondrik et al., 2019) have attempted to take it a step
1021 further, towards estimation of PIC. This typically involves quantifying the number
1022 of coccoliths in surface waters, and making assumptions on per-coccolith PIC
1023 concentrations. Recent advancements in satellite-based PIC methods include: the
1024 development of band-difference PIC approaches (Mitchell et al., 2017), which
1025 have been seen to perform with better accuracy than standard methods (Balch
1026 et al., 2005) and found to be more resilient to errors in atmospheric-correction;
1027 methods that relate surface PIC to water-column integrated PIC (down to 100 m
1028 or to the euphotic depth, Balch et al., 2018), allowing quantification of PIC below
1029 the depths seen by the satellite (Hopkins et al., 2019); and quantification of
1030 the influence of coccolithophores on surface CO₂ concentrations and gas fluxes
1031 (Shutler et al., 2013; Kondrik et al., 2019).

1032 *4.2. Fluxes of carbon from space*

1033 *4.2.1. Primary Production from space*

1034 Following the development of the first satellite ocean-colour algorithms for
1035 deriving phytoplankton biomass, during the CZCS era, it became desirable to
1036 convert these fields of biomass into fields of primary production (Platt and Herman,
1037 1983; Robinson, 1983; Perry, 1986; Sathyendranath et al., 2019b). In the 1980's,
1038 there were some regional and basin-scale attempts to convert these fields directly
1039 (Smith et al., 1982; Brown et al., 1985; Eppley et al., 1985; Lohrenz et al., 1988).
1040 However, accurate conversion requires knowledge of, in addition to phytoplankton
1041 biomass (as indexed through satellite estimates of chlorophyll-a concentration),
1042 information on light availability (available through satellite Photosynthetically
1043 Available Radiation (PAR) products), and the response of the phytoplankton to
1044 the available light, through parameters that describe the photosynthesis-irradiance
1045 curve (assimilation number (maximum photosynthetic rate) and initial slope of

1046 the curve; Platt et al., 1980). Some of these components can vary over the day,
1047 with depth, species composition, physiological state, and with the wavelength
1048 and angular distribution of light (Platt and Herman, 1983; Platt et al., 1990;
1049 Sathyendranath and Platt, 1989). Platt (1986) and Platt et al. (1988) described the
1050 application of this approach in the context of satellite remote-sensing, variants of
1051 which have had subsequent success in quantifying primary production at local
1052 and regional scales (e.g. Platt and Sathyendranath, 1988, 1991; Sathyendranath
1053 et al., 1989, 1991, 1995; Kuring et al., 1990; Morel, 1991; Morel and André,
1054 1991). Platt and Sathyendranath (1993) provide a detailed user guide on the
1055 types of models used in computing marine primary production from remotely-
1056 sensed data on ocean colour, which illustrates, supported by more recent work
1057 (e.g. Sathyendranath and Platt, 2007; Sathyendranath et al., 2020b), that model
1058 variants conform to the same basic formulation, with the same set of parameters.
1059 Targeting the model parameters appears to be the key to accurate estimates of
1060 primary production from space (Platt et al., 1992).

1061 The first global estimates of satellite primary production using CZCS were
1062 provided by Longhurst et al. (1995), who estimated global net oceanic primary
1063 production to be 45 to 50 Gt C y⁻¹. Other global estimates using CZCS quickly
1064 followed (e.g. Antoine et al., 1996; Behrenfeld and Falkowski, 1997), with most
1065 techniques converging at around 50 Gt C y⁻¹ (see also Carr et al., 2006; Sathyen-
1066 dranath et al., 2019b), equivalent to primary production in the terrestrial biosphere
1067 (Field et al., 1998). Following the CZCS era, a variety of primary production
1068 models (including available light, absorbed light, inherent optical property based,
1069 and carbon based) have been applied to subsequent ocean-colour missions (Sea-
1070 WiFS, MODIS and MERIS) for mapping primary production (e.g. Bosc et al.,
1071 2004; Behrenfeld et al., 2005; Smyth et al., 2005; Platt et al., 2008; Westberry
1072 et al., 2008; Tilstone et al., 2015; Arrigo and van Dijken, 2015), demonstrating
1073 regulation of global primary production by climate variability (Behrenfeld et al.,
1074 2001, 2006; Racault et al., 2017; Taboada et al., 2019; Kulk et al., 2020). Kulk
1075 et al. (2020) provide the most recent global primary production estimates, using a
1076 20-year ocean-colour data record (Sathyendranath et al., 2019a) together with a

1077 global database on photosynthesis-irradiance curve parameters (Bouman et al.,
1078 2018) and vertical biomass parameters (Platt et al., 1988; Longhurst et al., 1995)
1079 partitioned into ecological provinces and varied seasonally, and quantified global
1080 primary production to be between 38.8 to 42.1 Gt C y⁻¹ over the period of 1998 to
1081 2018.

1082 Considerable resources have been invested by space agencies in round-robin
1083 comparisons and validation of products for estimating ocean primary production,
1084 for example, the NASA Primary Production Algorithm Round Robin series
1085 (PPARR; Campbell et al., 2002; Carr et al., 2006; Friedrichs et al., 2009; Saba
1086 et al., 2010, 2011; Lee et al., 2015a). These comparisons have emphasised that
1087 model performance varies with complexity and trophic state, and with region
1088 and season. The challenges in deriving trends in satellite primary production, the
1089 importance of minimising the uncertainties in model inputs, model parameters,
1090 and in the *in-situ* measurements used for validation, were also highlighted in the
1091 PPAAR series. In general, satellite daily, depth-integrated primary production
1092 models have an uncertainty (root mean square deviation) of around 0.2 to 0.5
1093 in log₁₀ space, when matched to and compared with *in-situ* data (e.g. Campbell
1094 et al., 2002; Friedrichs et al., 2009; Tilstone et al., 2009; Brewin et al., 2017d).
1095 Based on a formal error analysis, Platt et al. (1995) reported that uncertainties
1096 (standard error) in primary production were about 50 % on primary-production
1097 estimates at a single pixel.

1098 In addition to estimates of total primary production, there have been efforts
1099 to map primary production in different phytoplankton size classes from satellite
1100 data (Mouw and Yoder, 2005; Silió-Calzada et al., 2008; Uitz et al., 2009, 2010,
1101 2012; Hirata et al., 2009; Brewin et al., 2017d; Curran et al., 2018). This is useful
1102 considering cell size influences many key processes in biogeochemistry and marine
1103 ecology (Chisholm, 1992; Marañón, 2009, 2015) and many marine biogeochem-
1104 istry models use a size-based partitioning for phytoplankton (e.g. Aumont et al.,
1105 2003; Ward et al., 2012; Butenschön et al., 2016). Other satellite algorithms have
1106 been developed for computing new production (e.g. Sathyendranath et al., 1991;
1107 Goes et al., 2000; Coles et al., 2004; Tilstone et al., 2015), export production

1108 (see Section 4.2.2), and to account for the the inhibition of photosynthesis by
1109 ultraviolet radiation (Cullen et al., 2012).

1110 One of the principal difficulties in modelling primary production from space,
1111 considering that many models conform to the same formulation (Sathyendranath
1112 and Platt, 2007; Sathyendranath et al., 2020b), is in the assignment of the photo-
1113 synthetic parameters on a per-pixel basis. Various efforts have been made in this
1114 direction, including: direct use of *in-situ* data, by averaging data seasonally and re-
1115 gionally, using biogeographical provinces (Longhurst et al., 1995; Sathyendranath
1116 et al., 1995; Kulk et al., 2020), or interrogating the data using statistical methods
1117 such as nearest-neighbour techniques (Platt et al., 2008); and indirect methods that
1118 tie parameters to one (or more) environmental variable retrievable from satellite
1119 data, such as SST, light, chlorophyll and phytoplankton size structure (Eppley,
1120 1972; Behrenfeld and Falkowski, 1997; Bouman et al., 2005; Claustre et al., 2005;
1121 Uitz et al., 2008; Sathyendranath et al., 2009; Saux Picart et al., 2014; Brewin
1122 et al., 2017d; Tilstone et al., 2017). Future advances in this direction rely on
1123 the continued production and development of *in-situ* datasets (Richardson et al.,
1124 2016; Bouman et al., 2018; Kulk et al., 2020), and improvements in satellite
1125 PAR products (Frouin et al., 2018). The use of ecosystem models run in data
1126 assimilation mode is another avenue to infer model parameters (Roy et al., 2012;
1127 DeVries and Weber, 2017). Improving the vertical parametrisations of satellite
1128 models through integration of data from autonomous platforms (e.g. BGC-Argo
1129 floats) is another exciting avenue of work. For example, Richardson and Bendtsen
1130 (2019) have demonstrated that the depth of the nutricline, that can be measured by
1131 attaching nutrient sensors BGC-Argo floats, is useful for understanding vertical
1132 variations in primary production. For further discussions on future strategies to
1133 improving satellite-based ocean primary production models, the reader is referred
1134 to Lee et al. (2015b).

1135 4.2.2. *Export Production from space*

1136 Estimating Export Production (EP) from satellite-derived properties requires
1137 that we establish how much of primary production is exported out of the surface
1138 layer. Most of the carbon generated by primary production is consumed by het-

1139 erotrophs. The remaining carbon (net community production, NCP, defined as
1140 primary production minus community respiration) is, if aggregated over suffi-
1141 ciently large temporal and spatial scales, equivalent to EP, which is the amount of
1142 organic matter produced in the ocean by primary production that is not recycled
1143 (remineralised) before it sinks into the aphotic zone and which serves as the upper
1144 bound for carbon sequestration (Platt et al., 1989; Siegel et al., 2016). Currently,
1145 NCP and EP are not derived from physiological relationships, as is the case for
1146 primary production, since no such relationships are available for community respi-
1147 ration. Also, NCP and EP depend explicitly on the temporal and spatial domains
1148 over which they are defined. For example, *in-situ* measurements of mixed layer
1149 NCP cannot be converted directly to EP since the newly-produced biomass might
1150 be consumed before it can be exported to the aphotic zone. It is therefore not yet
1151 possible to define mechanistic relationships between EP and properties derived
1152 from remote sensing.

1153 Instead, a common approach used by the scientific community to estimate
1154 EP from satellite derived products, is to rely on empirical correlations of *in-situ*
1155 measurements of vertical carbon fluxes, with properties that can be derived from
1156 satellite. These approaches can be traced back to early work where proxies of
1157 export (e.g. the ratio of new production to total production, defined as the *f*-
1158 ratio, or particle fluxes from sediment traps) were empirically related to primary
1159 production, chlorophyll-a concentration and depth (Eppley and Peterson, 1979;
1160 Suess, 1980; Betzer et al., 1984; Pace et al., 1987; Wassman, 1990), or to nutrient
1161 concentrations (Platt and Harrison, 1985; Harrison et al., 1987). One of the first
1162 techniques, that directly used satellite data, was proposed by Laws et al. (2000).
1163 In this approach the ratio of export production to primary production (denoted as
1164 the *ef*-ratio) is approximated based on empirical relationships with SST. Once the
1165 *ef*-ratio is computed, it can be used with satellite primary production to estimate
1166 EP. The study estimated global EP at between 11.1 and 20.9 Pg C yr⁻¹. Their
1167 empirical model was tuned using a food-web ecosystem model, rather than *in-situ*
1168 data. However, Laws et al. (2011) presented updates to the approach, where
1169 the *ef*-ratio was approximated using an empirical equation driven by SST and

1170 primary production, and tuned to *in-situ* data. Application of the model to satellite
1171 data suggested global EP of around 9-13 Gt C y⁻¹. Other satellite-based empirical
1172 algorithms have been presented, for example, Dunne et al. (2005) modelled EP as
1173 an empirical function of SST, chlorophyll-a and primary production, and Henson
1174 et al. (2011) as an empirical function of SST and primary production. Using these
1175 empirical approaches, satellite-based global estimates of EP range between 4 and
1176 12 Pg C yr⁻¹. Though proven useful, these empirical approaches are, by their very
1177 nature, limited in their ability to predict EP (Stukel et al., 2015; Palevsky et al.,
1178 2016).

1179 Simple food-web based models, driven by satellite observations, that are more
1180 mechanistic in nature than the aforementioned empirical approaches, have also
1181 been proposed as a means for estimating EP from space. The link between size
1182 and export is relatively well established, with large cells thought to contribute
1183 more to EP than smaller phytoplankton. For example, Tremblay et al. (1997)
1184 demonstrated the fraction of large phytoplankton (>5µm) to total biomass to be
1185 linearly correlated with the *f*-ratio. These approaches have gained momentum
1186 owing partly to development of satellite algorithms for deriving phytoplankton
1187 size structure (IOCCG, 2014). Siegel et al. (2014) used a food-web model, driven
1188 by satellite estimates of primary production (Westberry et al., 2008), euphotic
1189 depth (Morel et al., 2007), and the slope of the particle size spectrum (Kostadinov
1190 et al., 2009), to predict the production of sinking zooplankton feces and algal
1191 aggregates, and consequently EP. Their model estimates global EP at 6 Pg C yr⁻¹.
1192 In an analysis of this approach, Stukel et al. (2015) found it to perform as well
1193 or better than purely empirical approaches, and suggest food-web relationships
1194 and grazing dynamics are crucial to improving the accuracy of export predictions
1195 made from satellite-derived products. Li et al. (2018) also found the Siegel et al.
1196 (2014) model to work reasonably well in the northern South China Sea. Despite
1197 this progress, considerable unexplained variance in export remains and needs to be
1198 explored to improve satellite EP estimates (Stukel et al., 2015). Moving towards
1199 more mechanistic relationships (e.g. DeVries et al., 2014) between satellite-
1200 derived products and EP is a major goal in the NASA EXPORTS programme

1201 (Siegel et al., 2016).

1202 As more *in-situ* data become available, improvements in both empirical and
1203 food-web based satellite EP models are expected. One solution is to tune the
1204 models on a more regional basis (Sathyendranath et al., 1991; Li et al., 2018).
1205 This could be done through the use of biogeochemical provinces, for example,
1206 Longhurst regions (e.g. Reygondeau et al., 2013), with sufficient data richness
1207 to perform the tuning. Other avenues of investigation include: studying the
1208 phytoplankton seasonal cycles (phenology) from space (Platt et al., 2009; Racault
1209 et al., 2012), critical in food web-dynamics (Platt et al., 2003), over long-time
1210 periods, which may offer insight into inter-annual variability in EP (Racault,
1211 2009); and consideration of the time-scales of variability, since ecosystems that
1212 vary on shorter timescales and exhibit more episodic production events are often
1213 expected to export a greater proportion of their primary production (Platt et al.,
1214 1989; Buesseler, 1998; Lutz et al., 2007; Henson et al., 2012; Brown et al., 2014).

1215 Of the three export pathways, the majority of studies estimating EP from
1216 satellite data focus on gravitational sinking, only implicitly including, or in
1217 some cases neglecting, the physical pathway and the migration pathway. Recent
1218 evidence that these other pathways contribute significantly to the OBCP (Boyd
1219 et al., 2019), has led to efforts to incorporate them explicitly into satellite estimates,
1220 for example, by including the contribution of zooplankton vertical migration
1221 (Archibald et al., 2019; Behrenfeld et al., 2019a) and the contribution to carbon
1222 export from fluctuations in the mixed-layer (Stramska, 2010; Dall’Olmo et al.,
1223 2016). As we learn more about these pathways, perhaps exploring and exploiting
1224 the use of ocean physical datasets, we can seek to improve their representation
1225 and consequently the space-based estimates of EP.

1226 4.2.3. *Loss rates from space*

1227 Individually, the loss rates (grazing, respiration, sinking, excretion, mortality)
1228 cannot be retrieved directly from remote-sensing. However, methods have been
1229 proposed to derive the total loss rate (sum of the losses) using remote sensing
1230 methods. These techniques typically involve monitoring changes in phytoplankton
1231 properties at a given location, over time. Zhai et al. (2008) implemented a method,

1232 proposed by Platt and Sathyendranath (2008), that involves taking a series of
1233 images of chlorophyll concentration that allow the calculation, by difference at
1234 successive time steps, of the rate of chlorophyll increase (difference between
1235 growth and total loss). The difference in the rate of chlorophyll increase and
1236 the photosynthetic rate (also estimated from satellite data), gives the total loss
1237 rate. The recovered loss rates showed clear seasonal cycles and abrupt shifts
1238 during the spring bloom in the North West Atlantic. Using a similar approach,
1239 Behrenfeld (2010) computed the rate of carbon increase (referred to as the net
1240 specific growth rate, the specific growth rate minus loss rate) from successive
1241 time steps in phytoplankton carbon concentrations retrieved from satellite data.
1242 The sign in net specific growth rate was subsequently used to monitor the balance
1243 between specific growth and loss rates, and used for interpreting phytoplankton
1244 blooms (Behrenfeld, 2014).

1245 To make best use of this sequential time-series approach, one needs to correct
1246 for the effect of physical processes (advection and mixing; Zhai et al., 2008).
1247 This requires additional information on velocity components, and horizontal and
1248 vertical eddy diffusivity. The magnitude and importance of this correction is
1249 likely to vary regionally. One solution to addressing this is through Lagrangian-
1250 based analysis of satellite-data, to track the water mass, which can be achieved
1251 through combining satellite biological observations (ocean colour) with ocean
1252 circulation velocity fields derived from an operational model (Jönsson et al.,
1253 2009) or derived through physical satellite ocean observations (Lehahn et al.,
1254 2018; Nencioli et al., 2018). Other exciting avenues for determining information
1255 on loss rates from ocean colour include harnessing recent, and soon to be launched,
1256 geostationary ocean-colour satellites (see Section 7) together with diel optical
1257 techniques (Dall’Olmo et al., 2011; Kheireddine and Antoine, 2014).

1258 4.2.4. Air-sea CO₂ transfer-related variables from space

1259 Regional, indirect approaches have been proposed for estimating the exchange
1260 of CO₂ between the the ocean and atmosphere from satellite data (see Section 4.1.1
1261 and Land et al., 2015). As discussed in Section 4.1.1, these approaches involve
1262 forcing empirical equations or statistical models, typically tuned with *in-situ*

1263 observations, with satellite retrievals of SST, SSS and chlorophyll-a, individually
1264 or in combination (Ono et al., 2004; Sarma et al., 2006; Gledhill et al., 2008;
1265 Friedrich and Oschlies, 2009). For further reviews on the topic the reader is
1266 referred to Land et al. (2015), Land et al. (2019) and Shutler et al. (2019).

1267 4.3. *Uncertainties in space-based carbon estimates*

1268 4.3.1. *Uncertainties in individual satellite products*

1269 To enable responsible and informed uptake of satellite carbon products by the
1270 user community, it is essential that uncertainties in individual carbon products be
1271 quantified, ideally on a per-pixel basis (Moore et al., 2009; Jackson et al., 2017a;
1272 Sathyendranath et al., 2017, 2019a). This helps algorithm providers to establish
1273 whether the products meet user requirements, and to identify areas where further
1274 development is needed. Two common approaches to quantify uncertainties are
1275 through validation of satellite products with independent *in-situ* data or through
1276 error propagation methods.

1277 Determining uncertainties through validation of satellite products typically
1278 requires matching the satellite data in time and space with the *in-situ* observa-
1279 tions, having characterised the uncertainties in the *in-situ* observations. Such
1280 comparisons will never be perfect, owing to the differences in the spatial scales
1281 between satellite and *in-situ* observations. Once a match-up dataset is produced,
1282 the two data streams can be compared quantitatively, using a common set of
1283 statistical tests (Brewin et al., 2015c, 2016; Seegers et al., 2018), for example,
1284 the root mean square deviation. With a sufficiently large dataset, the match-ups
1285 can be partitioned into trophic categories, regions, or by using other discretisation
1286 methods. One approach that has been gaining momentum is the use of optical-
1287 class-based, fuzzy-logic methods (Moore et al., 2009; Jackson et al., 2017a). In
1288 this method, metrics are calculated for all the match-up data in each optical class.
1289 By deriving the fuzzy membership probabilities of a given pixel's spectrum to the
1290 set of optical classes, per-pixel metrics can be computed by weighing the metric in
1291 each class by the memberships of the pixel. This method of computing per-pixel
1292 uncertainties has been used for mapping uncertainties in satellite-based estimates

1293 of POC, phytoplankton carbon and phytoplankton chlorophyll in different size
1294 classes or in different functional types (Brewin et al., 2017a; Evers-King et al.,
1295 2017; Martínez-Vicente et al., 2017). Further refinements to this approach could
1296 be made by incorporating functions that relate uncertainties to the known factors
1297 that might influence the quality of a satellite product (e.g. Land et al., 2018).

1298 Determining uncertainties through error propagation techniques involves quan-
1299 tifying uncertainty in all components of the measurement equation, starting with
1300 instrument calibration, and propagating the errors through to the derived carbon
1301 products, using either the principles of formal analytical error propagation, or
1302 using statistical methods like Monte-Carlo techniques. Standardised frameworks
1303 exist (e.g. BIPM, 2008) and should ideally be used consistently across products.
1304 Error propagation techniques have been used previously in satellite primary pro-
1305 duction models (e.g. Sathyendranath et al., 1991; Platt et al., 1995; Brewin et al.,
1306 2017d) and phytoplankton carbon models (e.g. Kostadinov et al., 2009, 2016).
1307 For a comprehensive review on uncertainties in satellite ocean-colour products,
1308 the reader is referred to the recent IOCCG report on the topic (IOCCG, 2019).

1309 *4.3.2. Uncertainties in multiple satellite products*

1310 In the context of quantifying the ocean carbon budget, in which all the pools
1311 and fluxes have to fit in a mutually consistent way, it is important to not only
1312 consider the uncertainties in individual products, but to analyse multiple products
1313 to identify discrepancies and associated uncertainties with a view to close the
1314 ocean carbon budget in a satisfactory manner. This requires that we analyse each
1315 of the products in relation to all the other products, and see whether they hold
1316 together in a coherent fashion. Similarity, bio-optical closure among input data
1317 products is equally important. In the case of carbon products, we can illustrate
1318 this point with a couple of examples taken from the current status of the field.
1319 The bio-available, labile DOC pool is currently estimated to be about 0.2 Pg with
1320 annual production rate of 15-25 Pg C y⁻¹ (Hansell, 2013). This yields a turnover
1321 rate of 100 times per year, or roughly once in every 3-4 days. The source of this
1322 labile pool is phytoplankton (Hansell and Carlson, 2013). According to Falkowski
1323 et al. (1998), the size of the phytoplankton pool is 1 Pg. With global primary

1324 production estimated to be about 50 Pg C y^{-1} , we get a turnover rate of 50 per
1325 year for phytoplankton. We immediately note a discrepancy of a factor of two
1326 between the two turnover rates, which merits further investigation. How can
1327 phytoplankton, turning over once every week, generate a labile DOC pool that
1328 is turning over twice as fast? Clearly, this is an indication of uncertainty in the
1329 overall budget, that can be reduced only if the two turnover rates can be brought
1330 closer to each other, or if we find another explanation for the discrepancy (e.g.
1331 microbial activity at the interface between labile and semi-labile DOC enhancing
1332 the DOC rates). This example demonstrates that, to reduce uncertainties in the
1333 overall carbon budget, future efforts are needed to compare individual products
1334 against others, to check for consistency, and to reduce discrepancies.

1335 **5. Integrating satellite observations with models**

1336 As highlighted in Table 3, many components of the OBCP are not directly
1337 observable from space. Furthermore, the components that are observable are
1338 limited to conditions (e.g. a cloud-free atmosphere) that allow for satellite remote-
1339 sensing. One avenue to infer the hidden pools and fluxes, and to fill gaps in data, is
1340 through assimilation of satellite-based observations into ecosystem models. There
1341 are increasing efforts to integrate radiative transfer models into ecosystem models,
1342 such that the ecosystem models themselves become capable of simulating ocean
1343 colour data (e.g. Jones et al., 2016; Gregg et al., 2017; Dutkiewicz et al., 2018,
1344 2019). Integrating satellite observations with models can be used to improve
1345 model parameterisation, improve hindcasts and forecasts of biogeochemical pools
1346 and fluxes, and identify processes poorly represented by models, that can be
1347 subsequently improved in future model design (Fennel et al., 2019).

1348 Using satellite data assimilation to improve model parameters is a powerful
1349 method of inferring rates not accessible from space. For example, Roy et al.
1350 (2012) assimilated satellite-based chlorophyll data into a nutrient-phytoplankton-
1351 zooplankton (NPZ) model to infer specific growth rates and mortality rates of
1352 phytoplankton. DeVries and Weber (2017) developed a global model of the
1353 OBCP that assimilates satellite primary production and particle size data with

1354 oceanographic tracer observations to constrain rates and patterns of organic mat-
1355 ter production, export, and remineralization in the ocean. Their OBCP model
1356 combines an ecosystem model, an ocean circulation model and an organic matter
1357 transport and remineralisation model. Model parameters are adjusted by an itera-
1358 tive process to achieve optimal consistency with observed global-scale data sets
1359 of sinking POC fluxes, DOC concentrations and dissolved O₂ distributions. The
1360 model outputs an export flux of 9 Pg C y⁻¹, and offers insight into the controls and
1361 distributions of various pools and fluxes not seen from space. Major challenges in
1362 model parameter optimisation using data-assimilation techniques are the often
1363 large number of parameters used in models, that some parameters are correlated,
1364 and that errors in some parameters can be compensated by errors in others. Ulti-
1365 mately, the success of these approaches depend somewhat on the complexity of
1366 the model (Friedrichs et al., 2006).

1367 Satellite data assimilation can also be used directly to improve hindcasts and
1368 forecasts of carbon pools and fluxes. The NASA Ocean Biogeochemical Model
1369 (NOBM), a coupled, atmosphere, ecosystem, radiative transfer and circulation
1370 model, has a history of being used for such purposes (Gregg, 2001, 2008). Decadal
1371 trends in phytoplankton biomass, primary production and phytoplankton compo-
1372 sition have been estimated using the NOBM with ocean-colour data assimilation
1373 (Rousseaux and Gregg, 2015; Gregg et al., 2017; Gregg and Rousseaux, 2019).
1374 The model has also been used used to estimate pCO₂ and carbon dioxide fluxes
1375 (Gregg et al., 2014; Ott et al., 2015). The assimilation of satellite chlorophyll
1376 data into various ecosystem models has demonstrated improvements in carbon
1377 cycle variables (e.g. Ford and Barciela, 2017; Pradhan et al., 2019). Ciavatta et al.
1378 (2018) assimilated satellite-based chlorophyll data for four different phytoplank-
1379 ton groups (using the model of Brewin et al., 2017c), into the European Regional
1380 Seas Ecosystem Model (ERSEM) and showed improvements in the ability of
1381 the model to hindcast the air-sea flux of CO₂. Similar results were also found
1382 in a forecast simulation with a (pre)operational model (Skákala et al., 2018). A
1383 prerequisite for successful data assimilation is accurate assignment of uncertain-
1384 ties in the satellite observations and the model simulations. A point to note is

1385 that increased performance in carbon fluxes and pools using data assimilation
1386 might be accompanied by reduced performance in other model compartments
1387 (Ciavatta et al., 2018). For a comprehensive review on synergy between satellite
1388 and ecosystem model data, the reader is referred to the recent IOCCG report on
1389 the topic (IOCCG, 2020).

1390 **6. Bringing satellite observations into the limelight**

1391 As this review demonstrates, recent years have seen great progress in the use
1392 of satellite observations to detect or infer various pools and fluxes of carbon in
1393 the ocean as well as air-sea fluxes of carbon. Much of the information necessary
1394 to establish OBCP is already accessible to remote sensing, and the potential
1395 exists for improving the products and for generating additional products (Table
1396 3). Satellite observations meet the requirements for global coverage and high
1397 spatial and temporal resolution. With ocean-colour observations, the creation
1398 of long-term, climate-quality products has been a challenge, because of the
1399 finite life span of sensors in space, in combination with the differences in the
1400 characteristics of each sensor launched into space (e.g. wavebands), making
1401 it difficult to eliminate inter-sensor biases. But that situation is changing now,
1402 with bias-corrected, multi-sensor, error-characterised products being generated
1403 (Sathyendranath et al., 2019a), and the length of the time series now exceeding
1404 two decades. The prospects for further improvements in the quality of the products
1405 and in the length of the uninterrupted time series is excellent, with initiatives
1406 such as the ESA's Sentinel and NASA's PACE missions (Donlon et al., 2012;
1407 Remer et al., 2019). The access to many of the key components of the OBCP
1408 implies that we are now in a position to examine not only the influence of the
1409 ocean biota on the air-sea flux of carbon dioxide, but also to evaluate any potential
1410 impact of climate change on the integrity of marine ecosystems. When combined
1411 with *in-situ* observing systems (Tables 1 and 2), we are in a position to close the
1412 biological carbon budget of the ocean with unprecedented rigour, and to develop
1413 a predictive, mechanistic understanding of the processes involved, rather than
1414 solely rely on empirical relationships.

1415 Notwithstanding the benefits of integrating satellite remote sensing with
1416 ecosystem and climate models, as well as with autonomous observations and
1417 with other field datasets, as discussed above, producing a purely satellite-based
1418 carbon budget for the oceans, for the pools and fluxes that can be estimated, could
1419 be a useful way of independently verifying ecosystem and climate models. The
1420 international Global Carbon project was established to produce a common and
1421 mutually agreed knowledge base to support policy debate and action to slow
1422 down and ultimately stop the increase of greenhouse gases in the atmosphere
1423 (<https://www.globalcarbonproject.org/about/index.htm>). Every year, a picture of
1424 the global carbon cycle is produced, including both its biophysical and human
1425 dimensions, together with the interactions and feedbacks between them, based on
1426 a combination of models and observations. The latest report (Friedlingstein et al.,
1427 2019) suggests the oceans currently absorb 2.5 Gt C y^{-1} ($\pm 0.6 \text{ Gt C y}^{-1}$), close to
1428 the figure for the terrestrial biosphere ($3.2 \pm 0.6 \text{ Gt C y}^{-1}$), and accounting for the
1429 absorption of around 24 % of the fossil CO₂ emissions. The results also suggest
1430 in recent periods (2009-2018), the ocean CO₂ sink appears to have intensified.
1431 This work emphasises the importance of the oceans in the global carbon cycle.
1432 Yet, large uncertainties still remain in how the oceans will respond to increased
1433 CO₂ emissions in the future. The conclusions drawn from the latest Global
1434 Carbon project are from models which, at best, include satellite-observations
1435 implicitly in their simulations (e.g. through validation). One conclusion from
1436 the Friedlingstein et al. (2019) work is that the ocean models underestimate CO₂
1437 variability outside the tropics. DeVries et al. (2019) have also noted that ocean
1438 biogeochemistry models tend to underestimate inter-annual variability in ocean
1439 uptake of atmospheric carbon, compared with *in-situ* observation-based methods.
1440 Similar comparisons with satellite-based observations are essential, to improve
1441 our understanding of the current state of the OBCP as well as model-based
1442 forecasts. Here, we argue that it is time for our community to bring satellite-based
1443 ocean carbon observations into the limelight. Our understanding of the ocean
1444 carbon cycle can improve with new opportunities in space, and it is our duty to use
1445 satellite observations to help strive towards a characterisation and understanding

1446 of the ocean carbon cycle, and its role in the Earth carbon cycle, that is better
1447 than anything that has been achieved before. This is the objective of the ESA
1448 Biological Pump and Carbon Exchange (BICEP) project.

1449 **7. New opportunities in space and future recommendations**

1450 In this section, we highlight a series of opportunities and make recommenda-
1451 tions that can facilitate the advancement of satellite-based ocean carbon observa-
1452 tions.

- 1453 • **Satellite data records.** Over recent years, there has been large interna-
1454 tional investment in the production of satellite data records (Cazenave
1455 et al., 2019; Groom et al., 2019; O’Carroll et al., 2019; Vinogradova et al.,
1456 2019). These efforts typically involve stitching together satellite data from
1457 different platforms and sensors, correcting for differences in wavelengths
1458 and for systematic biases, and producing a seamless data record, suitable
1459 for monitoring long-term (climate) change. The European Space Agency
1460 (ESA) Climate Change Initiative (CCI) is one such example (Hollmann
1461 et al., 2013), where ocean data records have been produced for many of
1462 the input datasets needed for producing carbon-based products, such as
1463 ocean colour (OC-CCI; Sathyendranath et al., 2019a), SST (SST-CCI; Mer-
1464 chant et al., 2014, 2019), and sea-level (SST-CCI; Legeais et al., 2018).
1465 NASA and NOAA have also developed similar initiatives (e.g. NASA’s
1466 MEaSUREs programme and NOAA’s Climate Data Record Programme;
1467 Maritorena et al., 2010; Bates et al., 2016). Many of these programmes are
1468 developed with consideration of commitments made by space agencies and
1469 intergovernmental organisations, for continued support of operational ocean
1470 satellites in the coming decades (e.g. Sentinel Copernicus programme).
1471 These records provide the ideal platform for exploring long-term change in
1472 carbon pools and fluxes (e.g. Mélin, 2016; Mélin et al., 2017; Kulk et al.,
1473 2020).

- 1474 • **Increased spectral resolution of ocean colour.** At present, the majority
1475 of operational ocean-colour satellite sensors are multispectral by nature,
1476 with select wavebands (typically 6-10) spread out over the visible spectral
1477 range, with each band having a spectral response function (band-width) in
1478 the order of 10-20 nm. By increasing the spectral resolution of the sensors,
1479 it is feasible to acquire additional information on the properties of phyto-
1480 plankton and other water constituents, such as phytoplankton composition,
1481 by monitoring spectral features (e.g. from accessory pigment absorption)
1482 associated with different phytoplankton types (IOCCG, 2014; Cael et al.,
1483 2020). Direct measurements of phytoplankton composition would help
1484 improve OBCP analysis, owing to the differing roles of phytoplankton in
1485 the cycling of carbon (IOCCG, 2014). Additionally, increased spectral
1486 resolution in the UV and short wave infra-red regions (as well as satellite
1487 polarimetry) are expected to improve atmospheric-correction (Frouin et al.,
1488 2019). Planned hyperspectral ocean-colour sensors like NASA's PACE (Re-
1489 mer et al., 2019) and ESA's CHIME (one of the 6 High Priority Candidate
1490 missions for the Copernicus Expansion) will facilitate these developments,
1491 though challenges remain, for example, in treating the signal to noise ratio
1492 for narrower bands, and that the degrees of freedom in hyperspectral data
1493 are likely a lot less than the number of bands (Cael et al., 2020).
- 1494 • **Increased spatial and temporal coverage.** New satellite platforms are
1495 opening the door to improved spatial and temporal coverage. Geostationary
1496 ocean colour sensors like the Korean GOCI satellite, have the capability to
1497 monitor diel cycles in phytoplankton properties, and dramatically enhance
1498 daily coverage of ocean colour (Choi et al., 2012). Under the most recent
1499 NASA Earth Venture Instrument solicitation, a geostationary, hyperspectral,
1500 ocean-colour instrument was selected. The instrument, Geostationary Lit-
1501 toral Imaging and Monitoring Radiometer (GLIMR) gathers data at hourly
1502 frequencies and is expected to launch in the 2026 time frame. Our com-
1503 munity is well-positioned to take advantage of developments in micro- and
1504 nano- satellites (CubeSats; Vanhellemont, 2019). These small platforms

1505 can be launched cheaply, in large swarms, and, when cross-calibrated, have
1506 the potential to monitor the ocean with unprecedented spatial and temporal
1507 coverage. There is already an example of a successful launch of an ocean-
1508 colour CubeSats (e.g. SeaHawk; Schueler and Holmes, 2016). Tapping
1509 into high resolution satellites (e.g. Landsat and Sentinel-2) for improved
1510 monitoring of the carbon cycle in coastal waters and lakes is also an exciting
1511 avenue of research (Pahlevan et al., 2020).

1512 • **New satellite approaches.** There have been successful examples of re-
1513 search using satellite sensors originally designed for other purposes (e.g.
1514 atmospheric monitoring) for monitoring ocean properties relevant to the
1515 OBCP. For instance, the SCIAMACHY instrument onboard ESA ENVISAT,
1516 developed originally for monitoring atmospheric constituents, has found
1517 use for monitoring phytoplankton composition in the ocean (Bracher et al.,
1518 2009; Losa et al., 2017). Similarly, the on-going ESA S5p+ project is inves-
1519 tigating the use of the atmospheric TROPOMI sensor onboard Sentinel-5p
1520 to retrieve new ocean-colour products such as phytoplankton functional
1521 types, sun-induced marine fluorescence and light attenuation. Satellite
1522 lidar sensors, like those onboard the NASA and CNES CALIPSO satellite,
1523 designed for monitoring aerosol composition and clouds, have found use
1524 in ocean ecosystem monitoring (see reviews by Neukermans et al., 2018;
1525 Jamet et al., 2019). Similar applications could emerge from the Doppler
1526 wind lidar on-board ESA's Earth Explorer mission Aeolus. With a long
1527 history in monitoring ocean properties from aircraft (Churnside, 2014),
1528 attaching these active ocean-colour sensors to satellite platforms can reveal
1529 parts of the ocean not viewable with passive systems (e.g. polar ocean
1530 in winter), monitor at night and see further in the depth dimension. This
1531 has led to new insight relevant to the OBCP, for example, resolving the
1532 full seasonal cycles of phytoplankton in the polar ocean (Behrenfeld et al.,
1533 2017), and viewing the diel migration of zooplankton (Behrenfeld et al.,
1534 2019a).

- 1535 • **New statistical tools.** Driven by developments in big data (extremely large
1536 data sets), rapid advances in cloud-based computing (e.g. Google Earth En-
1537 gine) and statistical techniques, such as artificial intelligence, are underway.
1538 These tools are well-placed to help address some of the challenges we face
1539 in monitoring the OBCP from space: for instance, developing techniques
1540 that use multiple satellite products to target pools and fluxes of carbon not
1541 currently feasible to monitor from space, or for integrating satellite data
1542 with field data, models and autonomous observations. Advanced statisti-
1543 cal and machine learning techniques can be useful for highly non-linear
1544 inversion algorithm development (e.g. neural networks) and model data
1545 assimilation.

- 1546 • **Open Science.** Open Science is the way forward for accelerating the re-
1547 search process and maximising impact. It is essential that our community
1548 follows an approach of data sharing and knowledge transfer. This involves
1549 promoting: open access datasets, in community standard data formats,
1550 available in open-access repositories; open sharing of methods, for repro-
1551 ducibility and knowledge transfer, with code documented in open software
1552 repositories; open source publications; and openly available education re-
1553 sources, promoting the importance of the work to younger generations of
1554 scientists, students and the general public.

- 1555 • ***In situ* observations.** Considering the development, evaluation, uncer-
1556 tainty computation, and calibration of satellite remote-sensing algorithms
1557 for carbon pools and fluxes are highly-dependent on *in situ* observations, in-
1558 creasing resources should be assigned to improving *in situ* methods for mea-
1559 suring carbon pools and fluxes, embracing new technologies, autonomous
1560 platforms, and developing community protocols for *in situ* data gathering,
1561 with high emphasis on uncertainty characterisation. Additionally, and con-
1562 sidering the importance of system vicarious calibration of ocean colour
1563 sensors and the validation of core satellite products used as input to carbon
1564 algorithms (e.g., remote sensing reflectance), sustained support should be

1565 placed on funding campaigns to obtain Fiducial Reference Measurements
1566 (Banks et al., 2020).

1567 • **Bridging scales in observations and models.** Given the need to integrate
1568 satellite, *in situ* and model-based datasets, for improving our understanding
1569 of carbon pools and fluxes, increasing emphasis should be placed of meth-
1570 ods that can address the challenge in bridging the contrasting temporal and
1571 spatial scales applicable to these datasets.

1572 • **Harmonising carbon products across different planetary domains.**
1573 Moving beyond the ocean carbon cycle towards the Earth’s carbon bud-
1574 get, increasing emphasis should be placed on harmonising satellite carbon
1575 products across different planetary domains (ocean, land, ice and air). This
1576 harmonisation should consider consistency in data product format and algo-
1577 rithm approach. For example, the fundamental equation of photosynthesis
1578 is the same for the ocean and land, offering scope to develop unified al-
1579 gorithms of primary production. This harmonisation and consistency will
1580 ultimately improve Earth carbon budgets and estimates of cross-domain
1581 carbon fluxes.

1582 • **Improved data distribution of satellite carbon products.** Significant
1583 improvements have been made in recent years by space agencies and opera-
1584 tional satellite services to provide satellite data to end users in a variety of
1585 formats, and with a faster turn-around from data capture to delivery (Groom
1586 et al., 2019). Increasing emphasis should be placed on integrating satellite-
1587 based carbon products into these data streams, to ensure easy access to end
1588 users.

1589 **8. Summary**

1590 The ocean biological carbon pump (OBCP) transfers organic carbon from the
1591 surface to the deep ocean, helping to regulate atmospheric CO₂ concentrations.
1592 Monitoring the OBCP is vital to predicting changes in the Earth’s carbon cycle,

1593 and consequently changes in life and climate. In this paper, we have defined the
1594 pools and fluxes of carbon that make up the OBCP and reviewed *in-situ* (sampling
1595 from ships and autonomous platforms) and remote methods for monitoring them,
1596 with a major focus on satellite remote sensing. We discussed the advantages of
1597 producing a satellite-based carbon budget for the oceans, as an independent means
1598 for evaluating ecosystem models, but also advantages of integrating satellite-
1599 based observations with ecosystems models, to access the pools not currently
1600 retrievable from space, and also to integrate datasets (*in situ* and satellite) together
1601 in one platform and provide global coverage. We finished by touching on future
1602 opportunities in space, with the goal of bringing satellite observations to the
1603 attention of Earth System carbon research.

1604 **Competing Interest Statement**

1605 The authors declare that the research was conducted in the absence of any
1606 commercial or financial relationships that could be construed as a potential conflict
1607 of interest.

1608 **Author Contributions**

1609 Robert J. W. Brewin wrote the original draft with significant input from
1610 Shubha Sathyedranath & Trevor Platt. All authors contributed to the writing and
1611 editing of subsequent versions.

1612 **Acknowledgments**

1613 During the writing of this review, we very sadly lost one of our co-authors
1614 Professor Trevor Platt FRS. Trevor's input to this review was substantial. The topic
1615 of the ocean carbon cycle, and the use of optical measurements for monitoring
1616 and understanding carbon cycling, has been at the centre of Trevor's research over
1617 the past five decades. His contributions to the topic have been pioneering. He has
1618 left an enduring mark on our field and his presence will continue in those he has
1619 worked with and alongside, and through his vast body of publications. He will be
1620 dearly missed. We dedicate this paper to the memory of Trevor.

1621 **Funding**

1622 This work was funded through a European Space Agency (ESA) project
1623 "Biological Pump and Carbon Exchange Processes (BICEP)" and by the Simons
1624 Foundation Project "Collaboration on Computational Biogeochemical Modeling
1625 of Marine Ecosystems (CBIOMES)" (549947, SS). It was also supported by the
1626 UK National Centre for Earth Observation (NCEO). Additional support from the
1627 Ocean Colour Component of the Climate Change Initiative of the European Space
1628 Agency (ESA) is gratefully acknowledged.

1629 **References**

- 1630 Agustí, S., Satta, M.P., Mura, M.P., Benavent, E., 1998. Dissolved esterase
1631 activity as a tracer of phytoplankton lysis: evidence of high phytoplankton lysis
1632 rates in the northwestern mediterranean. *Limnology and Oceanography* 43,
1633 1836–1849. doi:10.4319/lo.1998.43.8.1836.
- 1634 Alcaraz, M., Saiz, E., Calbet, A., Trepát, I., Broglio, E., 2003. Estimating
1635 zooplankton biomass through image analysis. *Marine Biology* 143., 307–315.
1636 doi:10.1007/s00227-003-1094-8.
- 1637 Alkire, M.B., Lee, C., D’Asaro, E., Perry, M.J., Briggs, N., C.I., Gray, A.,
1638 2014. Net community production and export from Seaglider measurements in
1639 the North Atlantic after the spring bloom. *Journal of Geophysical Research:
1640 Oceans* 119, 6121–6139. URL: <https://doi.org/10.1002/2014JC010105>, doi:10.
1641 1002/2014JC010105.
- 1642 Allison, D.B., Stramski, D., Mitchell, B.G., 2010. Empirical ocean color algo-
1643 rithms for estimating particulate organic carbon in the Southern Ocean. *Journal
1644 of Geophysical Research: Oceans* 115, C06002. doi:10.1029/2009JC00604.
- 1645 Anderson, E.E., Wilson, C., Knap, A.H., Villareal, T.A., 2018. Summer diatom
1646 blooms in the eastern North Pacific gyre investigated with a long-endurance
1647 autonomous surface vehicle. *PeerJ* 6, e5387. URL: [https://doi.org/10.7717/
1648 peerj.5387](https://doi.org/10.7717/peerj.5387), doi:10.7717/peerj.5387.

- 1649 Antoine, D., André, J.M., Morel, A., 1996. Ocean primary production. 2 Esti-
1650 mation at global scale from satellite (coastal zone color scanner) chlorophyll.
1651 *Global Biogeochemical Cycles* 10, 57–69.
- 1652 Archibald, K., Siegel, D.A., Doney, S.C., 2019. Modeling the impact of zooplank-
1653 ton diel vertical migration on the carbon export flux of the biological pump.
1654 *Global Biogeochemical Cycles* 33, 181–199. doi:10.1029/2018GB005983.
- 1655 Ardyna, M., Lacour, L., Sergi, S., d’Ovidio, F., Sallée, J.B., Rembauville, M.,
1656 Blain, S., Tagliabue, A., Schlitzer, R., Jeandel, C., Arrigo, K.R., Claustre,
1657 H., 2019. Hydrothermal vents trigger massive phytoplankton blooms in the
1658 southern ocean. *Nature Communications* 10, 2451. URL: [https://doi.org/10.](https://doi.org/10.1038/s41467-019-09973-6)
1659 [1038/s41467-019-09973-6](https://doi.org/10.1038/s41467-019-09973-6), doi:10.1038/s41467-019-09973-6.
- 1660 Arrigo, K.R., van Dijken, G.L., 2015. Continued increases in Arctic Ocean
1661 primary production. *Progress in Oceanography* 136, 60–70.
- 1662 Arrigo, K.R., Pabi, S., van Dijken, G.L., Maslowski, W., 2010. Air-sea flux
1663 of CO₂ in the Arctic Ocean, 1998-2003. *Journal of Geophysical Research:*
1664 *Biogeosciences* 115, G04024. URL: <https://doi.org/10.1029/2009JG001224>,
1665 doi:10.1029/2009JG001224.
- 1666 Aumont, O., Maier-Reimer, E., Blain, S., Monfray, P., 2003. An ecosystem model
1667 of the global ocean including Fe, Si, P colimitations. *Global Biogeochemical*
1668 *Cycles* 17, 1060. doi:10.1029/2001GB001745.
- 1669 Aurin, D., Mannino, A., Lary, D.J., 2018. Remote sensing of CDOM, CDOM
1670 spectral slope, and Dissolved Organic Carbon in the Global Ocean. *Applied*
1671 *Sciences* 8, 2687. URL: <https://doi.org/10.3390/app8122687>, doi:10.3390/
1672 [app8122687](https://doi.org/10.3390/app8122687).
- 1673 Bakker, D.C.E., Pfeil, B., Landa, C.S., Metzl, N., O’Brien, K.M., Olsen, A., Smith,
1674 K., Cosca, C., Harasawa, S., Jones, S.D., Nakaoka, S., Nojiri, Y., Schuster, U.,
1675 Steinhoff, T., Sweeney, C., Takahashi, T., Tilbrook, B., Wada, C., Wanninkhof,
1676 R., Alin, S.R., Balestrini, C.F., Barbero, L., Bates, N.R., Bianchi, A.A., Bonou,
1677 F., Boutin, J., Bozec, Y., Burger, E.F., Cai, W.J., Castle, R.D., Chen, L.,
1678 Chierici, M., Currie, K., Evans, W., Featherstone, C., Feely, R.A., Fransson,
1679 A., Goyet, C., Greenwood, N., Gregor, L., Hankin, S., Hardman-Mountford,

1680 N.J., Harlay, J., Hauck, J., Hoppema, M., Humphreys, M.P., Hunt, C.W., Huss,
1681 B., Ibáñez, J.S.P., Johannessen, T., Keeling, R., Kitidis, V., Körtzinger, A.,
1682 Kozyr, A., Krasakopoulou, E., Kuwata, A., Landschützer, P., Lauvset, S.K.,
1683 Lefèvre, N., Lo Monaco, C., Manke, A., Mathis, J.T., Merlivat, L., Millero, F.J.,
1684 Monteiro, P.M.S., Munro, D.R., Murata, A., Newberger, T., Omar, A.M., Ono,
1685 T., Paterson, K., Pearce, D., Pierrot, D., Robbins, L.L., Saito, S., Salisbury, J.,
1686 Schlitzer, R., Schneider, B., Schweitzer, R., Sieger, R., Skjelvan, I., Sullivan,
1687 K.F., Sutherland, S.C., Sutton, A.J., Tadokoro, K., Telszewski, M., Tuma, M.,
1688 van Heuven, S.M.A.C., Vandemark, D., Ward, B., Watson, A.J., Xu, S., 2016.
1689 A multi-decade record of high-quality fCO₂ data in version 3 of the Surface
1690 Ocean CO₂ atlas (SOCAT). *Earth System Science Data* 8, 383–413. URL:
1691 <https://doi.org/10.5194/essd-8-383-2016>, doi:10.5194/essd-8-383-2016.
1692 Balch, W.M., Bowler, B.C., Drapeau, D.T., Lubelczyk, L.C., Lyczkowski,
1693 E., 2018. Vertical distributions of coccolithophores, PIC, POC, biogenic
1694 silica, and chlorophyll a throughout the global ocean. *Global Biogeo-*
1695 *chemical Cycles* 32, 2–17. URL: <https://doi.org/10.1002/2016GB005614>,
1696 doi:10.1002/2016GB005614.
1697 Balch, W.M., Gordon, H.R., Bowler, B.C., Drapeau, D.T., Booth, E.S., 2005. Cal-
1698 cium carbonate measurements in the surface global ocean based on Moderate-
1699 Resolution Imaging Spectroradiometer data. *Journal of Geophysical Research*
1700 110, C0700. doi:10.1029/2004JC002560.
1701 Bale, N.J., Airs, R.L., Llewellyn, C.A., 2011. Type I and Type II chlorophyll-a
1702 transformation products associated with algal senescence. *Organic Geochem-*
1703 *istry* 42, 451–464. doi:10.1016/j.orggeochem.2011.03.016.
1704 Banks, A.C., Vendt, R., Alikas, K., Bialek, A., Kuusk, J., Lerebourg, C., Ruddick,
1705 K., Tilstone, G., Vabson, V., Donlon, C., Casal, T., 2020. Fiducial reference
1706 measurements for satellite ocean colour (FRM4SOC). *Remote Sensing* 12,
1707 1322. doi:10.3390/rs12081322.
1708 Basedow, S.L., McKee, D., Lefering, I., Gislason, A., Daase, M., Trudnowska,
1709 E., Egeland, E.S., Choquet, M., Falk-Petersen, S., 2019. Remote sensing of
1710 zooplankton swarms. *Scientific Reports* 9, 686. URL: <https://doi.org/10.1038/>

- 1711 s41598-018-37129-x, doi:10.1038/s41598-018-37129-x.
- 1712 Bates, J.J., Privette, J.L., Kearns, E.J., Glance, W., Zhao, X., 2016. Sustained
1713 production of multidecadal climate records: lessons from the NOAA Climate
1714 Data Record Program. *Bulletin of the American Meteorological Society* 97,
1715 1573–1581. doi:10.1175/BAMS-D-15-00015.1.
- 1716 Baumgartner, M.F., Fratantoni, D.M., Hurst, T.P., Brown, M.W., Cole, T.V.,
1717 Van Parijs, S.M., Johnson, M., 2013. Real-time reporting of baleen whale
1718 passive acoustic detections from ocean gliders. *The Journal of the Acoustical*
1719 *Society of America* 134, 1814–1823. URL: <https://doi.org/10.1121/1.4816406>,
1720 doi:10.1121/1.4816406.
- 1721 Beaton, A.D., Sieben, V.J., Floquet, C.F., Waugh, E.M., Bey, S.A.K., Ogilvie, I.R.,
1722 Mowlem, M.C., Morgan, H., 2011. An automated microfluidic colourimetric
1723 sensor applied in situ to determine nitrite concentration. *Sensors and actuators*
1724 *B: Chemical* 156, 1009–1014. URL: <https://doi.org/10.1016/j.snb.2011.02.042>,
1725 doi:10.1016/j.snb.2011.02.042.
- 1726 Behrenfeld, M., Boss, E., Siegel, D.A., Shea, D.M., 2005. Carbon-based ocean
1727 productivity and phytoplankton physiology from space. *Global Biogeochemical*
1728 *Cycles* 19, 1–14. doi:10.1029/2004GB002299.
- 1729 Behrenfeld, M.J., 2010. Abandoning Sverdrup’s critical depth hypothesis on
1730 phytoplankton blooms. *Ecology* 91, 977–989. doi:10.1890/09-1207.1.
- 1731 Behrenfeld, M.J., 2014. Climate-mediated dance of the plankton. *Nature Climate*
1732 *Change* 4, 880–887. doi:10.1038/nclimate2349.
- 1733 Behrenfeld, M.J., Falkowski, P.G., 1997. Photosynthetic rates derived from
1734 satellite-based chlorophyll concentration. *Limnology and Oceanography* 42,
1735 1–20.
- 1736 Behrenfeld, M.J., Gaube, P., Della Penna, A., O’Malley, R.T., Burt, W.J., Hu,
1737 Y., Bontempi, P.S., Steinberg, D.K., Boss, E.S., Siegel, D.A., Hostetler, C.A.,
1738 2019a. Global satellite-observed daily vertical migrations of ocean animals.
1739 *Nature* 576, 257–261.
- 1740 Behrenfeld, M.J., Hu, Y., O’Malley, R.T., Boss, E.S., Hostetler, C.A., Siegel,
1741 D.A., Sarmiento, J.L., Schulien, J., Hair, J.W., Lu, X., Rodier, S., 2017. Annual

1742 boom-bust cycles of polar phytoplankton biomass revealed by space-based
1743 lidar. *Nature Geoscience* 10, 118–122. doi:10.1038/ngeo2861.

1744 Behrenfeld, M.J., Moore, R.H., Hostetler, C.A., Graff, J., Gaube, P., Russell, L.M.,
1745 Chen, G., Doney, S.C., Giovannoni, S., Liu, H., Proctor, C., Bolaños, L.M.,
1746 Baetge, N., Davie-Martin, C., Westberry, T.K., Bates, T.S., Bell, T.G., Bidle,
1747 K.D., Boss, E.S., Brooks, S.D., Cairns, B., Carlson, C., Halsey, K., Harvey,
1748 E.L., Hu, C., Karp-Boss, L., Kleb, M., Menden-Deuer, S., Morison, F., Quinn,
1749 P.K., Scarino, A.J., Anderson, B., Chowdhary, J., Crosbie, E., Ferrare, R., Hair,
1750 J.W., Hu, Y., Janz, S., Redemann, J., Saltzman, E., Shook, M., Siegel, D.A.,
1751 Wisthaler, A., Martin, M.Y., Ziemba, L., 2019b. The North Atlantic Aerosol and
1752 Marine Ecosystem Study (NAAMES): Science motive and mission overview.
1753 *Frontiers in Marine Science* 6, 122. doi:10.3389/fmars.2019.00122.

1754 Behrenfeld, M.J., O'Malley, R.T., Siegel, D.A., McClain, C.R., Sarmiento, J.L.,
1755 Feldman, G.C., Milligan, A.J., Falkowski, P.G., Letelier, R.M., Boss, E.S., 2006.
1756 Climate-driven trends in contemporary ocean productivity. *Nature* 444, 752–
1757 755. URL: <https://doi.org/10.1038/nature05317>, doi:10.1038/nature05317.

1758 Behrenfeld, M.J., Randerson, J.T., McClain, C.R., Feldman, G.C., Los, S.O.,
1759 Tucker, C.J., Falkowski, P.G., Field, C.B., Frouin, R., Esaias, W.E., Kolber,
1760 D.D., 2001. Biospheric primary production during an ENSO transition. *Science*
1761 291, 2594–2597. doi:10.1126/science.1055071.

1762 Bellacicco, M., Cornec, M., Organelli, E., Brewin, R.J.W., Neukermans, G.,
1763 Volpe, G., Barbieux, M., Poteau, A., Schmechtig, C., D'Ortenzio, F., Marullo,
1764 S., Claustre, H., Pitarch, J., 2019. Global variability of optical backscattering
1765 by non-algal particles from a biogeochemical-Argo data set. *Geophysical*
1766 *Research Letters* 46, 9767–9776. URL: <https://doi.org/10.1029/2019GL084078>,
1767 doi:10.1029/2019GL084078.

1768 Bellacicco, M., Volpe, G., Briggs, N., Brando, V., Pitarch, J., Landolfi, A., Colella,
1769 S., Marullo, S., Santoleri, S., 2018. Global distribution of non-algal particles
1770 from ocean color data and implications for phytoplankton biomass detection.
1771 *Geophysical Research Letters* 45, 7672–7682. URL: <https://doi.org/10.1029/2018GL078185>,
1772 doi:10.1029/2018GL078185.

- 1773 Bellacicco, M., Volpe, G., Colella, S., Pitarch, J., Santoleria, R., 2016. Influence of
1774 photoacclimation on the phytoplankton seasonal cycle in the Mediterranean Sea
1775 as seen by satellite. *Remote Sensing of Environment* 184, 595–604. URL: <https://doi.org/10.1016/j.rse.2016.08.004>, doi:10.1016/j.rse.2016.08.004.
1776
- 1777 Berge, G., 1962. Discoloration of the sea due to *Coccolithus huxleyi* "bloom".
1778 *Sarsia* 6, 27–40.
- 1779 Betzer, P.R., Showers, W.J., Laws, E.A., Winn, C.D., DiTullio, G.R., Kroopnick,
1780 P.M., 1984. Primary productivity and particle fluxes on a transect of the equator
1781 at 153W in the Pacific Ocean. *Deep-Sea Research* 31, 1–11. doi:10.1016/
1782 0198-0149(84)90068-2.
- 1783 BIPM, 2008. Evaluation of measurement data – guide to the expression of
1784 uncertainty in measurement.
- 1785 Birkenes, E., Braarud, T., 1952. Phytoplankton in the Oslo Fjord during a
1786 "Coccolithus huxleyi-summer". *Avhandlingar utgitt av det Norske videnskaps*
1787 *akademii Oslo, Matematisk naturvidenskapelig Klasse 2*.
- 1788 Bishop, J., 1999. Transmissometer measurement of POC. *Deep Sea Re-*
1789 *search Part I: Oceanographic Research Papers* 46, 353–369. doi:10.1016/
1790 S0967-0637(98)00069-7.
- 1791 Bishop, J.K.B., Fong, M.B., Wood, T.J., 2016. Robotic observations of high
1792 wintertime carbon export in California coastal waters. *Biogeosciences* 13,
1793 3109–3129. doi:10.5194/bg-13-3109-2016.
- 1794 Bishop, J.K.B., Wood, T.J., 2009. Year-round observations of carbon biomass
1795 and flux variability in the Southern Ocean. *Global Biogeochemical Cycles* 23,
1796 GB2019. doi:10.1029/2008GB003206.
- 1797 Bishop, J.K.B., Wood, T.J., Davis, R.E., Sherman, J.T., 2004. Robotic observa-
1798 tions of enhanced carbon biomass and export at 55°S during SOFeX. *Science*
1799 304, 417–420. doi:10.1126/science.1087717.
- 1800 Bisson, K., Siegel, D.A., DeVries, T., 2020. Diagnosing mechanisms of ocean
1801 carbon export in a satellite-based food web model. *Frontiers in Marine Science*
1802 7, 505. doi:10.3389/fmars.2020.00505.
- 1803 Bol, R., Henson, S.A., Rumyantseva, A., Briggs, N., 2018. High-frequency

- 1804 variability of small-particle carbon export flux in the Northeast Atlantic.
1805 *Global Biogeochemical Cycles* 32, 1803–1814. URL: [https://doi.org/10.1029/](https://doi.org/10.1029/2018GB005963)
1806 [2018GB005963](https://doi.org/10.1029/2018GB005963), doi:10.1029/2018GB005963.
- 1807 Bork, K., Karstensen, J., Visbeck, M., Zimmermann, A., 2008. The legal regu-
1808 lation of floats and gliders—in quest of a new regime? *Ocean Development &*
1809 *International law* 39, 298–328. doi:10.1080/00908320802235338.
- 1810 Bosc, E., Bricaud, A., Antoine, D., 2004. Seasonal and interannual variability
1811 in algal biomass and primary production in the Mediterranean Sea, as derived
1812 from 4 years of SeaWiFS observations. *Global Biogeochemical Cycles* 18,
1813 GB1005. doi:10.1029/2003GB002034.
- 1814 Boss, E., Behrenfeld, M., 2010. In situ evaluation of the initiation of the North
1815 Atlantic phytoplankton bloom. *Geophysical Research Letters* 37, L18603.
1816 doi:10.1029/2010GL044174.
- 1817 Bouman, H., Platt, T., Sathyendranath, S., Stuart, V., 2005. Dependence of light-
1818 saturated photosynthesis on temperature and community structure. *Deep-Sea*
1819 *Research I* 52, 1284–1299.
- 1820 Bouman, H.A., Platt, T., Doblin, M., Figueiras, F.G., Gudmundsson, K., Gudfinns-
1821 son, H.G., Huang, B., Hickman, A., Hiscock, M., Jackson, T., Lutz, V.A.,
1822 Mélin, F., Rey, F., Pepin, P., Segura, V., Tilstone, G.H., van Dongen-Vogels,
1823 V., Sathyendranath, S., 2018. Photosynthesis-irradiance parameters of ma-
1824 rine phytoplankton: synthesis of a global data set. *Earth System Sci-*
1825 *ence Data* 10, 251–266. URL: <https://doi.org/10.5194/essd-10-251-2018>,
1826 doi:10.5194/essd-10-251-2018.
- 1827 Bowers, D.G., Evans, D., Thomas, D.N., Ellis, K., Williams, P.L.B., 2004. Inter-
1828 preting the colour of an estuary. *Estuarine, Coastal and Shelf Science* 59, 13–20.
1829 URL: [https://doi.org/10.1016/j.ecss.2003.](https://doi.org/10.1016/j.ecss.2003.06.001)
1830 [06.001](https://doi.org/10.1016/j.ecss.2003.06.001).
- 1831 Bowers, D.G., Harker, G.E.L., Smith, P.S.D., Tett, P., 2000. Optical properties
1832 of a region of freshwater influence (the Clyde Sea). *Estuarine, Coastal and*
1833 *Shelf Science* 50, 717–726. URL: <https://doi.org/10.1006/ecss.1999.0600>,
1834 doi:10.1006/ecss.1999.0600.

- 1835 Boyd, P., Claustre, H., Levy, M., Siegel, D.A., Weber, T., 2019. Multi-faceted
1836 particle pumps drive carbon sequestration in the ocean. *Nature* 568, 327–335.
1837 doi:10.1038/s41586-019-1098-2.
- 1838 Bracher, A., Bouman, H., Brewin, R.J.W., Bricaud, A., Brotas, V., Ciotti, A.M.,
1839 Clementson, L., Devred, E., Di Cicco, A., Dutkiewicz, S., Hardman-Mountford,
1840 N., Hickman, A.E., Hieronymi, M., Hirata, T., Losa, S., Mouw, C.B., Organelli,
1841 E., Raitzos, D.E., Uitz, J., Vogt, M., Wolanin, A., 2017. Obtaining Phytoplankton
1842 Diversity from Ocean Color: A Scientific Roadmap for Future Development.
1843 *Frontiers in Marine Science* 4, 1–15. doi:10.3389/fmars.2017.00055.
- 1844 Bracher, A., Vountas, M., Dinter, T., Burrows, J.P., Röttgers, R., Peeken, I.,
1845 2009. Quantitative observation of cyanobacteria and diatoms from space
1846 using PhytoDOAS on SCIAMACHY data. *Biogeosciences* 6, 751–764. URL:
1847 <https://doi.org/10.5194/bg-6-751-2009>, doi:10.5194/bg-6-751-2009.
- 1848 Bresnahan, P., Martz, T., de Almeida, J., Ward, B., Maguire, P., 2017a. Looking
1849 ahead: A profiling float Micro-Rosette. *Oceanography* 30, 32. URL: <https://doi.org/10.5670/oceanog.2017.215>, doi:10.5670/oceanog.2017.215.
- 1851 Bresnahan, P.J., Cyronak, T., Martz, T., Andersson, A., Waters, S., Stern, A.,
1852 Richard, J., Hammond, K., Griffin, J., Thompson, B., 2017b. Engineering a
1853 Smartfin for surf-zone oceanography, in: *OCEANS 2017 - Anchorage*, IEEE.
1854 pp. 1–4.
- 1855 Bresnahan, P.J., Wirth, T., Martz, T.R., Andersson, A.J., Cyronak, T., D’Angelo,
1856 S., Pennise, J., Melville, W.K., Lenain, L., Statom, N., 2016. A sensor package
1857 for mapping pH and oxygen from mobile platforms. *Methods in Oceanography*
1858 17, 1–13. doi:10.1016/j.mio.2016.04.004.
- 1859 Brewin, R.J.W., Ciavatta, S., Sathyendranath, S., Jackson, T., Tilstone, G., Cur-
1860 ran, K., Airs, R.L., Cummings, D., Brotas, V., Organelli, E., Dall’Olmo,
1861 G., Raitzos, D.E., 2017a. Uncertainty in ocean-color estimates of chloro-
1862 phyll for phytoplankton groups. *Frontiers in Marine Science* 4, 104. URL:
1863 <https://www.frontiersin.org/article/10.3389/fmars.2017.00104>, doi:10.3389/
1864 *fmars.2017.00104*.
- 1865 Brewin, R.J.W., Dall’Olmo, G., Pardo, S., van Dongen-Vogel, V., Boss, E.S.,

- 1866 2016. Underway spectrophotometry along the Atlantic Meridional Transect
1867 reveals high performance in satellite chlorophyll retrievals. *Remote Sensing of*
1868 *Environment* 183, 82–97. doi:10.1016/j.rse.2016.05.005.
- 1869 Brewin, R.J.W., Devred, E., Sathyendranath, S., Hardman-Mountford, N.J., Laven-
1870 der, S.J., 2011. Model of phytoplankton absorption based on three size classes.
1871 *Applied Optics* 50, 4535–4549. doi:10.1364/AO.50.004535.
- 1872 Brewin, R.J.W., Hyder, K., Andersson, A.J., Billson, O., Bresnahan, P.J., Brewin,
1873 T.G., Cyronak, T., Dall’Olmo, G., de Mora, L., Graham, G., Jackson, T.,
1874 Raitsos, D.E., 2017b. Expanding aquatic observations through recreation.
1875 *Frontiers in Marine Science* 4, 351. doi:10.3389/fmars.2017.00351.
- 1876 Brewin, R.J.W., de Mora, L., Billson, O., Jackson, T., Russell, P., Brewin,
1877 T.G., Shutler, J., Miller, P.I., Taylor, B.H., Smyth, T., Fishwick, J.R., 2017c.
1878 Evaluating operational AVHRR sea surface temperature data at the coast-
1879 line using surfers. *Estuarine, Coastal and Shelf Sciences* 196, 276–289.
1880 doi:10.1016/j.ecss.2017.07.011.
- 1881 Brewin, R.J.W., de Mora, L., Jackson, T., Brewin, T.G., Shutler, J., 2015a. On
1882 the potential of surfers to monitor environmental indicators in the coastal zone.
1883 *PLoS One* 10, e0127706.
- 1884 Brewin, R.J.W., Sathyendranath, S., Jackson, T., Barlow, R., Brotas, V., Airs, R.,
1885 Lamont, T., 2015b. Influence of light in the mixed layer on the parameters of a
1886 three-component model of phytoplankton size structure. *Remote Sensing of*
1887 *Environment* 168, 437–450. doi:10.1016/j.rse.2015.07.004.
- 1888 Brewin, R.J.W., Sathyendranath, S., Müller, D., Brockmann, C., Deschamps, P.Y.,
1889 Devred, E., Doerffer, R., Fomferra, N., Franz, B.A., Grant, M., Groom, S.,
1890 Horseman, A., Hu, C., Krasemann, H., Lee, Z.P., Maritorea, S., Mélin, F.,
1891 Peters, M., Platt, T., Regner, P., Smyth, T., Steinmetz, F., Swinton, J., Werdell,
1892 J., White III, G.N., 2015c. The Ocean Colour Climate Change Initiative: III. A
1893 round-robin comparison on in-water bio-optical algorithms. *Remote Sensing*
1894 *Environment* 162, 271–294. doi:10.1016/j.rse.2013.09.016.
- 1895 Brewin, R.J.W., Tilstone, G., Jackson, T., Cain, T., Miller, P., Lange, P.K., Misra,
1896 A., Airs, R., 2017d. Modelling size-fractionated primary production in the

- 1897 Atlantic Ocean from remote sensing. *Progress in Oceanography* 158, 130–149.
1898 URL: [https://doi.org/10.1016/j.pocean.](https://doi.org/10.1016/j.pocean.2017.02.002)
1899 2017.02.002.
- 1900 Bricaud, A., Babin, M., Claustre, H., Ras, J., Tiéche, F., 2010. Light absorp-
1901 tion properties and absorption budget of Southeast Pacific waters. *Journal of*
1902 *Geophysical Research* 115, C08009. doi:10.1029/2009JC005517.
- 1903 Briggs, N., Dall’Olmo, G., Claustre, H., 2020. Major role of particle fragmen-
1904 tation in regulating biological sequestration of CO₂ by the oceans. *Science*
1905 doi:10.1126/science.aay1790.
- 1906 Briggs, N., Perry, M.J.P., Cetinić, I., Lee, C., D’Asaro, E., Gray, A.M., Rehm, E.,
1907 2011. High-resolution observations of aggregate flux during a sub-polar North
1908 Atlantic spring bloom. *Deep Sea Research I* 58, 1031–1039. doi:10.1016/j.
1909 dsr.2011.07.007.
- 1910 Briggs, N.T., Slade, W.H., Boss, E., Perry, M.J., 2013. Method for estimating
1911 mean particle size from high-frequency fluctuations in beam attenuation or
1912 scattering measurements. *Applied Optics* 52, 6710. doi:10.1364/AO.52.
1913 006710.
- 1914 Brown, A., Thomson, J., Ellenson, A., Rollano, F.T., Özkan-Haller, H.T., Haller,
1915 M.C., 2019. Kinematics and statistics of breaking waves observed using SWIFT
1916 buoys. *IEEE Journal of Oceanic Engineering* 44, 1011–1023. doi:10.1109/
1917 JOE.2018.2868335.
- 1918 Brown, C.W., Schollaert Uz, S., Corliss, B.H., 2014. Seasonality of oceanic
1919 primary production and its interannual variability from 1998 to 2007. *Deep Sea*
1920 *Research Part I: Oceanographic Research Papers* 90, 166–175. doi:10.1016/
1921 j.dsr.2014.05.009.
- 1922 Brown, C.W., Yoder, J.A., 1994. Coccolithophorid blooms in the global ocean.
1923 *Journal of Geophysical Research: Oceans* 99, 7467–7482.
- 1924 Brown, O.B., Evans, R.H., Brown, J.W., Gordon, H.R., Smith, R.C., Baker, K.S.,
1925 1985. Phytoplankton blooming off the US east coast: A satellite description.
1926 *Science* 229, 163–167. doi:10.1126/science.229.4709.163.
- 1927 Buck, K.R., Chavez, F.P., Campbell, L., 1996. Basin-wide distributions of living

- 1928 carbon components and the inverted trophic pyramid of the central gyre of the
1929 North Atlantic Ocean, summer 1993. *Aquatic Microbial Ecology* 10, 283–298.
1930 doi:10.3354/ame010283.
- 1931 Buesseler, K.O., 1998. The decoupling of production and particulate export in
1932 the surface ocean. *Global Biogeochemical Cycles* 12, 297–310. doi:10.1029/
1933 97gb03366.
- 1934 Buesseler, K.O., Antia, A.N., Chen, M., Fowler, S.W., Gardner, W.D., Gustafsson,
1935 O., Harada, K., Michaels, A.F., Rutgers van der Loeff, M., Sarin, M., Steinberg,
1936 D.K., Trull, T., 2007. An assessment of the use of sediment traps for estimating
1937 upper ocean particle fluxes. *Journal of Marine Systems* 65, 345–416. doi:10.
1938 1357/002224007781567621.
- 1939 Buesseler, K.O., Boyd, P.W., Black, E.E., Siegel, D.A., 2020. Metrics that matter
1940 for assessing the ocean biological carbon pump. *Proceedings of the National
1941 Academy of Sciences* 117, 9679–9687. doi:10.1073/pnas.1918114117.
- 1942 Buitenhuis, E.T., Vogt, M., Moriarty, R., Bednaršek, N., Doney, S.C., Leblanc,
1943 K., Le Quéré, C., Luo, Y.W., O'Brien, C., O'Brien, T., Peloquin, J., Schiebel,
1944 R., Swan, C., 2013. MAREDAT: towards a world atlas of MARine Ecosystem
1945 DATA. *Earth System Science Data* 5, 227–239. URL: [https://doi.org/10.5194/
1946 essd-5-227-2013](https://doi.org/10.5194/essd-5-227-2013), doi:10.5194/essd-5-227-2013.
- 1947 Burd, A.B., Jackson, G.A., 2009. Particle aggregation. *Annual Review of Marine
1948 Science* 1, 65–90. doi:10.1146/annurev.marine.010908.163904.
- 1949 Burt, W.J., Tortell, P.D., 2018. Observations of zooplankton diel vertical
1950 migration from high-resolution surface ocean optical measurements. *Geo-
1951 physical Research Letters* 45, 13,396–13,404. URL: [https://doi.org/10.1029/
1952 2018GL079992](https://doi.org/10.1029/2018GL079992), doi:10.1029/2018GL079992.
- 1953 Burt, W.J., Westberry, T.K., Behrenfeld, M.J., Zeng, C., Izett, R.W., Tortell,
1954 P.D., 2018. Carbon: Chlorophyll ratios and net primary productivity of
1955 Subarctic Pacific surface waters derived from autonomous shipboard sensors.
1956 *Global Biogeochemical Cycles* 32, 267–288. URL: [https://doi.org/10.1002/
1957 2017GB005783](https://doi.org/10.1002/2017GB005783), doi:10.1002/2017GB005783.
- 1958 Bushinsky, S.M., Takeshita, Y., Williams, N.L., 2019. Observing changes in ocean

- 1959 carbonate chemistry: Our autonomous future. *Current Climate Change Reports*
1960 5, 207–220. URL: <https://doi.org/10.1007/s40641-019-00129-8>, doi:10.1007/
1961 s40641-019-00129-8.
- 1962 Butenschön, M., Clark, J., Aldridge, J.N., Allen, J.I., Artioli, Y., Blackford, J.,
1963 Bruggeman, J., Cazenave, P., Ciavatta, S., Kay, S., Lessin, G., van Leeuwen,
1964 S., van der Molen, J., de Mora, L., Polimene, L., Saille, S., Stephens, N., ,
1965 Torres, R., 2016. ERSEM 15.06: a generic model for marine biogeochemistry
1966 and the ecosystem dynamics of the lower trophic levels. *Geoscience Model*
1967 *Development* 9, 1293–1339. doi:10.5194/gmd-9-1293-2016.
- 1968 Byrne, R.H., 2014. Measuring ocean acidification: New technology for a new
1969 era of ocean chemistry. *Environmental Science & Technology* 48, 5352–5360.
1970 doi:10.1021/es405819p.
- 1971 Cael, B.B., Bisson, K., 2018. Particle flux parameterizations: Quantitative and
1972 mechanistic similarities and differences. *Frontiers in Marine Science* 5, 395.
1973 doi:10.3389/fmars.2018.00395.
- 1974 Cael, B.B., Chase, A., Boss, E., 2020. Information content of absorption spectra
1975 and implications for ocean color inversion. *Applied Optics* 59, 3971–3984.
1976 doi:10.1364/AO.389189.
- 1977 Call, M., Sanders, C.J., Macklin, P.A., Santos, I.R., Maher, D.T., 2019. Carbon
1978 outwelling and emissions from two contrasting mangrove creeks during the
1979 monsoon storm season in Palau, Micronesia. *Estuarine, Coastal and Shelf*
1980 *Science* 218, 340–348. doi:10.1016/j.ecss.2019.01.002.
- 1981 Campbell, J.W., Antoine, D., Armstrong, R.A., Arrigo, K.R., Balch, W., Barber,
1982 R., Behrenfeld, M., Bidigare, R., Bishop, J., Carr, M.E., Esaias, W., Falkowski,
1983 P., Hoepffner, N., Iverson, R., Kiefer, D.A., Lohrenz, S., Marra, J., Morel, A.,
1984 Ryan, J., Vedernikov, V., Waters, K., Yentch, C., Yoder, J., 2002. Comparison of
1985 algorithms for estimating ocean primary production from surface chlorophyll,
1986 temperature, and irradiance. *Global Biogeochemical Cycles* 16, 1035. doi:10.
1987 1029/2001GB001444.
- 1988 Carr, M.E., Friedrichs, M.A., Schmeltz, M., Aita, M.N., Antoine, D., Arrigo, K.R.,
1989 Asanuma, I., Aumont, O., Barber, R., Behrenfeld, M., Bidigare, R., Buitenhuis,

1990 E.T., Campbell, J.W., Ciotti, A.M., Dierssen, H.M., Dowell, M., Dunne, J.,
1991 Esaias, W., Gentili, B., Gregg, W.W., Groom, S., Hoepffner, N., Ishizaka, J.,
1992 Kameda, T., Le Quéré, C., Lohrenz, S., Marra, J., Mélin, F., Moore, K., Morel,
1993 A., Reddy, T.E., Ryan, J., Scardi, M., Smyth, T., Turpie, K., Tilstone, G.,
1994 Waters, K., Yamanaka, Y., 2006. A comparison of global estimates of marine
1995 primary production from ocean color. *Deep Sea Research Part II: Topical*
1996 *Studies in Oceanography* 53, 741–770. doi:10.1016/j.dsr2.2006.01.028.
1997 Carranza, M.M., Gille, S.T., Franks, P.J., Johnson, K.S., Pinkel, R., Girton,
1998 J.B., 2018. When mixed layers are not mixed. Storm-driven mixing and bio-
1999 optical vertical gradients in mixed layers of the Southern Ocean. *Journal of*
2000 *Geophysical Research: Oceans* 123, 7264–7289. URL: [https://doi.org/10.1029/](https://doi.org/10.1029/2018JC014416)
2001 [2018JC014416](https://doi.org/10.1029/2018JC014416), doi:10.1029/2018JC014416.
2002 Casey, J.R., Aucan, J.P., Goldberg, S.R., Lomas, M.W., 2013. Changes in
2003 partitioning of carbon amongst photosynthetic pico-and nano-plankton groups
2004 in the Sargasso Sea in response to changes in the North Atlantic Oscillation.
2005 *Deep Sea Research Part II: Topical Studies in Oceanography* 93, 58–70. doi:10.
2006 1016/j.dsr2.2013.02.002.
2007 Catlett, D., Siegel, D.A., 2018. Phytoplankton pigment communities can be
2008 modeled using unique relationships with spectral absorption signatures in a
2009 dynamic coastal environment. *Journal of Geophysical Research: Oceans* 123,
2010 246–264. doi:10.1002/2017JC013195.
2011 Cauchy, P., Heywood, K.J., Merchant, N.D., Queste, B.Y., Testor, P., 2018. Wind
2012 speed measured from underwater gliders using passive acoustics. *Journal of*
2013 *Atmospheric and Oceanic Technology* 35, 2305–2321. URL: [https://doi.org/10.](https://doi.org/10.1175/JTECH-D-17-0209.1)
2014 [1175/JTECH-D-17-0209.1](https://doi.org/10.1175/JTECH-D-17-0209.1), doi:10.1175/JTECH-D-17-0209.1.
2015 Cazenave, A., Hamlington, B., Horwath, M., Barletta, V.R., Benveniste, J., Cham-
2016 bers, D., Döll, P., Hogg, A.E., Legeais, J.F., Merrifield, M., Meyssignac, B.,
2017 Mitchum, G., Nerem, S., Pail, R., Palanisamy, H., Paul, F., von Schuckmann,
2018 K., Thompson, P., 2019. Observational requirements for long-term monitoring
2019 of the global mean sea level and its components over the altimetry era. *Frontiers*
2020 *in Marine Science* 6, 582. URL: <https://www.frontiersin.org/article/10.3389/>

2021 fmars.2019.00582, doi:10.3389/fmars.2019.00582.

2022 CEOS, 2014. CEOS strategy for carbon observations from space. The Committee
2023 on Earth Observation Satellites (CEOS) response to the Group on Earth Ob-
2024 servations (GEO) carbon strategy. September 30th 2014, printed in Japan by
2025 JAXA and I&A Corporation.

2026 Chai, F., Johnson, K.S., Claustre, H., Xing, X., Wang, Y., Boss, E., Riser, S.,
2027 Fennel, K., Schofield, O. and Sutton, A., 2020. Monitoring ocean biogeochem-
2028 istry with autonomous platforms. *Nature Reviews Earth and Environment* 1,
2029 315–326. doi:10.1038/s43017-020-0053-y.

2030 Chami, M., Marken, E., Stamnes, J., Khomenko, G.A., Korotaev, G.K., 2006. Vari-
2031 ability of the relationship between the particulate backscattering coefficient and
2032 the volume scattering function measured at fixed angles. *Journal of Geophysical*
2033 *Research: Oceans* 111, C05013. URL: <https://doi.org/10.1029/2005JC003230>,
2034 doi:10.1029/2005JC003230.

2035 Chaves, J.E., Cetinić, I., Dall’Olmo, G., Estapa, M., Gardner, W., Goñi, M.,
2036 Graff, J.R., Hernes, P., Lam, P.J., Liu, Z., Lomas, M.W., 2020. Particulate
2037 Organic Carbon Sampling and Measurement Protocols: Consensus Towards
2038 Future Ocean Color Missions. Technical Report. International Ocean Colour
2039 Coordinating Group. URL: [https://ioccg.org/wp-content/uploads/2019/11/poc_
2040 ioccg_protocol_2019_public_draft-18nov-2019.pdf](https://ioccg.org/wp-content/uploads/2019/11/poc_ioccg_protocol_2019_public_draft-18nov-2019.pdf).

2041 Chisholm, S.W., 1992. Phytoplankton size, in: Falkowski, P.G., Woodhead, A.D.
2042 (Eds.), *Primary Productivity and Biogeochemical Cycles in the Sea*. Springer,
2043 New York, pp. 213–237.

2044 Choi, J.K., Park, Y.J., Ahn, J.H., Lim, H.S., Eom, J., Ryu, J.H., 2012. GOCI, the
2045 world’s first geostationary ocean color observation satellite, for the monitoring
2046 of temporal variability in coastal water turbidity. *Journal of Geophysical*
2047 *Research* 117, C09004. doi:10.1029/2012JC008046.

2048 Church, M., Cullen, J., Karl, D., 2019. Approaches to measuring primary produc-
2049 tion, in: Cochran, J.K., Bokuniewicz, J.H., Yager, L.P. (Eds.), *Encyclopedia of*
2050 *Ocean Sciences*, 3rd Edition. Elsevier. volume 1, pp. 484–492.

2051 Churnside, J.H., 2014. Review of profiling oceanographic lidar. *Optical Engi-*

2052 neering 53, 1–13. doi:10.1117/1.OE.53.5.051405.

2053 Ciavatta, S., Brewin, R.J.W., Skákala, J., Polimene, L., de Mora, L., Artioli,
2054 Y., Allen, J.I., 2018. Assimilation of ocean-color plankton functional types
2055 to improve marine ecosystem simulations. *Journal of Geophysical Research*
2056 *Oceans* 123, 834–854. doi:10.1002/2017JC013490.

2057 Claustre, H., Antoine, D., Boehme, L., Boss, E., D’Ortenzio, F., Fanton D’Andon,
2058 O., Guinet, C., Gruber, N., Handegard, N.O., Hood, M., Johnson, K., Lampitt,
2059 R., LeTraon, P.Y., LeQuéré, C., Lewis, M., Perry, M.J., Platt, T., Roemmich, D.,
2060 Testor, P., Sathyendranath, S., Send, U., Yoder, J., 2010. Guidelines towards an
2061 integrated ocean observation system for ecosystems and biogeochemical cycles,
2062 in: Hall, J., Harrison, D.E., Stammer, D. (Eds.), *Proceedings of OceanObs’09:*
2063 *Sustained Ocean Observations and Information for Society* (Vol. 1), ESA
2064 Publication WPP-306. doi:10.5270/OceanObs09.pp.14.

2065 Claustre, H., Babin, M., Merien, D., Ras, J., Prieur, L., Dallot, S., Prasil, O.,
2066 Dousova, H., Moutin, T., 2005. Towards a taxon-specific parameterization of
2067 bio-optical models of primary production: A case study in the North Atlantic.
2068 *Journal of Geophysical Research* 110, C07S12. doi:10.1029/2004JC002634.

2069 Claustre, H., Johnson, K.S., Takeshita, Y., 2020. Observing the global ocean
2070 with Biogeochemical-Argo. *Annual Review of Marine Science* 12, 23–48.
2071 URL: <https://doi.org/10.1146/annurev-marine-010419-010956>, doi:10.1146/
2072 [annurev-marine-010419-010956](https://doi.org/10.1146/annurev-marine-010419-010956).

2073 Claustre, H., Morel, A., Babin, M., Cailliau, C., Marie, D., Marty, J.C., Tailliez, D.,
2074 Vaultot, D., 1999. Variability in particle attenuation and chlorophyll fluorescence
2075 in the tropical Pacific: Scales, patterns, and biogeochemical implications.
2076 *Journal of Geophysical Research: Oceans* 104, 3401–3422. URL: <https://doi.org/10.1029/98JC01334>, doi:10.1029/98JC01334.

2078 Coles, V.J., Wilson, C., Hood, R.R., 2004. Remote sensing of new production
2079 fuelled by nitrogen fixation. *Geophysical Research Letters* 31. URL: <https://doi.org/10.1029/2003GL019018>, doi:10.1029/2003GL019018.

2081 Corrigan, C.E., Roberts, G.C., Ramana, M.V., Kim, D., Ramanathan, V., 2008.
2082 Capturing vertical profiles of aerosols and black carbon over the Indian Ocean

2083 using autonomous unmanned aerial vehicles. *Atmospheric Chemistry and*
2084 *Physics* 8, 737–747. URL: <https://doi.org/10.5194/acp-8-737-2008>, doi:10.
2085 5194/acp-8-737-2008.

2086 Cullen, J.J., Davis, R.F., Huot, Y., 2012. Spectral model of depth-integrated
2087 water column photosynthesis and its inhibition by ultraviolet radiation. *Global*
2088 *Biogeochemical Cycles* 26, GB1011. doi:10.1029/2010GB003914.

2089 Cunningham, A., McKee, D., Craig, S., Tarran, G., Widdicombe, C., 2003. Fine-
2090 scale variability in phytoplankton community structure and inherent optical
2091 properties measured from an autonomous underwater vehicle. *Journal of*
2092 *Marine Systems* 43, 51–59. doi:10.1016/S0924-7963(03)00088-5.

2093 Curran, K., Brewin, R.J.W., Tilstone, G.H., Bouman, H.A., Hickman, A., 2018.
2094 Estimation of size-fractionated primary production from satellite ocean colour
2095 in UK shelf seas. *Remote Sensing* 10, 1389. URL: <https://doi.org/10.3390/rs10091389>,
2096 doi:10.3390/rs10091389.

2097 Cury, P.M., Shin, Y.J., Planque, B., Durant, J.M., Fromentin, J.M., Kramer-Schadt,
2098 S., Stenseth, N.C., Travers, M., Grimm, V., 2008. Ecosystem oceanography
2099 for global change in fisheries. *Trends in Ecology & Evolution* 23, 338–346.
2100 URL: [https://doi.org/10.1016/j.tree.2008.](https://doi.org/10.1016/j.tree.2008.02.005)
2101 02.005.

2102 Dall’Olmo, G., Boss, E., Behrenfeld, M., Westberry, T.K., Courties, C., Prieur,
2103 L., Pujo-Pay, M., Hardman-Mountford, N.J., Moutin, T., 2011. Inferring
2104 phytoplankton carbon and eco-physiological rates from diel cycles of spectral
2105 particulate beam-attenuation coefficient. *Biogeosciences* 8, 3423–3439. doi:10.
2106 5194/bg-8-3423-2011.

2107 Dall’Olmo, G., Dingle, J., Polimene, L., Brewin, R.J.W., Claustre, H., 2016.
2108 Substantial energy input to the mesopelagic ecosystem from the seasonal
2109 mixed-layer pump. *Nature Geoscience* 9, 820–823. doi:10.1038/ngeo2818.

2110 Dall’Olmo, G., Mork, K.A., 2014. Carbon export by small particles in the
2111 Norwegian Sea. *Geophysical Research Letters* 41, 2921–2927. doi:10.1002/
2112 2014GL059244.

2113 Dall’Olmo, G., Westberry, T.K., Behrenfeld, M.J., Boss, E., Slade, W.H., 2009.

2114 Significant contribution of large particles to optical backscattering in the open
2115 ocean. *Biogeosciences* 6, 947–967. doi:10.5194/bg-6-947-2009.

2116 Dall’Olmo, G., Brewin, R.J.W., Nencioli, F., Organelli, E., Lefering, I., McKee,
2117 D., Röttgers, R., Mitchell, C., Boss, E., Bricaud, A., Tilstone, G., 2017. De-
2118 termination of the absorption coefficient of chromophoric dissolved organic
2119 matter from underway spectrophotometry. *Optics Express* 25, A1079–A1095.
2120 doi:10.1364/OE.25.0A1079.

2121 Daniel, T., Manley, J., Trenaman, N., 2011. The Wave Glider: enabling a new
2122 approach to persistent ocean observation and research. *Ocean Dynamics* 61,
2123 1509–1520. URL: <https://doi.org/10.1007/s10236-011-0408-5>, doi:10.1007/
2124 s10236-011-0408-5.

2125 Daniels, C.J., Poulton, A.J., Balch, W.M., Marañón, E., Adey, T., Bowler, B.C.,
2126 Cermeño, P., Charalampopoulou, A., Crawford, D.W., Drapeau, D., Feng,
2127 Y., Fernández, A., Fernández, E., Fragoso, G.M., González, N., Graziano,
2128 L. M and, H.R., Holligan, P.M., Hopkins, J., Huete-Ortega, M., Hutchins,
2129 D.A., Lam, P.J., Lipsen, M.S., López-Sandoval, D.C., Loucaides, S., Marchetti,
2130 A., Mayers, K.M.J., Rees, A.P., Sobrino, C., Tynan, E., Tyrrell, T., 2018. A
2131 global compilation of coccolithophore calcification rates. *Earth System Science*
2132 *Data* 10, 1859–1876. URL: <https://doi.org/10.5194/essd-10-1859-2018>, doi:10.
2133 5194/essd-10-1859-2018.

2134 Daro, M.H., 1978. A simplified ^{14}C method for grazing measurements on natural
2135 planktonic populations. *Helgoländer wissenschaftliche Meeresuntersuchungen*
2136 31, 241.

2137 DeVries, T., Le Quéré, C., Andrews, A., Berthet, S., Hauck, J., Ilyina, T., Land-
2138 schützer, P., Lenton, A., Lima, I.D., Nowicki, M., Schwinger, J., Séférian, R.,
2139 2019. Decadal trends in the ocean carbon sink. *Proceedings of the National*
2140 *Academy of Sciences of the United States of America* 116, 11646–11651.
2141 doi:10.1073/pnas.1900371116.

2142 DeVries, T., Liang, J.H., Deutsch, C., 2014. A mechanistic particle flux model
2143 applied to the oceanic phosphorus cycle. *Biogeosciences* 11, 5381–5398.
2144 doi:10.5194/bg-11-5381-2014.

- 2145 DeVries, T., Weber, T., 2017. The export and fate of organic matter in the
2146 ocean: New constraints from combining satellite and oceanographic tracer
2147 observations. *Global Biogeochemical Cycles* 31, 535–555. doi:10.1002/
2148 2016GB005551.
- 2149 Dilling, L., Alldredge, A.L., 2000. Fragmentation of marine snow by swimming
2150 macrozooplankton: A new process impacting carbon cycling in the sea. *Deep
2151 Sea Research Part I: Oceanographic Research Papers* 47, 1227–1245. doi:10.
2152 1016/S0967-0637(99)00105-3.
- 2153 Donlon, C., Berruti, B., Buongiorno, A., Ferreira, M.H., Féménias, P. and Frerick,
2154 J., Goryl, P., Klein, U., Laur, H., Mavrocordatos, C., Nieke, J., Rebhan, H.,
2155 Seitz, B., Stroede, J., Sciarra, R., 2012. The Global Monitoring for Environment
2156 and Security (GMES) Sentinel-3 mission. *Remote Sensing of Environment*
2157 120, 37–57. doi:10.1016/j.rse.2011.07.024.
- 2158 Donlon, C., Robinson, I.S., Wimmer, W., Fisher, G., Reynolds, M., Edwards,
2159 R., Nightingale, T.J., 2008. An infrared sea surface temperature autonomous
2160 radiometer (ISAR) for deployment aboard volunteer observing ships (VOS).
2161 *Journal of Atmospheric and Oceanic Technology* 25, 93–113. doi:10.1175/
2162 2007JTECH0505.1.
- 2163 Druffel, E.R.M., Griffin, S.N., Coppola, A.I., Walker, B.D., 2016. Radiocarbon in
2164 dissolved organic carbon of the Atlantic Ocean. *Geophysical Research Letters*
2165 43, 5279–5286. doi:10.1002/2016GL068746.
- 2166 Druon, J.N., Hélaouët, P., Beaugrand, G., Fromentin, J.M., Palialexis, A.,
2167 Hoepffner, N., 2019. Satellite-based indicator of zooplankton distribution
2168 for global monitoring. *Scientific Reports* 9, 1–13. URL: [https://doi.org/10.
2169 1038/s41598-019-41212-2](https://doi.org/10.1038/s41598-019-41212-2), doi:10.1038/s41598-019-41212-2.
- 2170 Duforêt-Gaurier, L., Loisel, H., Dessailly, D., Nordkvist, K., Alvain, S., 2010.
2171 Estimates of particulate organic carbon over the euphotic depth from in situ
2172 measurements. Application to satellite data over the global ocean. *Deep Sea
2173 Research Part I: Oceanographic Research Papers* 57, 351–367. URL: [https:
2174 //doi.org/10.1016/j.dsr.2009.12.007](https://doi.org/10.1016/j.dsr.2009.12.007), doi:10.1016/j.dsr.2009.12.007.
- 2175 Dugdale, R.C., Goering, J.J., 1967. Uptake of new and regenerated forms of

2176 nitrogen in primary productivity. *Limnology and Oceanography* 12, 196–206.
2177 doi:10.4319/lo.1967.12.2.0196.

2178 Dunne, J.P., Armstrong, R.A., Gnanadesikan, A., Sarmiento, J.L., 2005. Empirical
2179 and mechanistic models for the particle export ratio. *Global Biogeochemical*
2180 *Cycles* 19, GB4026. doi:10.1029/2004GB002390.

2181 Durban, J.W., Moore, M.J., Chiang, G., Hickmott, L.S., Bocconcelli, A., Howes,
2182 G., Bahamonde, P.A., Perryman, W.L., LeRoi, D.J., 2016. Photogrammetry
2183 of blue whales with an unmanned hexacopter. *Marine Mammal Science* 32,
2184 1510–1515. doi:10.1111/mms.12328.

2185 Dutkiewicz, S., Hickman, A.E., Jahn, O., 2018. Modelling ocean colour derived
2186 Chlorophyll-a. *Biogeoscience* 15, 613–630. doi:10.5194/bg-15-613-2018.

2187 Dutkiewicz, S., Hickman, A.E., Jahn, O., Henson, S., Beaulieu, C., Moneir, E.,
2188 2019. Ocean colour signature of climate change. *Nature Communications* 10,
2189 578. doi:10.1038/s41467-019-08457-x.

2190 Eppley, R.W., 1972. Temperature and phytoplankton growth in the sea. *Fishery*
2191 *Bulletin* 70, 1063–1085.

2192 Eppley, R.W., Peterson, B.J., 1979. Particulate organic matter flux and planktonic
2193 new production in the deep ocean. *Nature* 282, 677–680. doi:10.1038/
2194 282677a0.

2195 Eppley, R.W., Stewart, E., Abbott, M.R., Heyman, U., 1985. Estimating
2196 ocean primary production from satellite chlorophyll. introduction to re-
2197 gional differences and statistics for the southern california bight. *Journal*
2198 *of Plankton Research* 7, 57–70. URL: <https://doi.org/10.1093/plankt/7.1.57>,
2199 doi:10.1093/plankt/7.1.57.

2200 Eriksen, C.C., Osse, T.J., Light, R.D., Wen, T., Lehman, T.W., Sabin, P.L., Ballard,
2201 J.W., Chiodi, A.M., 2001. Seaglider: a long-range autonomous underwater
2202 vehicle for oceanographic research. *IEEE Journal of Oceanic Engineering* 26,
2203 424–436. doi:10.1109/48.972073.

2204 Estapa, M.L., Feen, M.L., Breves, E., 2019. Direct observations of biological
2205 carbon export from profiling floats in the subtropical North Atlantic. *Global*
2206 *Biogeochemical Cycles* 33, 282–300. doi:10.1029/2018GB006098.

- 2207 Evers-King, H., Martinez-Vicente, V., Brewin, R.J.W., Dall’Olmo, G., Hick-
2208 man, A.E., Jackson, T., Kostadinov, T.S., Krasemann, H., Loisel, H., Röttgers,
2209 R., Roy, S., Stramski, D., Thomalla, S., Platt, T., Sathyendranath, S., 2017.
2210 Validation and intercomparison of ocean color algorithms for estimating par-
2211 ticulate organic carbon in the oceans. *Frontiers in Marine Science* 4, 251.
2212 doi:10.3389/fmars.2017.00251.
- 2213 Falkowski, P.G., Barber, R.T., Smetacek, V., 1998. Biogeochemical controls and
2214 feedbacks on ocean primary production. *Science* 281, 200–206. doi:10.1126/
2215 science.281.5374.200.
- 2216 Fedak, M., 2004. Marine animals as platforms for oceanographic sampling: a
2217 "winwin" situation for biology and operational oceanography. *Memoirs of*
2218 *National Institute of Polar Research*. Special issue 58, 133–147.
- 2219 Fedak, M.A., 2013. The impact of animal platforms on polar ocean observation.
2220 *Deep Sea Research Part II: Topical Studies in Oceanography* 88, 7–13. doi:10.
2221 1016/j.dsr2.2012.07.007.
- 2222 Feely, R.A., Sabine, C.L., Lee, K., Berelson, W., Kleypas, J., Fabry, V.J., Millero,
2223 F.J., 2004. Impact of anthropogenic CO₂ on the CaCO₃ system in the oceans.
2224 *Science* 305, 362–366. doi:10.1126/science.1097329.
- 2225 Fennel, K., Gehlen, M., Brasseur, P., Brown, C.W., Ciavatta, S., Cossarini, G.,
2226 Crise, A., Edwards, C., Ford, D., Friedrichs, M.A.M., Gregoire, M., Jones, E.,
2227 Kim, H.C., Lamouroux, J., Murtugudde, R., Perruche, C., 2019. Advancing
2228 marine biogeochemical and ecosystem reanalyses and forecasts as tools for
2229 monitoring and managing ecosystem health. *Frontiers in Marine Science* 6, 89.
2230 doi:10.3389/fmars.2019.00089.
- 2231 Ferrari, G.M., Dowell, M.D., Grossi, S., Targa, C., 1996. Relationship between
2232 the optical properties of chromophoric dissolved organic matter and total
2233 concentrations of dissolved organic carbon in the southern Baltic Sea region.
2234 *Marine Chemistry* 55, 299–316. URL: [https://doi.org/10.1016/S0304-4203\(96\)](https://doi.org/10.1016/S0304-4203(96)00061-8)
2235 [00061-8](https://doi.org/10.1016/S0304-4203(96)00061-8), doi:10.1016/S0304-4203(96)00061-8.
- 2236 Fichot, C., Kaiser, K., Hooker, S.B., Amon, R., Babin, M., Belanger, S., Walker,
2237 S., Benner, R., 2013. Pan-arctic distributions of continental runoff in the arctic

2238 ocean. Scientific Reports 3, 1053. URL: <https://doi.org/10.1038/srep01053>,
 2239 doi:10.1038/srep01053.

2240 Fichot, C.G., Benner, R., 2012. The spectral slope coefficient of chromophoric
 2241 dissolved organic matter ($S_{275-295}$) as a tracer of terrigenous dissolved organic
 2242 carbon in river-influenced ocean margins. Limnology and Oceanography 57,
 2243 1453–1466.

2244 Field, C.B., Behrenfeld, M.J., Randerson, J.T., Falkowski, P.G., 1998. Primary
 2245 production of the biosphere: integrating terrestrial and oceanic components.
 2246 Science 281, 237–240.

2247 Fogg, G.E., 1952. Extracellular products of phytoplankton and the estimation of
 2248 primary productivity. Rapp. P.-V. Reun., Cons, Int. Explor. Mer 144, 56–60.

2249 Ford, D., Barciela, R., 2017. Global marine biogeochemical reanalyses assimila-
 2250 ating two different sets of merged ocean colour products. Remote Sensing of
 2251 Environment 203, 40–54. doi:10.1016/j.rse.2017.03.040.

2252 Ford, T.E., Colwell, R.R., Rose, J.B., Morse, S.S., Rogers, D.J., Yates, T.L., 2009.
 2253 Using satellite images of environmental changes to predict infectious disease
 2254 outbreaks. Emerging Infectious Diseases 15, 1341–1346. doi:10.3201/eid/
 2255 1509.081334.

2256 Friedlingstein, P., Jones, M.W., O’Sullivan, M., Andrew, R.M., Hauck, J., Peters,
 2257 G.P., Peters, W., Pongratz, J., Sitch, S., Le Quéré, C., Bakker, D.C.E., Canadell,
 2258 J.G., Ciais, P., Jackson, R.B., Anthoni, P., Barbero, L., Bastos, A., Bastrikov,
 2259 V., Becker, M., Bopp, L., Buitenhuis, E., Chandra, N., Chevallier, F., Chini,
 2260 L.P., Currie, K.I., Feely, R.A., Gehlen, M., Gilfillan, D., Gkritzalis, T., Goll,
 2261 D.S., Gruber, N., Gutekunst, S., Harris, I., Haverd, V., Houghton, R.A., Hurtt,
 2262 G., Ilyina, T., Jain, A.K., Joetzjer, E., Kaplan, J.O., Kato, E., Klein Goldewijk,
 2263 K., Korsbakken, J.I., Landschützer, P., Lauvset, S.K., Lefèvre, N., Lenton, A.,
 2264 Lienert, S., Lombardozi, D., Marland, G., McGuire, P.C., Melton, J.R., Metzl,
 2265 N., Munro, D.R., Nabel, J.E.M.S., Nakaoka, S.I., Neill, C., Omar, A.M., Ono,
 2266 T., Peregon, A., Pierrot, D., Poulter, B., Rehder, G., Resplandy, L., Robertson,
 2267 E., Rödenbeck, C., Séférian, R., Schwinger, J., Smith, N., Tans, P.P., Tian, H.,
 2268 Tilbrook, B., Tubiello, F.N., van der Werf, G.R., Wiltshire, A.J., Zaehle, S.,

2269 2019. Global carbon budget 2019. *Earth System Science Data* 11, 1783–1838.
2270 doi:10.5194/essd-11-1783-2019.

2271 Friedrich, T., Oschlies, A., 2009. Neural network-based estimates of North
2272 Atlantic surface pCO₂ from satellite data: A methodological study. *Journal of*
2273 *Geophysical Research: Oceans* 114, C03020. doi:10.1029/2007JC00464.

2274 Friedrichs, M.A., Hood, R.R., Wiggert, J.D., 2006. Ecosystem model complexity
2275 versus physical forcing: Quantification of their relative impact with assimilated
2276 Arabian Sea data. *Deep Sea Research Part II: Topical Studies in Oceanography*
2277 53, 576–600. doi:10.1016/j.dsr2.2006.01.026.

2278 Friedrichs, M.A.M., Carr, M.E., Barber, R.T., Scardi, M., Antoine, D., Armstrong,
2279 R.A., Asanuma, I., Behrenfeld, M., Buitenhuis, E.T., Chai, F., Christian, J.R.,
2280 Ciotti, A.M., Doney, S.C., Dowell, M., Dunne, J., Gentili, B., Gregg, W.W.,
2281 Hoepffner, N., Ishizaka, J., Kameda, T., Lima, I., Marra, J., Mélin, F., Moore,
2282 J.K., Morel, A., O'Malley, R.T.O., O'Reilly, J.E., Saba, V.S., Schmeltz, M.,
2283 Smyth, T.J., Tjiputraw, J., Waters, K., Westberry, T.K., Winguth, A., 2009.
2284 Assessing the uncertainties of model estimates of primary productivity in the
2285 tropical Pacific Ocean. *Journal of Marine Systems* 76, 113–133. doi:10.1016/
2286 j.jmarsys.2008.05.010.

2287 Frouin, R., Ramon, D., Boss, E., Jolivet, D., Compiègne, M., Tan, J., Bouman, H.,
2288 Jackson, T., Franz, B., Platt, T., Sathyendranath, S., 2018. Satellite radiation
2289 products for ocean biology and biogeochemistry: Needs, state-of-the-art, gaps,
2290 development priorities, and opportunitie. *Frontiers in Marine Science* 5, 3.
2291 URL: <https://www.frontiersin.org/article/10.3389/fmars.2018.00003>, doi:10.
2292 3389/fmars.2018.00003.

2293 Frouin, R.J., Franz, B.A., Ibrahim, A., Knobelspiesse, K., Ahmad, Z., Cairns,
2294 B., Chowdhary, J., Dierssen, H.M., Tan, J., Dubovik, O., Huang, X., Davis,
2295 A.B., Kalashnikova, O., Thompson, D.R., Remer, L.A., Boss, E., Coddington,
2296 O., Deschamps, P.Y., Gao, B.C., Gross, L., Hasekamp, O., Omar, A., Pelletier,
2297 B., Ramon, D., Steinmetz, F., Zhai, P.W., 2019. Atmospheric correction of
2298 satellite ocean-color imagery during the PACE era. *Frontiers in Earth Science*
2299 7, 145. URL: <https://www.frontiersin.org/article/10.3389/feart.2019.00145>,

2300 doi:10.3389/feart.2019.00145.

2301 Fuhrman, J.A., Azam, F., 1980. Bacterioplankton secondary production estimates
2302 for coastal waters of British Columbia, Antarctica, and California. *Applied and*
2303 *Environmental Microbiology* 30, 1085–1095.

2304 Fukuda, R., Ogawa, H., Nagata, T., Koike, I., 1998. Direct determination of carbon
2305 and nitrogen contents of natural bacterial assemblages in marine environments.
2306 *Applied and Environmental Microbiology* 64, 3352–3358. URL: [https://aem.](https://aem.asm.org/content/64/9/3352)
2307 [asm.org/content/64/9/3352](https://aem.asm.org/content/64/9/3352).

2308 Gallienne, C.P., Robins, D.B., Pilgrim, D.A., 1996. Measuring abundance and
2309 size distribution of zooplankton using the optical plankton counter in underway
2310 mode. *Underwater Technology* 21, 15–21.

2311 Gardner, W., Walsh, I., Richardson, M.J., 1993. Biophysical forcing of particle
2312 production and distribution during a spring bloom in the North Atlantic. *Deep*
2313 *Sea Research Part I: Oceanographic Research Papers* 40, 171–195. doi:10.
2314 1016/0967-0645(93)90012-C.

2315 Gardner, W.D., Mishonov, A.V., Richardson, M.J., 2006. Global POC concentra-
2316 tions from in-situ and satellite data. *Deep Sea Research Part II: Topical Studies*
2317 *in Oceanography* 53, 718–740. URL: [https://doi.org/10.1016/j.dsr2.2006.01.](https://doi.org/10.1016/j.dsr2.2006.01.029)
2318 [029](https://doi.org/10.1016/j.dsr2.2006.01.029), doi:10.1016/j.dsr2.2006.01.029.

2319 Gentemann, C.L., Scott, J.P., Mazzini, P.L., Pianca, C., Akella, S., Minnett,
2320 P.J., Cornillon, P., Fox-Kemper, B., Cetinić, I., Chin, T.M., Gomez-Valdes, J.,
2321 Vazquez-Cuervo, J., Tsontos, V., Yu, L., Jenkins, R., De Halleux, S., Peacock,
2322 D., Cohen, N., 2020. Saildrone: adaptively sampling the marine environment.
2323 *Bulletin of the American Meteorological Society* URL: [https://doi.org/10.1175/](https://doi.org/10.1175/BAMS-D-19-0015.1)
2324 [BAMS-D-19-0015.1](https://doi.org/10.1175/BAMS-D-19-0015.1), doi:10.1175/BAMS-D-19-0015.1.

2325 Giering, S.L.C., Cavan, E.L., Basedow, S.L., Briggs, N., Burd, A.B., Darroch,
2326 L.J., Guidi, L., Irisson, J.O., Iversen, M.H., Kiko, R., Lindsay, D., Marcolin,
2327 C.R., McDonnell, A.M.P., Möller, K.O., Passow, U., Thomalla, S., Trull, T.W.,
2328 Waite, A.M., 2020. Sinking organic particles in the ocean—Flux estimates
2329 from in situ optical devices. *Frontiers in Marine Science* 6, 834. URL: [https://](https://www.frontiersin.org/article/10.3389/fmars.2019.00834)
2330 [www.frontiersin.org/article/10.3389/fmars.](https://www.frontiersin.org/article/10.3389/fmars.2019.00834)

2331 2019.00834.

2332 Regaudie-de Gioux, A., Lasternas, S., Agustí, S., Duarte, C.M., 2014. Com-
2333 paring marine primary production estimates through different methods and
2334 development of conversion equations. *Frontiers in Marine Science* 1, 19.
2335 doi:10.3389/fmars.2014.00019.

2336 Gittings, J.A., Raitsos, D.E., Kheireddine, M., Racault, M.F., Claustre, H., Hoteit,
2337 I., 2019. Evaluating tropical phytoplankton phenology metrics using contem-
2338 porary tools. *Scientific Reports* 9, 674. doi:10.1038/s41598-018-37370-4.

2339 Gledhill, D.K., Wanninkhof, R., Millero, F.J., Eakin, M., 2008. Ocean acidifi-
2340 cation of the Greater Caribbean Region 1996-2006. *Journal of Geophysical*
2341 *Research: Oceans* 113, C10031. doi:10.1029/2007JC004629.

2342 Goes, J.I., Saino, T., Oaku, H., Ishizaka, J., Wong, C.S., Nojiri, Y., 2000.
2343 Basin scale estimates of sea surface nitrate and new production from re-
2344 motely sensed sea surface temperature and chlorophyll. *Geophysical Re-*
2345 *search Letters* 27, 1263–1266. URL: <https://doi.org/10.1029/1999GL002353>,
2346 doi:10.1029/1999GL002353.

2347 Goldthwait, S., Yen, J., Brown, J., Alldredge, A., 2004. Quantification of marine
2348 snow fragmentation by swimming euphausiids. *Limnology and Oceanography*
2349 49, 940–952. doi:10.4319/lo.2004.49.4.0940.

2350 Gomez-Pereira, P.R., Fuchs, B.M., Alonso, C., Oliver, M.J., Van Beusekom,
2351 J.E., Amann, R., 2010. Distinct flavobacterial communities in contrasting
2352 water masses of the North Atlantic ocean. *The ISME journal* 4, 472–487.
2353 doi:10.1038/ismej.2009.142.

2354 Gordon, H.R., Boynton, G.C., Balch, W.M., Groom, S.B., Harbour, D.S., Smyth,
2355 T.J., 2001. Retrieval of coccolithophore calcite concentration from SeaWiFS
2356 imagery. *Geophysical Research Letters* 28, 1587–1590. URL: [https://doi.org/](https://doi.org/10.1029/2000GL012025)
2357 [10.1029/2000GL012025](https://doi.org/10.1029/2000GL012025), doi:10.1029/2000GL012025.

2358 Gorsky, G., Picheral, M., Stemann, L., 2000. Use of the underwater video pro-
2359 filer for the study of aggregate dynamics in the North Mediterranean. *Estuarine,*
2360 *Coastal and Shelf Science* 50, 121–128. doi:10.1006/ecss.1999.0539.

2361 Graff, J.R., Westberry, T.K., Milligan, A.J., Brown, M.B., Dall’Olmo, G., van

- 2362 Dongen-Vogels, V., Reifel, K.M., Behrenfeld, M.J., 2015. Analytical phy-
2363 toplankton carbon measurements spanning diverse ecosystems. *Deep Sea*
2364 *Research Part I: Oceanographic Research Papers* 102, 16–25. doi:10.1016/j.
2365 dsr.2015.04.006.
- 2366 Gregg, W.W., 2001. Tracking the SeaWiFS record with a coupled physi-
2367 cal/biogeochemical/radiative model of the global oceans. *Deep Sea Re-*
2368 *search Part II: Topical Studies in Oceanography* 49, 81–105. doi:10.1016/
2369 S0967-0645(01)00095-9.
- 2370 Gregg, W.W., 2008. Assimilation of SeaWiFS ocean chlorophyll data into a three-
2371 dimensional global ocean model. *Journal of Marine Systems* 69, 205–225.
2372 doi:10.1016/j.jmarsys.2006.02.015.
- 2373 Gregg, W.W., Casey, N.W., Rousseaux, C.S., 2014. Sensitivity of simulated
2374 global ocean carbon flux estimates to forcing by reanalysis products. *Ocean*
2375 *Modelling* 80, 24–35. doi:10.1016/j.ocemod.2014.05.002.
- 2376 Gregg, W.W., Rousseaux, C.S., 2019. Global ocean primary production trends in
2377 the modern ocean color satellite record (1998-2015). *Environmental Research*
2378 *Letters* 14, 124011. doi:10.1088/1748-9326/ab4667.
- 2379 Gregg, W.W., Rousseaux, C.S., Franz, B.A., 2017. Global trends in ocean
2380 phytoplankton: a new assessment using revised ocean colour data. *Remote*
2381 *Sensing Letters* 8, 1102–1111. doi:10.1080/2150704X.2017.1354263.
- 2382 GREMPA, 1988. Satellite (AVHRR/NOAA-9) and ship studies of a coccol-
2383 ithophorid bloom in the Western English Channel. *Marine Nature* 1, 1–14.
- 2384 Grimes, D.J., Ford, T.E., Colwell, R.R., Baker-Austin, C., Martinez-Urtaza, J.,
2385 Subramaniam, A., Capone, D.G., 2014. Viewing marine bacteria, their activity
2386 and response to environmental drivers from orbit. *Microbial Ecology* 67,
2387 489–500. URL: <https://doi.org/10.1007/s00248-013-0363-4>, doi:10.1007/
2388 s00248-013-0363-4.
- 2389 Groom, S., Sathyendranath, S., Ban, Y., Bernard, S., Brewin, R.J.W., Brotas, V.,
2390 Brockmann, C., Chauhan, P., Choi, J., Chuprin, A., Ciavatta, S., Cipollini, P.,
2391 Donlon, C., Franz, B., He, X., Hirata, T., Jackson, T., Kampel, M., Krasemann,
2392 H., Lavender, S., Pardo-Martinez, S., Mélin, F., Platt, T., Santoleri, R., Skakala,

- 2393 J., Schaeffer, B., Smith, M., Steinmetz, F., Valente, A., Wang, M., 2019.
2394 Satellite ocean colour: Current status and future perspective. *Frontiers in*
2395 *Marine Science* 6, 485. URL: <https://www.frontiersin.org/article/10.3389/fmars.2019.00485>, doi:10.3389/fmars.2019.00485.
- 2397 Groom, S.B., Holligan, P.M., 1987. Remote sensing of coccolithophore
2398 blooms. *Advances in Space Research* 7, 73–78. URL: [https://doi.org/10.1016/0273-1177\(87\)90166-9](https://doi.org/10.1016/0273-1177(87)90166-9), doi:10.1016/0273-1177(87)90166-9.
- 2400 Grossart, H.P., Thorwest, M., Plitzko, I., Brinkhoff, T., Simon, M., Zeeck, A.,
2401 2009. Production of a blue pigment (Glaukothalin) by marine *Rheinheimera spp.*
2402 *International journal of Microbiology* 2009, 1–7. doi:10.1155/2009/701735.
- 2403 Gruber, N., Landschützer, P., Lovenduski, N.S., 2019. The variable southern
2404 ocean carbon sink. *Annual Review of Marine Science* 11, 159–186. doi:10.
2405 1146/annurev-marine-121916-063407.
- 2406 Guihen, D., Fielding, S., Murphy, E.J., Heywood, K.J., Griffiths, G., 2014. An
2407 assessment of the use of ocean gliders to undertake acoustic measurements of
2408 zooplankton: the distribution and density of Antarctic krill (*Euphausia superba*)
2409 in the Weddell Sea. *Limnology and Oceanography: Methods* 12, 373–389.
2410 URL: <https://doi.org/10.4319/lom.2014.12.373>, doi:10.4319/lom.2014.12.
2411 373.
- 2412 Gülzow, W., Rehder, G., Schneider von Deimling, J., Seifert, S., Tóth, Z., 2013.
2413 One year of continuous measurements constraining methane emissions from
2414 the Baltic Sea to the atmosphere using a ship of opportunity. *Biogeosciences*
2415 10, 81–99. doi:10.4319/lom.2011.9.176.
- 2416 Haëntjens, N., Della, P.A., Briggs, N., Karp-Boss, L., Gaube, P., Claustre, H.,
2417 Boss, E., 2020. Detecting mesopelagic organisms using biogeochemical-Argo
2418 floats. *Geophysical Research Letters* e2019GL086088.
- 2419 Haney, J.F., 1971. An in situ method for the measurement of zooplankton grazing
2420 rates. *Limnology and Oceanography* 16, 970–977. doi:10.4319/lo.1971.16.
2421 6.0970.
- 2422 Hansell, D.A., 2013. Recalcitrant dissolved organic carbon frac-
2423 tions. *Annual Review of Marine Science* 5, 421–445. URL:

2424 <https://doi.org/10.1146/annurev-marine-120710-100757>, doi:10.1146/
2425 annurev-marine-120710-10075.

2426 Hansell, D.A., Carlson, C., 2013. Localised refractory dissolved organic carbon
2427 sinks in the deep ocean. *Global Biogeochemical Cycles* 27, 705–710.

2428 Harcourt, R., Sequeira, A.M.M., Zhang, X., Roquet, F., Komatsu, K., He-
2429 upel, M., McMahon, C., Whoriskey, F., Meekan, M., Carroll, G., Brodie,
2430 S., Simpfendorfer, C., Hindell, M., Jonsen, I., Costa, D.P., Block, B., Muelbert,
2431 M., Woodward, B., Weise, M., Aarestrup, K., Biuw, M., Boehme, L., Bograd,
2432 S.J., Cazau, D., Charrassin, J.B., Cooke, S.J., Cowley, P., de Bruyn, P.J.N.,
2433 Jeanniard du Dot, T., Duarte, C., Eguluz, V.M., Ferreira, L.C., Fernández-
2434 Gracia, J., Goetz, K., Goto, Y., Guinet, C., Hammill, M., Hays, G.C., Hazen,
2435 E.L., Hückstädt, L.A., Huveneers, C., Iverson, S., Jaaman, S.A., Kittiwat-
2436 tanawong, K., Kovacs, K.M., Lydersen, C., Moltmann, T., Naruoka, M.,
2437 Phillips, L., Picard, B., Queiroz, N., Reverdin, G., Sato, K., Sims, D.W.,
2438 Thorstad, E.B., Thums, M., Treasure, A.M., Trites, A.W., Williams, G.D.,
2439 Yonehara, Y., Fedak, M.A., 2019. Animal-borne telemetry: An integral
2440 component of the ocean observing toolkit. *Frontiers in Marine Science*
2441 6, 326. URL: <https://www.frontiersin.org/article/10.3389/fmars.2019.00326>,
2442 doi:10.3389/fmars.2019.00326.

2443 Harrison, W.G., Platt, T., Lewis, M.R., 1987. F-ratio and its relationship to
2444 ambient nutrient concentration in coastal waters. *Journal of Plankton Research*
2445 9, 225–248.

2446 Hedges, J.I., 1992. Global biogeochemical cycles: progress and problems. *Marine*
2447 *Chemistry* , 67–93.

2448 Heldal, M., Scanlan, D.J., Norland, S., Thingstad, F., Mann, N.H., 2003. Element-
2449 tal composition of single cells of various strains of marine *Prochlorococcus*
2450 and *Synechococcus* using X-ray microanalysis. *Limnology and Oceanography*
2451 5, 1732–1743. doi:10.4319/lo.2003.48.5.1732.

2452 Hemsley, V.S., Smyth, T.J., Martin, A.P., Frajka-Williams, E., Thompson, A.F.,
2453 Damerell, G., Painter, S.C., 2015. Estimating oceanic primary production
2454 using vertical irradiance and chlorophyll profiles from ocean gliders in the

2455 north atlantic. *Environmental Science & Technology* 49, 11612–11621. URL:
2456 <https://doi.org/10.1021/acs.est.5b00608>, doi:10.1021/acs.est.5b00608.

2457 Henson, S.A., Sanders, R., Madsen, E., 2012. Global patterns in efficiency
2458 of particulate organic carbon export and transfer to the deep ocean. *Global*
2459 *Biogeochemical Cycles* 26, GB1028. doi:10.1029/2011gb004099.

2460 Henson, S.A., Sanders, R., Madsen, E., Morris, P.J., Le Moigne, F., Quartly, G.D.,
2461 2011. A reduced estimate of the strength of the ocean’s biological carbon pump.
2462 *Geophysical Research Letters* 38, L04606. doi:10.1029/2011GL046735.

2463 Hirata, T., Hardman-Mountford, N.J., Barlow, R., Lamont, T., Brewin, R.J.W.,
2464 Smyth, T., Aiken, J., 2009. An inherent optical property approach to the estima-
2465 tion of size-specific photosynthetic rates in eastern boundary upwelling zones
2466 from satellite ocean colour: an initial assessment. *Progress in Oceanography*
2467 83, 393–397. doi:10.1016/j.pocean.2009.07.019.

2468 Hirata, T., Hardman-Mountford, N.J., Brewin, R.J.W., 2012. Comparing Satellite-
2469 Based Phytoplankton Classification Methods. *EOS, Transactions American*
2470 *Geophysical Union* 93, 59–60. doi:10.1029/2012E0060008.

2471 Holligan, P.M., Viollier, M., Harbour, D.S., Camus, P., Champagne-Philippe,
2472 M., 1983. Satellite and ship studies of coccolithophore production along a
2473 continental shelf edge. *Nature* 304, 339–342. URL: [https://doi.org/10.1038/](https://doi.org/10.1038/304339a0)
2474 [304339a0](https://doi.org/10.1038/304339a0), doi:10.1038/304339a0.

2475 Hollmann, R., Merchant, C.J., Saunders, R., Downy, C., Buchwitz, M., Cazenave,
2476 A., Chuvieco, E., Defourny, P., de Leeuw, G., Forsberg, R., Holzer-Popp, T.,
2477 2013. The ESA climate change initiative: Satellite data records for essential
2478 climate variables. *Bulletin of the American Meteorological Society* 94, 1541–
2479 1552. doi:10.1175/BAMS-D-11-00254.1.

2480 Hopkins, J., Henson, S.A., Poulton, A.J., Balch, W.M., 2019. Regional char-
2481 acteristics of the temporal variability in the global particulate inorganic
2482 carbon inventory. *Global Biogeochemical Cycles* 33, 1328–1338. URL:
2483 <https://doi.org/10.1029/2019GB006300>, doi:10.1029/2019GB006300.

2484 Hu, C., Carder, K.L., Muller-Karger, F.E., 2000. Atmospheric correction of Sea-
2485 WiFS imagery over turbid coastal waters: a practical method. *Remote Sensing*

2486 of Environment 74, 195–206. doi:10.1016/S0034-4257(00)00080-8.

2487 Iglesias-Rodríguez, M.D., Brown, C.W., Doney, S.C., Kleypas, J., Kolber, D.,
2488 Kolber, Z., Hayes, P.K., Falkowski, P.G., 2002. Representing key phyto-
2489 plankton functional groups in ocean carbon cycle models: Coccolithophorids.
2490 Global Biogeochemical Cycles 16, 47–1–47–20. URL: [https://doi.org/10.1029/
2491 2001GB001454](https://doi.org/10.1029/2001GB001454), doi:10.1029/2001GB001454.

2492 IOCCG, 2000. Remote Sensing of Ocean Colour in Coastal, and Other Optically
2493 Complex waters. Technical Report. Sathyendranath, S. (e.d.), Reports of the
2494 International Ocean-Colour Coordinating Group, No. 3, IOCCG, Dartmouth,
2495 Canada.

2496 IOCCG, 2014. Phytoplankton Functional Types from Space. Technical Report.
2497 Sathyendranath, S. (e.d.), Reports of the International Ocean-Colour Coordi-
2498 nating Group, No. 15, IOCCG, Dartmouth, Canada.

2499 IOCCG, 2019. Uncertainties in Ocean Colour Remote Sensing. Technical Re-
2500 port. Mélin, F. (e.d.), Reports of the International Ocean-Colour Coordinating
2501 Group, No. 18, IOCCG, Dartmouth, Canada. URL: [http://dx.doi.org/10.25607/
2502 OBP-696](http://dx.doi.org/10.25607/OBP-696).

2503 IOCCG, 2020. Synergy between Ocean Colour and Biogeochemical/Ecosystem
2504 Models. Technical Report. Dutkiewicz, S. (ed.), IOCCG Report Series, No. 19,
2505 International Ocean Colour Coordinating Group, Dartmouth, Canada. URL:
2506 <http://dx.doi.org/10.25607/OBP-711>.

2507 Jackson, T., Sathyendranath, S., Mélin, F., 2017a. An improved optical clas-
2508 sification scheme for the Ocean Colour Essential Climate Variable and its
2509 applications. Remote Sensing of Environment 203, 152–161. URL: <https://doi.org/10.1016/j.rse.2017.03.036>, doi:10.1016/j.rse.2017.03.036.

2511 Jackson, T., Sathyendranath, S., Platt, T., 2017b. An exact solution for modeling
2512 photoacclimation of the carbon-to-chlorophyll ratio in phytoplankton. Frontiers
2513 in Marine Science 4, 283. URL: [https://www.frontiersin.org/article/10.3389/
2514 fmars.2017.00283](https://www.frontiersin.org/article/10.3389/fmars.2017.00283), doi:10.3389/fmars.2017.00283.

2515 Jacobson, A.R., Mikaloff Fletcher, S.E., Gruber, N., Sarmiento, J.L., Gloor, M.,
2516 2007. A joint atmosphere-ocean inversion for surface fluxes of carbon dioxide:

- 2517 1. Methods and global-scale fluxes. *Global Biogeochemical Cycles* 21, GB1019.
2518 doi:10.1029/2005GB002556.
- 2519 Jamet, C., Ibrahim, A., Ahmad, Z., Angelini, F., Babin, M., Behrenfeld, M.J.,
2520 Boss, E., Cairns, B., Churnside, J., Chowdhary, J., Davis, A.B., Dionisi, D.,
2521 Duforêt-Gaurier, L., Franz, B., Frouin, R., Gao, M., Gray, D., Hasekamp,
2522 O., He, X., Hostetler, C., Kalashnikova, O.V., Knobelspiesse, K., Lacour,
2523 L., Loisel, H., Martins, V., Rehm, E., Remer, L., Sanhaj, I., Stamnes, K.,
2524 Stamnes, S., Victori, S., Werdell, J., Zhai, P.W., 2019. Going beyond standard
2525 ocean color observations: Lidar and polarimetry. *Frontiers in Marine Science*
2526 6, 251. URL: <https://www.frontiersin.org/article/10.3389/fmars.2019.00251>,
2527 doi:10.3389/fmars.2019.00251.
- 2528 Jennings, S., Mélin, F., Blanchard, J.L., Forster, R.M., Dulvy, N.K., Wilson,
2529 R.W., 2008. Global-scale predictions of community and ecosystem properties
2530 from simple ecological theory. *Proceedings of the Royal Society B: Biologi-*
2531 *cal Sciences* 275, 1375–1383. URL: <https://doi.org/10.1098/rspb.2008.0192>,
2532 doi:10.1098/rspb.2008.0192.
- 2533 Johnson, K.S., Berelson, W.M., Boss, E.S., Chase, Z., Claustre, H., Emerson,
2534 S.R., Gruber, N., Körtzinger, A., Perry, M.J., Riser, S.C., 2009. Observing bio-
2535 geochemical cycles at global scales with profiling floats and gliders: prospects
2536 for a global array. *Oceanography* 22, 216–225.
- 2537 Johnson, K.S., Coletti, L.J., Jannasch, H.W., Sakamoto, C.M., Swift, D.D., Riser,
2538 S.C., 2013. Long-term nitrate measurements in the ocean using the In Situ
2539 Ultraviolet Spectrophotometer: sensor integration into the Apex profiling float.
2540 *Journal of Atmospheric and Oceanic Technology* 30, 1854–1866. URL: <https://doi.org/10.1175/JTECH-D-12-00221.1>, doi:10.1175/JTECH-D-12-00221.
2541 1.
2542
- 2543 Johnston, D.W., 2019. Unoccupied aircraft systems in marine science
2544 and conservation. *Annual Review of Marine Science* 11, 439–463.
2545 URL: <https://doi.org/10.1146/annurev-marine-010318-095323>, doi:10.1146/
2546 [annurev-marine-010318-095323](https://doi.org/10.1146/annurev-marine-010318-095323).
- 2547 Jónasdóttir, S.H., Visser, A.W., Richardson, K., Heath, M.R., 2015. Seasonal

2548 copepod lipid pump promotes carbon sequestration in the deep North Atlantic.
2549 Proceedings of the National Academy of Sciences 112, 12122–12126.

2550 Jones, E.M., Baird, M.E., Mongin, M., Parslow, J., Skerratt, J., Lovell, J., Margve-
2551 lashvili, N., Matear, R.J., Wild-Allen, K., Robson, B., Rizwi, F., Oke, P., King,
2552 E., Schroeder, T., Steven, A., Taylor, J., 2016. Use of remote-sensing reflectance
2553 to constrain a data assimilating marine biogeochemical model of the Great Bar-
2554 rier Reef. *Biogeosciences* 13, 6441–6469. doi:10.5194/bg-13-6441-2016.

2555 Jönsson, B.F., Salisbury, J.E., Mahadevan, A., 2009. Extending the use and inter-
2556 pretation of ocean satellite data using Lagrangian modelling. *International Jour-
2557 nal of Remote Sensing* 30, 3331–3341. doi:10.1080/01431160802558758.

2558 Kaiser, K., Benner, R., 2012. Organic matter transformations in the upper
2559 mesopelagic zone of the North Pacific: Chemical composition and linkages to
2560 microbial community structure. *Journal of Geophysical Research: Oceans* 117,
2561 1–12. doi:10.1029/2011JC007141.

2562 Keates, T.R., Kudela, R.M., Holser, R.R., Hückstädt, L.A., Simmons, S.E., Costa,
2563 D.P., 2020. Chlorophyll fluorescence as measured in situ by animal-borne
2564 instruments in the northeastern Pacific Ocean. *Journal of Marine Systems* 203,
2565 103265. URL: <https://doi.org/10.1016/j.jmarsys.2019.103265>, doi:10.1016/j.jmarsys.2019.103265.

2567 Kheireddine, M., Antoine, D., 2014. Diel variability of the beam attenuation and
2568 backscattering coefficients in the northwestern Mediterranean Sea (BOUS-
2569 SOLE site). *Journal of Geophysical Research: Oceans* 119, 5465–5482.
2570 doi:10.1002/2014JC010007.

2571 Kirchman, D., 1999. Phytoplankton death in the sea. *Nature* 398, 293–294.
2572 doi:10.1038/18570.

2573 Kondrik, D., Kazakov, E., Pozdnyakov, D., 2019. A synthetic satellite dataset of
2574 the spatio-temporal distributions of *Emiliana huxleyi* blooms and their impacts
2575 on Arctic and sub-Arctic marine environments (1998-2016). *Earth System
2576 Science Data* 11, 119–128. doi:10.5194/essd-11-119-2019.

2577 Kostadinov, T.S., Cabré, A., Vedantham, H., Marinov, I., Bracher, A., Brewin,
2578 R.J.W., Bricaud, A., Hirata, T., Hirawake, T., Hardman-Mountford, N.J., Mouw,

2579 C., Roy, S., Uitz, J., 2017. Inter-comparison of phytoplankton functional type
2580 phenology metrics derived from ocean color algorithms and earth system
2581 models. *Remote Sensing of Environment* 190, 162–177. URL: [https://doi.org/](https://doi.org/10.1016/j.rse.2016.11.014)
2582 [10.1016/j.rse.2016.11.014](https://doi.org/10.1016/j.rse.2016.11.014), doi:10.1016/j.rse.2016.11.014.

2583 Kostadinov, T.S., Milutinović, S., Marinov, I., Cabré, A., 2016. Carbon-based phy-
2584 toplankton size classes retrieved via ocean color estimates of the particle size
2585 distribution. *Ocean Sciences* 12, 561–575. doi:10.5194/os-12-561-2016.

2586 Kostadinov, T.S., Siegel, D.A., Maritorena, S., 2009. Retrieval of the particle size
2587 distribution from satellite ocean color observations. *Journal of Geophysical*
2588 *Research* 114, C09015. doi:10.1029/2009jc005303.

2589 Kostadinov, T.S., Siegel, D.A., Maritorena, S., Guillocheau, N., 2007. Ocean
2590 color observations and modeling for an optically complex site: Santa Barbara
2591 Channel, California, USA. *Journal of Geophysical Research: Oceans* 112,
2592 C07011. doi:10.1029/2006JC003526.

2593 Kovač, Ž., Platt, T., Ninčević Gladan, Ž., Morović, M., Sathyendranath, S.,
2594 Raitsos, D.E., Grbec, B., Matic, F., Veža, J., 2018a. A 55-year time series
2595 station for primary production in the Adriatic Sea: Data correction, extraction
2596 of photosynthesis parameters and regime shifts. *Remote Sensing* 10, 1460.
2597 doi:10.3390/rs10091460.

2598 Kovač, Ž., Platt, T., Sathyendranath, S., Lomas, M.W., 2018b. Extraction of
2599 photosynthesis parameters from time series measurements of in situ production:
2600 Bermuda atlantic time-series study. *Remote Sensing* 10, 915. URL: <https://doi.org/10.3390/rs10060915>, doi:10.3390/rs10060915.

2602 Kulk, G., Platt, T., Dingle, J., Jackson, T., Jönsson, B.F., Bouman, H.A., Babin, M.,
2603 Brewin, R.J.W., Doblin, M., Estrada, M., Figueiras, F.G., Furuya, K., González-
2604 Benítez, N., Gudfinnsson, H.G., Gudmundsson, K., Huang, B., Isada, T., Kovač,
2605 Ž., Lutz, V.A., Marañón, E., Raman, M., Richardson, K., Rozema, P.D., Poll,
2606 W.H., Segura, V., Tilstone, G.H., Uitz, J., Dongen-Vogels, V., Yoshikawa, T.,
2607 Sathyendranath, S., 2020. Primary production, an index of climate change in
2608 the ocean: Satellite-based estimates over two decades. *Remote Sensing* 12,
2609 826. URL: <https://doi.org/10.3390/rs12050826>, doi:10.3390/rs12050826.

2610 Kuring, N., Lewis, M.R., Platt, T., O'Reilly, J.E., 1990. Satellite-derived estimates
2611 of primary production on the northwest Atlantic continental shelf. *Continental*
2612 *Shelf Research* 10, 461–484. URL: [https://doi.org/10.1016/0278-4343\(90\)](https://doi.org/10.1016/0278-4343(90)90050-V)
2613 [90050-V](https://doi.org/10.1016/0278-4343(90)90050-V), doi:10.1016/0278-4343(90)90050-V.

2614 Lacour, L., Ardyna, M., Stec, K., Claustre, H., Prieur, L., Ribera D'Alcala,
2615 M., Iudicone, D., 2017. Unexpected winter phytoplankton blooms in the
2616 North Atlantic Subpolar Gyre. *Nature Geoscience* 10, 836–839. URL: <https://doi.org/10.1038/ngeo3035>, doi:10.1038/NGEO3035.

2618 Lacour, L., Briggs, N., Claustre, H., Ardyna, M., Dall'Olmo, G., 2019. The
2619 intraseasonal dynamics of the mixed layer pump in the subpolar north atlantic
2620 ocean: A biogeochemical-argo float approach. *Global Biogeochemical Cycles*
2621 33, 266–281. doi:10.1029/2018GB005997.

2622 Lancelot, C., 1979. Gross excretion rates of natural marine phytoplankton and het-
2623 erotrophic uptake of excreted products in the southern North Sea, as determined
2624 by short-term kinetics. *Marine Ecological Progress Series* 1, 179–186.

2625 Land, P.E., Bailey, T.C., Taberner, M., Pardo, S., Sathyendranath, S., Neja-
2626 bati Zenouz, K., Brammall, V., Shutler, J.D., Quartly, G.D., 2018. A statistical
2627 modeling framework for characterising uncertainty in large datasets: Applica-
2628 tion to ocean colour. *Remote Sensing* 10, 695. doi:10.3390/rs10050695.

2629 Land, P.E., Findlay, H.S., Shutler, J.D., Ashton, I.G., Holding, T., Grouazel, A.,
2630 Girard-Ardhuin, F., Reul, N., Piolle, J.F., Chapron, B., Quilfen, Y., Bellerby,
2631 R.G.J., Bhadury, P., Salsbury, J., Vandemark, D., Sabia, R., 2019. Op-
2632 timum satellite remote sensing of the marine carbonate system using em-
2633 pirical algorithms in the global ocean, the greater caribbean, the amazon
2634 plume and the bay of bengal. *Remote Sensing of Environment* 235, 111469.
2635 doi:10.1016/j.rse.2019.111469.

2636 Land, P.E., Shutler, J.D., Findlay, H.S., Girard-Ardhuin, F., Sabia, R., Reul, N.,
2637 Piolle, J.F., Chapron, B., Quilfen, Y., Salsbury, J., Vandemark, D., Bellerby,
2638 R., Bhadury, P., 2015. Salinity from space unlocks satellite-based assessment
2639 of ocean acidification. *Environmental Science & Technology* 49, 1987–1994.
2640 doi:10.1021/es504849s.

- 2641 Landry, M.R., Hassett, R., 1982. Estimating the grazing impact of marine micro-
2642 zooplankton. *Marine Biology* 67, 283–288. doi:10.1007/BF00397668.
- 2643 Landschützer, P., Gruber, N., Bakker, D.C.E., 2016. Decadal variations and trends
2644 of the global ocean carbon sink. *Global Biogeochemical Cycles* 30, 1396–1417.
2645 doi:10.1002/2015GB005359.
- 2646 Landwehr, S., Miller, S.D., Smith, M.J., Bell, T.G., Saltzman, E.S., Ward, B.,
2647 2018. Using eddy covariance to measure the dependence of air-sea CO₂
2648 exchange rate on friction velocity. *Atmospheric Chemistry and Physics* 18,
2649 4297–4315. doi:10.5194/acp-18-4297-2018.
- 2650 Lange, P.K., Brewin, R.J.W., Dall’Olmo, G., Tarran, G.A., Sathyendranath, S.,
2651 Zubkov, M., Bouman, H.A., 2018. Scratching beneath the surface: A model
2652 to predict the vertical distribution of *Prochlorococcus* using remote sensing.
2653 *Remote Sensing* 10, 847. URL: <https://doi.org/10.3390/rs10060847>, doi:10.
2654 3390/rs10060847.
- 2655 Lapota, D., Galt, C., Losee, J.R., Huddell, H.D., Orzech, J.K., Neilson, K.H.,
2656 1988. Observations and measurements of planktonic bioluminescence in and
2657 around a milky sea. *Journal of Experimental Marine Biology and Ecology* 119,
2658 55–81. URL: [https://doi.org/10.1016/0022-0981\(88\)90152-9](https://doi.org/10.1016/0022-0981(88)90152-9), doi:10.1016/
2659 0022-0981(88)90152-9.
- 2660 Larsen, P.E., Scott, N., Post, A.F., Field, D., Knight, R., Hamada, Y., Gilbert, J.A.,
2661 2015. Satellite remote sensing data can be used to model marine microbial
2662 metabolite turnover. *ISME* 9, 166–179. URL: [https://doi.org/10.1038/ismej.](https://doi.org/10.1038/ismej.2014.107)
2663 2014.107, doi:10.1038/ismej.2014.107.
- 2664 Laws, E.A., D’Sa, E., Naik, P., 2011. Simple equations to estimate ratios of new
2665 or export production to total production from satellite-derived estimates of sea
2666 surface temperature and primary production. *Limnology and Oceanography:*
2667 *Methods* 9, 593–601. doi:10.4319/lom.2011.9.593.
- 2668 Laws, E.A., Falkowski, P.G., Smith Jr, W.O., Ducklow, H., McCarth, J.J., 2000.
2669 Temperature effects on export production in the open ocean. *Global Biogeo-*
2670 *chemical Cycles* 14, 1231–1246. doi:10.1029/1999GB001229.
- 2671 Le, C., Lehrter, J.C., Hu, C., MacIntyre, H., Beck, M., 2017. Satellite obser-

2672 vation of particulate organic carbon dynamics in two river-dominated estuar-
2673 ies. *Journal of geophysical research. Oceans* 122, 555–569. doi:10.1002/
2674 2016JC012275.

2675 Le, C., Zhou, X., Hu, C., Lee, Z. and Li, L., Stramski, D., 2018. A color-index-
2676 based empirical algorithm for determining particulate organic carbon concen-
2677 tration in the ocean from satellite observations. *Journal of Geophysical Re-*
2678 *search: Oceans* 123, 7407–7419. URL: <https://doi.org/10.1029/2018JC014014>,
2679 doi:10.1029/2018JC014014.

2680 Le Fèvre, J., Viollier, M., Le Corre, P., Dupouy, C., Grall, J. R., ..., 1983. Remote
2681 sensing observations of biological material by LANDSAT along a tidal thermal
2682 front and their relevancy to the available field data. *Estuarine, Coastal and*
2683 *Shelf Science* 16, 37–50. URL: [https://doi.org/10.1016/0272-7714\(83\)90093-8](https://doi.org/10.1016/0272-7714(83)90093-8),
2684 doi:10.1016/0272-7714(83)90093-8.

2685 Le Fouest, V., Matsuoka, A., Manizza, M., Shernetsky, M., Tremblay, B., Babin,
2686 M., 2018. Towards an assessment of riverine dissolved organic carbon in
2687 surface waters of the western Arctic Ocean based on remote sensing and
2688 biogeochemical modeling. *Biogeosciences* 15, 1335–1346. doi:10.5194/
2689 bg-15-1335-2018.

2690 Le Menn, M., Poli, P., David, A., Sagot, J., Lucas, M., O'Carroll, A., Bel-
2691 beoch, M., Herklotz, K., 2019. Development of surface drifting buoys
2692 for fiducial reference measurements of sea-surface temperature. *Frontiers*
2693 *in Marine Science* 6, 578. URL: <https://doi.org/10.3389/fmars.2019.00578>,
2694 doi:10.3389/fmars.2019.00578.

2695 Le Moigne, F.A.C., 2019. Pathways of organic carbon downward transport
2696 by the oceanic biological carbon pump. *Frontiers in Marine Science* 6, 634.
2697 doi:10.3389/fmars.2019.00634.

2698 Lee, E., Yoon, H., Hyun, S.P., Burnett, W.C., Koh, D.C., Ha, K., Kim, D.J.,
2699 Kim, Y., Kang, K.M., 2016. Unmanned aerial vehicles (UAVs)-based thermal
2700 infrared (TIR) mapping, a novel approach to assess groundwater discharge
2701 into the coastal zone. *Limnology and Oceanography Methods* 14, 725–735.
2702 doi:10.1002/lom3.10132.

- 2703 Lee, Y.J., Matrai, P.A., Friedrichs, M.A.M., Saba, V.S., Antoine, D., Ardyna, M.,
2704 Asanuma, I., Babin, M., Bélanger, S., Benoît-Gagné, M., Devred, E., Fernández-
2705 Méndez, M., Gentili, B., Hirawake, T., Kang, S.H., Kameda, T., Katlein, C.,
2706 Lee, S.H., Lee, Z., Mélin, F., Scardi, M., Smyth, T.J., Tang, S., Turpie, K.,
2707 Waters, K.J., Westberry, T.K., 2015a. An assessment of phytoplankton primary
2708 productivity in the Arctic Ocean from satellite ocean color/in situ chlorophyll-a
2709 based models. *Journal of Geophysical Research: Oceans* 120, 6508–6541.
2710 URL: <https://agupubs.onlinelibrary.wiley.com/doi/abs/10.1002/2015JC011018>,
2711 doi:10.1002/2015JC011018.
- 2712 Lee, Z., Marra, J., Perry, M.J., Kahru, M., 2015b. Estimating oceanic primary
2713 productivity from ocean color remote sensing: A strategic assessment. *Journal*
2714 *of Marine Systems* 149, 50–59. URL: [http://dx.doi.org/10.1016/j.jmarsys.2014.](http://dx.doi.org/10.1016/j.jmarsys.2014.11.015)
2715 11.015, doi:10.1016/j.jmarsys.2014.11.015.
- 2716 Legeais, J.F., Ablain, M., Zawadzki, L., Zuo, H., Johannessen, J.A., Scharf-
2717 fenberg, M.G., Fenoglio-Marc, L., Fernandes, M.J., Andersen, O., Rudenko,
2718 S., Cipollini, P., 2018. An improved and homogeneous altimeter sea level
2719 record from the ESA Climate Change Initiative. *Earth System Science Data*
2720 10, 281–301. doi:10.5194/essd-10-281-2018.
- 2721 Lehahn, Y., d’Ovidio, F., Koren, I., 2018. A satellite-based lagrangian view
2722 on phytoplankton dynamics. *Annual Review of Marine Science* 10, 99–119.
2723 doi:10.1146/annurev-marine-121916-063204.
- 2724 Lévy, M., Bopp, L., Karleskind, P., Resplandy, L., Ethe, C., Pinsard, F., 2013.
2725 Physical pathways for carbon transfers between the surface mixed layer and
2726 the ocean interior. *Global Biogeochemical Cycles* , 1001–1012doi:10.1002/
2727 gbc.20092.
- 2728 Lévy, M., Klein, P., Treguier, A.M., 2001. Impact of sub-mesoscale physics on
2729 production and subduction of phytoplankton in an oligotrophic regime. *Journal*
2730 *of Marine Research* 59, 535–565. doi:10.1357/002224001762842181.
- 2731 Li, T., Bai, Y., He, X., Xie, Y., Chen, X., Gong, F., Pan, D., 2018. Satellite-based
2732 estimation of particulate organic carbon export in the northern South China
2733 Sea. *Journal of Geophysical Research: Oceans* 123, 8227–8246. doi:10.1029/

- 2734 2018jc014201.
- 2735 Liu, X., Byrne, R.H., Adornato, L., Yates, K.K., Kaltenbacher, E., Ding, X.,
2736 Yang, B., 2013. In Situ spectrophotometric measurement of dissolved inorganic
2737 carbon in seawater. *Environmental Science & Technology* 47, 11106–11114.
2738 doi:10.1021/es4014807.
- 2739 Llewellyn, C.A., Fishwick, J.R., Blackford, J.C., 2005. Phytoplankton community
2740 assemblage in the English Channel: a comparison using chlorophyll a derived
2741 from HPLC-CHEMTAX and carbon derived from microscopy cell counts.
2742 *Journal of Plankton Research* 27, 103–119. doi:10.1093/plankt/fbh158.
- 2743 Llorc, J., Langlais, C., Matear, R., Moreau, S., Lenton, A., Strutton, P.G.,
2744 2018. Evaluating southern ocean carbon eddy-pump from biogeochemical-
2745 argo floats. *Journal of Geophysical Research – Ocean* 123, 971–984.
2746 doi:10.1002/2017JC012861.
- 2747 Lobitz, B., Beck, L., Huq, A., Wood, B., Fuchs, G., Faruque, A.S.G., Colwell,
2748 R., 2000. Climate and infectious disease: use of remote sensing for detection
2749 of *Vibrio cholerae* by indirect measurement. *Proceedings of the National*
2750 *Academy of Sciences of the United States of America* 97, 1438–1443. URL:
2751 <https://doi.org/10.1073/pnas.97.4.1438>, doi:10.1073/pnas.97.4.1438.
- 2752 Lohrenz, S.E., Arone, R.A., Wiesenburg, D.A., DePalma, I.P., 1988. Satellite de-
2753 tection of transient enhanced primary production in the western Mediterranean
2754 Sea. *Nature* 335, 245–247.
- 2755 Loisel, H., Bosc, E., Stramski, D., Oubelkheir, K., Deschamps, P., 2001. Seasonal
2756 variability of the backscattering coefficient in the Mediterranean Sea based on
2757 satellite SeaWiFS imager. *Geophysical Research Letters* .
- 2758 Loisel, H., Nicolas, J.M., Deschamps, P.Y., Frouin, R., 2002. Seasonal and inter-
2759 annual variability of particulate organic matter in the global ocean. *Geophysical*
2760 *Research Letters* 29, 491–494. doi:10.1029/2002GL015948.
- 2761 Loisel, H., Vantrepotte, V., Dessailly, D., Mériaux, X., 2014. Assessment of the
2762 colored dissolved organic matter in coastal waters from ocean color remote
2763 sensing. *Optics Express* 22, 13109. doi:10.1364/OE.22.013109.
- 2764 Longhurst, A., Sathyendranath, S., Platt, T., Caverhill, C., 1995. An estimate of

- 2765 global primary production in the ocean from satellite radiometer data. *Journal*
2766 *of Plankton Research* 17, 1245–1271.
- 2767 Longhurst, A.R., 2007. *Ecological Geography of the Sea* (Second Edition).
2768 Elsevier.
- 2769 Longhurst, A.R., Bedo, A.W., Harrison, W.G., Head, E.J.H., Sameoto, D.D., 1990.
2770 Vertical flux of respiratory carbon by oceanic diel migrant biota. *Deep Sea*
2771 *Research Part A: Oceanographic Research Papers* 37, 685–694. doi:10.1016/
2772 0198-0149(90)90098-G.
- 2773 Losa, S.N., Soppa, M.A., Dinter, T., Wolanin, A., Brewin, R.J.W., Bricaud, A.,
2774 Oelker, J., Peeken, I., Gentili, B., Rozanov, V., Bracher, A., 2017. Synergistic
2775 exploitation of hyper- and multi-spectral precursor sentinel measurements to
2776 determine phytoplankton functional types (SynSenPFT). *Frontiers in Marine*
2777 *Science* 4, 203. doi:10.3389/fmars.2017.00203.
- 2778 Loukos, H., Vivier, F., Murphy, P.P., Harrison, D.E., Le Quéré, C., 2000. In-
2779 terannual variability of equatorial Pacific CO₂ fluxes estimated from temper-
2780 ature and salinity data. *Geophysical Research Letters* 27, 1735–1738. URL:
2781 <https://doi.org/10.1029/1999GL011013>, doi:10.1029/1999GL011013.
- 2782 Loveday, B.R., Smyth, T., 2018. A 40-year global data set of visible-
2783 channel remote-sensing reflectances and coccolithophore bloom occurrence
2784 derived from the Advanced Very High Resolution Radiometer catalogue.
2785 *Earth System Science Data* 10, 2043–2054. URL: [https://doi.org/10.5194/](https://doi.org/10.5194/essd-10-2043-2018)
2786 [essd-10-2043-2018](https://doi.org/10.5194/essd-10-2043-2018), doi:10.5194/essd-10-2043-2018.
- 2787 Lutz, M.J., Caldeira, K., Dunbar, R.B., Behrenfeld, M.J., 2007. Seasonal rhythms
2788 of net primary production and particulate organic carbon flux to depth describe
2789 the efficiency of biological pump in the global ocean. *Journal of Geophysical*
2790 *Research - Oceans* 112, C10011. doi:10.1029/2006JC003706.
- 2791 Lydersen, C., Nost, O.A., Lovell, P., McConnell, B.J., Gammelsrod, T., Hunter, C.,
2792 Fedak, M.A., Kovacs, K.M., 2002. Salinity and temperature structure of a freez-
2793 ing Arctic fjord—monitored by white whales (*Delphinapterus leucas*). *Geophys-*
2794 *ical Research Letters* 29, 2119. URL: <https://doi.org/10.1029/2002GL015462>,
2795 doi:10.1029/2002GL015462.

- 2796 Lyu, P., Malang, Y., Liu, H.H., Lai, J., Liu, J., Jiang, B., Qu, M., Anderson,
2797 S., Lefebvre, D.D., Wang, Y., 2017. Autonomous cyanobacterial harmful
2798 algal blooms monitoring using multirotor UAS. *International Journal of Re-*
2799 *remote Sensing* 38, 2818–2843. URL: [https://doi.org/10.1080/01431161.2016.](https://doi.org/10.1080/01431161.2016.1275058)
2800 [1275058](https://doi.org/10.1080/01431161.2016.1275058), doi:10.1080/01431161.2016.1275058.
- 2801 de Magny, G.C., Mozumder, P.K., Grim, C.J., Hasan, N.A., Naser, M.N., Alam,
2802 M., Sack, R.B., Huq, A., Colwell, R.R., 2011. Role of zooplankton diversity
2803 in vibrio cholerae population dynamics and in the incidence of cholera in
2804 the bangladesh sundarbans. *Applied and Environmental Microbiology* 77,
2805 6125–6132. doi:10.1128/AEM.01472-10.
- 2806 Mahesh, R., Saravanakumar, A., Thangaradjou, T., Solanki, H.U., Raman, M.,
2807 2018. A regional algorithm to model mesozooplankton biomass along the
2808 southwestern Bay of Bengal. *Environmental Monitoring and Assessment*
2809 volume 190, 1–14. URL: <https://doi.org/10.1007/s10661-018-6578-6>, doi:10.
2810 [1007/s10661-018-6578-6](https://doi.org/10.1007/s10661-018-6578-6).
- 2811 Mannino, A., Novak, M.G., Hooker, S.B., Hyde, K., Aurin, D., 2014. Algorithm
2812 development and validation of CDOM properties for estuarine and continental
2813 shelf waters along the northeastern US coast. *Remote Sensing of Environment*
2814 152, 576–602. URL: <https://doi.org/10.1016/j.rse.2014.06.027>, doi:10.1016/
2815 [j.rse.2014.06.027](https://doi.org/10.1016/j.rse.2014.06.027).
- 2816 Mannino, A., Russ, M.E., Hooker, S.B., 2008. Algorithm development for
2817 satellite-derived distributions of DOC and CDOM in the U.S. Middle Atlantic
2818 Bight. *Journal of Geophysical Research: Oceans* 113, C07051. doi:10.1029/
2819 [2007JC004493](https://doi.org/10.1029/2007JC004493).
- 2820 Mannino, A., Signorini, S.R., Novak, M.G., Wilkin, J., Friedrichs, M.A.M.,
2821 Najjar, R.G., 2016. Dissolved organic carbon fluxes in the Middle Atlantic
2822 Bight: An integrated approach based on satellite data and ocean model products.
2823 *Journal of Geophysical Research: Biogeosciences* 21, 312–336. doi:10.1002/
2824 [2015JG003031](https://doi.org/10.1002/2015JG003031).
- 2825 Marañón, E., 2009. Phytoplankton size structure, in: Steele, J.H., Turekian, K.,
2826 Thorpe, S.A. (Eds.), *Encyclopedia of Ocean Sciences*. Academic Press, Oxford.

- 2827 Marañón, E., 2015. Cell size as a key determinant of phytoplankton metabolism
2828 and community structure. *Annual Review of Marine Science* 7, 241–264.
2829 doi:10.1146/annurev-marine-010814-015955.
- 2830 Marañón, E., Cermeño, P., Huete-Ortega, M., López-Sandoval, D.C., Mouriño
2831 Carballido, B., Rodríguez-Ramos, T., 2014. Resource supply overrides temper-
2832 ature as a controlling factor of marine phytoplankton growth. *PLoS ONE* 9,
2833 e99312. doi:10.1371/journal.pone.0099312.
- 2834 Maritorena, S., Fanton d'Andon, O.H., Mangin, A., Siegel, D.A., 2010. Merged
2835 satellite ocean color data products using a bio-optical model: Characteristics,
2836 benefits and issues. *Remote Sensing Environment* 114, 1791–1804. doi:10.
2837 1016/j.rse.2010.04.002.
- 2838 Maritorena, S., Siegel, D.A., Peterson, A.R., 2002. Optimization of a semian-
2839 alytical ocean color model for global-scale applications. *Applied Optics* 41,
2840 2705–2714. doi:10.1364/AO.41.002705.
- 2841 Martin, P., Lampitt, R.S., Perry, M.J., Sanders, R., Lee, C., D'Asaro, E., 2011.
2842 Export and mesopelagic particle flux during a north atlantic spring diatom
2843 bloom. *Deep Sea Research Part I: Oceanographic Research Papers* 58, 338–
2844 349. doi:10.1016/j.dsr.2011.01.006.
- 2845 Martínez-Vicente, V., Dall'Olmo, G., Tarran, G., Boss, E., Sathyendranath, S.,
2846 2013. Optical backscattering is correlated with phytoplankton carbon across
2847 the Atlantic Ocean. *Geophysical Research Letters* 40, 1154–1158. doi:10.
2848 1002/grl.50252.
- 2849 Martínez-Vicente, V., Evers-King, H., Roy, S., Kostadinov, T.S., Tarran, G.A.,
2850 Graff, J.R., Brewin, R.J.W., Dall'Olmo, G., Jackson, T., Hickman, A.E.,
2851 Röttgers, R., Krasemann, H., Marañón, E., Platt, T., Sathyendranath, S., 2017.
2852 Intercomparison of ocean color algorithms for picophytoplankton carbon in the
2853 ocean. *Frontiers in Marine Science* 4, 378. doi:10.3389/fmars.2017.00378.
- 2854 Martínez-Vicente, V., Sathyendranath, S., Platt, T., Evers-King, H., Dall'Olmo, G.,
2855 Roy, S., Hickman, A. and Rottgers, R., 2016. Pools of Carbon in the Ocean
2856 (POCO): Requirements Baseline Document (D1.1) and Algorithm Theoretical
2857 Baseline Document (D1.2).

- 2858 Martínez-Vicente, V., Tilstone, G., Sathyendranath, S., Miller, P., Groom, S.,
2859 2012. Contributions of phytoplankton and bacteria to the optical backscattering
2860 coefficient over the mid-atlantic ridge. *Marine Ecological Progress Series* 445,
2861 37–51. doi:10.3354/meps09388.
- 2862 Martiny, A.C., Vrugt, J.A., Lomas, M.W., 2014. Concentrations and ratios
2863 of particulate organic carbon, nitrogen, and phosphorus in the global ocean.
2864 *Scientific Data* 1, 1–7. doi:10.1038/sdata.2014.48.
- 2865 Martz, T.R., Daly, K.L., Byrne, R.H., Stillman, J.H., Turk, D., 2015. Technology
2866 for ocean acidification research: Needs and availability. *Oceanography* 28,
2867 40–47. URL: <https://www.jstor.org/stable/24861869>.
- 2868 Matsuoka, A., Boss, E., Babin, M., Karp-Boss, L., Hafez, M., Chekalyuk, A.,
2869 Proctor, C.W., Werdell, P.J., Bricaud, A., 2017. Pan-Arctic optical character-
2870 istics of colored dissolved organic matter: Tracing dissolved organic carbon
2871 in changing Arctic waters using satellite ocean color data. *Remote Sensing*
2872 of Environment 200, 89–101. URL: <https://doi.org/10.1016/j.rse.2017.08.009>,
2873 doi:10.1016/j.rse.2017.08.009.
- 2874 Matsuoka, A., Bricaud, A., Benner, R., Para, J., Sempéré, R., Prieur, L., Bélanger,
2875 S., Babin, M., 2012. Tracing the transport of colored dissolved organic matter
2876 in water masses of the Southern Beaufort Sea: relationship with hydrographic
2877 characteristics. *Biogeosciences* 9, 925–940. URL: [https://doi.org/10.5194/](https://doi.org/10.5194/bg-9-925-2012)
2878 [bg-9-925-2012](https://doi.org/10.5194/bg-9-925-2012), doi:10.5194/bg-9-925-2012.
- 2879 McCollum, J.R., Krajewski, W.F., 1997. Oceanic rainfall estimation:
2880 Sampling studies of the fractional-time-in-rain method. *Journal of At-*
2881 *mospheric and Oceanic Technology* 14, 133–142. URL: [https://doi.](https://doi.org/10.1175/1520-0426(1997)014<0133:ORESSO>2.0.CO;2)
2882 [org/10.1175/1520-0426\(1997\)014<0133:ORESSO>2.0.CO;2](https://doi.org/10.1175/1520-0426(1997)014<0133:ORESSO>2.0.CO;2), doi:10.1175/
2883 [1520-0426\(1997\)014<0133:ORESSO>2.0.CO;2](https://doi.org/10.1175/1520-0426(1997)014<0133:ORESSO>2.0.CO;2).
- 2884 McIntyre, E.M., Gasiewski, A., 2007. An ultra-lightweight L-band digital Lobe-
2885 Differencing Correlation Radiometer(LDCR) for airborne UAV SSS mapping,
2886 in: *IEEE International Geoscience and RemoteSensing Symposium*, pp. 1095–
2887 1097.
- 2888 McMahan, C.R., Autret, E., Houghton, J.D.R., Lovell, P., Myers, A.E., Hays,

- 2889 G.C., 2005. Animal-borne sensors successfully capture the real-time thermal
2890 properties of ocean basins. *Limnology and Oceanography Methods* 3, 392–398.
2891 doi:10.4319/lom.2005.3.392.
- 2892 Mélin, F., 2016. Impact of inter-mission differences and drifts on chlorophyll-
2893 a trend estimates. *International Journal of Remote Sensing* 37, 2233–2251.
2894 doi:10.1080/01431161.2016.1168949.
- 2895 Mélin, F., Hoepffner, N., 2011. Monitoring phytoplankton productivity from
2896 satellite—An aid to marine resources management, in: Morales, J., Stuart, V.,
2897 Platt, T., Sathyendranath, S. (Eds.), *Handbook of Satellite Remote Sensing*
2898 *Image Interpretation: Applications for Marine Living Resources Conservation*
2899 *and Management*, EU PRESPO and IOCCG. pp. 79–93.
- 2900 Mélin, F., Vantrepotte, V., Chuprin, A., Grant, M., Jackson, T., Sathyendranath, S.,
2901 2017. Assessing the fitness-for-purpose of satellite multi-mission ocean color
2902 climate data records: A protocol applied to OC-CCI chlorophyll-a data. *Remote*
2903 *Sensing of Environment* 203, 139–151. doi:10.1016/j.rse.2017.03.039.
- 2904 Merchant, C.J., Embury, O., Bulgin, C.E., Block, T., Corlett, G.K., Fiedler, E.,
2905 Good, S.A., Mittaz, J., Rayner, N.A., Berry, D., Eastwood, S., 2019. Satellite-
2906 based time-series of sea-surface temperature since 1981 for climate applications.
2907 *Scientific data* 6, 223. doi:10.1038/s41597-019-0236-x.
- 2908 Merchant, C.J., Embury, O., Roberts-Jones, J., Fiedler, E., Bulgin, C.E., Corlett,
2909 G.K., Good, S., McLaren, A., Rayner, N., Morak-Bozzo, S., Donlon, C., 2014.
2910 Sea surface temperature datasets for climate applications from Phase 1 of the
2911 European Space Agency Climate Change initiative (SST CCI). *Geoscience*
2912 *Data Journal* 1, 179–191. doi:10.1002/gdj3.20.
- 2913 Meredith, M.P., Nicholls, K.W., Renfrew, I.A., Boehme, L., Biuw, M., Fedak,
2914 M., 2011. Seasonal evolution of the upper-ocean adjacent to the South Orkney
2915 Islands, Southern Ocean: results from a "lazy biological mooring". *Deep Sea*
2916 *Research Part II: Topical Studies in Oceanography* 58, 1569–1579. doi:10.
2917 1016/j.dsr2.2009.07.008.
- 2918 Meyer, R.A., 1979. Light scattering from biological cells: dependence of backscat-
2919 ter radiation on membrane thickness and refractive index. *Applied Optics* 18,

2920 585–588. doi:10.1364/AO.18.000585.

2921 Mignot, A., Ferrari, R., Claustre, H., 2018. Floats with bio-optical sensors reveal
2922 what processes trigger the North Atlantic bloom. *Nature Communications*
2923 9, 190. URL: <https://doi.org/10.1038/s41467-017-02143-6>, doi:10.1038/
2924 s41467-017-02143-6.

2925 Miles, T.N., Kohut, J., Slade, W., Gong, D., 2018. Suspended particle characteris-
2926 tics from a glider integrated LISST sensor, pp. 1–5.

2927 Miller, S.D., Haddock, S.H.D., Elvidge, C.D., Lee, T.F., 2005. Detection of a
2928 bioluminescent milky sea from space. *Proceedings of the National Academy*
2929 *of Sciences of the United States of America* 102, 14181–14184. URL: <https://doi.org/10.1073/pnas.0507253102>, doi:10.1073/pnas.0507253102.

2930

2931 Mishonov, A.V., Gardner, W.D., Richardson, M.J., 2003. Remote sensing and
2932 surface POC concentration in the South Atlantic. *Deep Sea Research Part*
2933 *II: Topical Studies in Oceanography* 50, 2997–3015. URL: <https://doi.org/10.1016/j.dsr2.2003.07.007>, doi:10.1016/j.dsr2.2003.07.007.

2934

2935 Mitarai, S., McWilliams, J.C., 2016. Wave glider observations of surface winds
2936 and currents in the core of Typhoon Danas. *Geophysical Research Letters* 43,
2937 11,312–11,319. doi:10.1002/2016GL071115.

2938 Mitchell, C., Hu, C., Bowler, B., Drapeau, D., Balch, W.M., 2017. Estimating Par-
2939 ticulate Inorganic Carbon concentrations of the global ocean from ocean color
2940 measurements using a reflectance difference approach. *Journal of Geophysical*
2941 *Research: Oceans* 122, 8707–8720. doi:10.1002/2017JC013146.

2942 Moore, T.S., Brown, C.W., 2020. Incorporating environmental data in abundance-
2943 based algorithms for deriving phytoplankton size classes in the Atlantic Ocean.
2944 *Remote Sensing of Environment* 240, 111689. URL: <https://doi.org/10.1016/j.rse.2020.111689>, doi:10.1016/j.rse.2020.111689.

2945

2946 Moore, T.S., Campbell, J.W., Dowell, M.D., 2009. A class-based approach to
2947 characterizing and mapping the uncertainty of the MODIS ocean chlorophyll
2948 product. *Remote Sensing Environment* 113, 2424–2430. doi:10.1016/j.rse.
2949 2009.07.016.

2950 Moore, T.S., Dowell, M.D., Franz, B.A., 2012. Detection of coccolithophore

2951 blooms in ocean color satellite imagery: A generalized approach for use with
2952 multiple sensors. *Remote Sensing of Environment* 117, 249–263. doi:10.
2953 1016/j.rse.2011.10.001.

2954 Morel, A., 1991. Light and marine photosynthesis: a spectral model with geo-
2955 chemical and climatological implications. *Progress in Oceanography* 26, 263–
2956 306.

2957 Morel, A., André, J.M., 1991. Pigment distribution and primary production in
2958 the western mediterranean as derived and modeled from coastal zone color
2959 scanner observations. *Journal of Geophysical Research* 96, 12,685–12,698.
2960 URL: <https://doi.org/10.1029/91JC00788>, doi:10.1029/91JC00788.

2961 Morel, A., Huot, Y., Gentili, B., Werdell, P.J., Hooker, S.B., Franz, B.A., 2007.
2962 Examining the consistency of products derived from various ocean color sensors
2963 in open ocean (case 1) waters in the perspective of a multi-sensor approach.
2964 *Remote Sensing of Environment* 111, 69–88. doi:10.1016/j.rse.2007.03.
2965 012.

2966 Mouw, C.B., Barnett, A., McKinley, G.A., Gloege, L., Pilcher, D., 2016a.
2967 Global ocean particulate organic carbon flux merged with satellite parame-
2968 ters. PANGAEA. URL: <https://doi.org/10.1594/PANGAEA.855600>, doi:10.
2969 1594/PANGAEA.855600.

2970 Mouw, C.B., Barnett, A., McKinley, G.A., Gloege, L., Pilcher, D., 2016b. Global
2971 ocean particulate organic carbon flux merged with satellite parameters. *Earth*
2972 *System Science Data* 8, 531–541. URL: [https://www.earth-syst-sci-data.net/8/
2973 531/2016/](https://www.earth-syst-sci-data.net/8/531/2016/), doi:10.5194/essd-8-531-2016.

2974 Mouw, C.B., Hardman-Mountford, N.J., Alvain, S., Bracher, A., Brewin, R.J.W.,
2975 Bricaud, A., Ciotti, A.M., Devred, E., Fujiwara, A., Hirata, T., Hirawake, T.,
2976 Kostadinov, T.S., Roy, S., Uitz, J., 2017. A consumer’s guide to satellite remote
2977 sensing of multiple phytoplankton groups in the global ocean. *Frontiers in*
2978 *Marine Science* 4, 1–19. doi:10.3389/fmars.2017.00041.

2979 Mouw, C.B., Yoder, J., 2005. Primary production calculations in the Mid-Atlantic
2980 Bight, including effects of phytoplankton community size structure. *Limnology*
2981 *and Oceanography* 50, 1232–1243.

- 2982 Murray, C.N., Riley, J.P., 1971. The solubility of gases in distilled water and sea
2983 water–IV. Carbon dioxide. *Deep Sea Research* 18, 533–541. doi:10.1016/
2984 0011-7471(71)90077-5.
- 2985 Nelson, N.B., Siegel, D.A., 2013. The Global Distribution and Dynamics of
2986 Chromophoric Dissolved Organic Matter. *Annual Review of Marine Science* 5,
2987 20.1–20.3. doi:10.1146/annurev-marine-120710-100751.
- 2988 Nelson, N.B., Siegel, D.A., Carlson, C.A., Swan, C., Smethie Jr, W.M., Khatiwala,
2989 S., 2007. Hydrography of chromophoric dissolved organic matter in the North
2990 Atlantic. *Deep Sea Research Part I: Oceanographic Research Papers* 54, 710–
2991 731. doi:10.1016/j.dsr.2007.02.006.
- 2992 Nencioli, F., Dall’Olmo, G., Quartly, G.D., 2018. Agulhas ring transport efficiency
2993 from combined satellite altimetry and Argo profiles. *Journal of Geophysical*
2994 *Research: Oceans* 123, 5874–5888.
- 2995 Neukermans, G., Harmel, T., Galí, M., Rudorff, N., Chowdhary, J., Dubovik, O.,
2996 Hostetler, C., Hu, Y., Jamet, C., Knobelspiesse, K., Lehahn, Y., Litvinov, P.,
2997 Sayer, A.M., Ward, B., Boss, E., Koren, I., Miller, L.A., 2018. Harnessing
2998 remote sensing to address critical science questions on ocean-atmosphere
2999 interactions. *Elementa Science of the Anthropocene* 6, 71. doi:10.101525/
3000 elementa.331.
- 3001 Olson, R.J., Shalapyonok, A., Sosik, H.M., 2003. An automated submersible flow
3002 cytometer for analyzing pico-and nanophytoplankton: FlowCytobot. *Deep Sea*
3003 *Research Part I: Oceanographic Research Papers* 50, 301–315. doi:10.1016/
3004 S0967-0637(03)00003-7.
- 3005 Omand, M.M., D’Asaro, E.A., Lee, C.M., Perry, M.J., Briggs, N., Cetinić, I.,
3006 Mahadevan, A., 2015. Eddy-driven subduction exports particulate organic
3007 carbon from the spring bloom. *Science* 348, 222–225. doi:10.1126/science.
3008 1260062.
- 3009 Ono, T., Saino, T., Kurita, N., Sasaki, K., 2004. Basin-scale extrapolation of
3010 shipboard pCO₂ data by using satellite SST and Chl_a. *International Journal of*
3011 *Remote Sensing* 25, 3803–3815. doi:10.1080/01431160310001657515.
- 3012 Ore, J.P., Elbaum, S., Burgin, A., Detweiler, C., 2015. Autonomous aerial water

3013 sampling. *Journal of Field Robotics* 32, 1095–1013. URL: <https://doi.org/10.1002/rob.21591>, doi:10.1002/rob.21591.

3014

3015 Organelli, E., Claustre, H., Bricaud, A., Schmechtig, C., Poteau, A., Xing, X.,
3016 Prieur, L., D’Ortenzio, F., Dall’Olmo, G., Vellucci, V., 2016. A novel near
3017 real-time quality-control procedure for radiometric profiles measured by Bio-
3018 Argo floats: protocols and performances. *Journal of Atmospheric and Oceanic*
3019 *Technology* 33, 937–951. doi:10.1175/JTECH-D-15-0193.1.

3020 Organelli, E., Dall’Olmo, G., Brewin, R.J.W., Tarran, G.A., Boss, E., Bricaud, A.,
3021 2018. The open-ocean missing backscattering is in the structural complexity
3022 of particles. *Nature Communications* 9, 1–11. URL: [https://doi.org/10.1038/](https://doi.org/10.1038/s41467-018-07814-6)
3023 [s41467-018-07814-6](https://doi.org/10.1038/s41467-018-07814-6), doi:10.1038/s41467-018-07814-6.

3024 Ott, L.E., Pawson, S., Collatz, G.J., Gregg, W.W., Menemenlis, D., Brix, H.,
3025 Rousseaux, C.S., Bowman, K.W., Liu, J., Eldering, A., Gunson, M.R., Kawa,
3026 S.R., 2015. Assessing the magnitude of CO₂ flux uncertainty in atmospheric CO₂
3027 records using products from NASA’s Carbon Monitoring Flux Pilot Project.
3028 *Journal of Geophysical Research: Atmospheres* 120, 734–765. doi:10.1002/
3029 2014JD022411.

3030 O’Carroll, A.G., Armstrong, E.M., Beggs, H.M., Bouali, M., Casey, K.S., Corlett,
3031 G.K., Dash, P., Donlon, C.J., Gentemann, C.L., Hoyer, J.L., Ignatov, A.,
3032 Kabobah, K., Kachi, M., Kurihara, Y., Karagali, I., Maturi, E., Merchant, C.J.,
3033 Marullo, S., Minnett, P.J., Pennybacker, M., Ramakrishnan, B., Ramsankaran,
3034 R., Santoleri, R., Sunder, S., Saux Picart, S., Vázquez-Cuervo, J., Wimmer, W.,
3035 2019. Observational needs of sea surface temperature. *Frontiers in Marine*
3036 *Science* 6, 420. URL: [https://www.frontiersin.org/article/10.3389/fmars.2019.](https://www.frontiersin.org/article/10.3389/fmars.2019.00420)
3037 [00420](https://www.frontiersin.org/article/10.3389/fmars.2019.00420), doi:10.3389/fmars.2019.00420.

3038 Paasche, E., 1962. Coccolith formation. *Nature* 193, 1094–1095. doi:10.1038/
3039 1931094b0.

3040 Paasche, E., 1963. The adaptation of the Carbon-14 method for the measurement
3041 of coccolith production in *Coccolithus huxleyi*. *Physiologia Plantarum* 16,
3042 186–200. doi:10.1111/j.1399-3054.1963.tb08302.x.

3043 Pace, M.L., Knauer, G.A., Karl, D.M., Martin, J.H., 1987. Primary production,

- 3044 new production and vertical flux in the eastern Pacific Ocean. *Nature* 325,
3045 803–804. doi:10.1038/325803a0.
- 3046 Pahlevan, N., Smith, B., Schalles, J., Binding, C., Cao, Z., Ma, R., Alikas, K.,
3047 Kangro, K., Gurlin, D., Hà, N., Matsushita, B., Moses, W., Greb, S., Lehmann,
3048 M.K., Ondrusek, M., Oppelt, N., Stumpf, R., 2020. Seamless retrievals of
3049 chlorophyll-a from Sentinel-2 (MSI) and Sentinel-3 (OLCI) in inland and
3050 coastal waters: A machine-learning approach. *Remote Sensing of Environment*
3051 240, 111604. doi:10.1016/j.rse.2019.111604.
- 3052 Palacz, A., John, M.S., Brewin, R.J.W., Hirata, T., Gregg, W.W., 2013. Distribu-
3053 tion of phytoplankton functional types in high-nitrate low-chlorophyll waters in
3054 a new diagnostic ecological indicator model. *Biogeosciences* 10, 7553–7574.
- 3055 Palevsky, H.I., Quay, P.D., Nicholson, D.P., 2016. Discrepant estimates of primary
3056 and export production from satellite algorithms, a biogeochemical model, and
3057 geochemical tracer measurements in the North Pacific Ocean. *Geophysical*
3058 *Research Letters* 43, 8645–8653. doi:10.1002/2016gl070226.
- 3059 Parekh, P., Dutkiewicz, S., Follows, M.J., Ito, T., 2006. Atmospheric carbon
3060 dioxide in a less dusty world. *Geophysical Research Letters* 33, L03610.
3061 doi:10.1029/2005GL025098.
- 3062 Passow, U., Alldredge, A.L., 1995. Aggregation of a diatom bloom in a mesocosm:
3063 The role of transparent exopolymer particles (tep). *Deep Sea Research Part II:*
3064 *Topical Studies in Oceanography* 42, 99–109. doi:10.1016/0967-0645(95)
3065 00006-C.
- 3066 Peperzak, L., Brussaard, C.P., 2011. Flow cytometric applicability of fluorescent
3067 vitality probes on phytoplankton. *Journal of Phycology* 47, 692–702. doi:10.
3068 1111/j.1529-8817.2011.00991.x.
- 3069 Perry, M.J., 1986. Assessing marine primary production from space. *BioScience*
3070 36, 461–467.
- 3071 Petersen, W., 2014. FerryBox systems: State-of-the-art in Europe and future
3072 development. *Journal of Marine Systems* 140, 4–12.
- 3073 Pierrot, D., Neill, C., Sullivan, K., Castle, R., Wanninkhof, R., Lüger, H., Johan-
3074 nessen, T., Olsen, A., Feely, R.A., Cosca, C.E., 2009. Recommendations for

3075 autonomous underway pCO₂ measuring systems and data-reduction routine.
3076 Deep Sea Research Part II: Topical Studies in Oceanography 56, 512–522.
3077 doi:10.1016/j.dsr2.2008.12.005.

3078 Platt, T. Caverhill, C., Sathyendranath, S., 1991. Basin-scale estimates of oceanic
3079 primary production by remote sensing: The North Atlantic. Journal of Geo-
3080 physical Research 96, 15,147–15,159.

3081 Platt, T., 1986. Primary production of the ocean water column as a function of
3082 surface light intensity: algorithms for remote sensing. Deep Sea Research Part
3083 A. Oceanographic Research Papers 33, 149–163. URL: [https://doi.org/10.1016/
3084 0198-0149\(86\)90115-9](https://doi.org/10.1016/0198-0149(86)90115-9), doi:10.1016/0198-0149(86)90115-9.

3085 Platt, T., Denman, K.L., 1977. Organisation in the pelagic ecosystem.
3086 Helgoländer Wissenschaftliche Meeresuntersuchungen 30, 575–581.

3087 Platt, T., Denman, K.L., 1978. The structure of pelagic marine ecosystems. Rapp.
3088 P.-v. Réun. Cons. perm. int. Explor. Mer , 60–65.

3089 Platt, T., Fuentes-Yaco, C., Frank, K., 2003. Spring algal bloom and larval fish
3090 survival. Nature 423, 398–399. doi:10.1038/423398b.

3091 Platt, T., Gallegos, C.L., Harrison, W.G., 1980. Photoinhibition of photosynthesis
3092 in natural assemblages of marine phytoplankton. Journal of Marine Research
3093 38, 687–701.

3094 Platt, T., Harrison, W.G., 1985. Biogenic fluxes of carbon and oxygen in the
3095 ocean. Nature 318, 55–58. doi:10.1038/318055a0.

3096 Platt, T., Harrison, W.G., Lewis, M., Li, W., Sathyendranath, S., Smith, R., Vezina,
3097 A., 1989. Biological production of the oceans: the case for a consensus. Marine
3098 Ecology Progress Series 52, 77–88. doi:10.3354/meps052077.

3099 Platt, T., Herman, A.W., 1983. Remote sensing of phytoplankton in the
3100 sea: surface-layer chlorophyll as an estimate of water-column chloro-
3101 phyll and primary production. International Journal of Remote Sensing 4,
3102 343–351. URL: <https://doi.org/10.1080/01431168308948552>, doi:10.1080/
3103 01431168308948552.

3104 Platt, T., Sathyendranath, S., 1988. Oceanic primary production: Estimation
3105 by remote sensing at local and regional scales. Science 241, 1613–1620.

3106 doi:10.1126/science.241.4873.1613.

3107 Platt, T., Sathyendranath, S., 1993. Estimators of primary production for interpre-
3108 tation of remotely sensed data on ocean color. *Journal of Geophysical Research*
3109 98, 14,561–14,576.

3110 Platt, T., Sathyendranath, S., 2008. Ecological indicators for the pelagic zone
3111 of the ocean from remote sensing. *Remote Sensing of Environment* 112,
3112 3426–3436. doi:10.1016/j.rse.2007.10.016.

3113 Platt, T., Sathyendranath, S., Caverhill, C.M., Lewis, M.R., 1988. Ocean
3114 primary production and available light: further algorithms for remote sens-
3115 ing. *Deep Sea Research Part A. Oceanographic Research Papers* 35, 855–
3116 879. URL: [https://doi.org/10.1016/0198-0149\(88\)90064-7](https://doi.org/10.1016/0198-0149(88)90064-7), doi:10.1016/
3117 0198-0149(88)90064-7.

3118 Platt, T., Sathyendranath, S., Forget, M.H., White III, G.N., Caverhill, C., Bouman,
3119 H., Devred, E., Son, S., 2008. Operational estimation of primary production at
3120 large geographical scales. *Remote Sensing of Environment* 112, 3437–3448.
3121 doi:10.1016/j.rse.2007.11.018.

3122 Platt, T., Sathyendranath, S., Longhurst, A., 1995. Remote sensing of primary
3123 production in the ocean: Promise and fulfilment. *Phil. Trans. R. Soc. Lond. B*
3124 348, 191–202. doi:10.1098/rstb.1995.0061.

3125 Platt, T., Sathyendranath, S., Ravindran, P., 1990. Primary production by phy-
3126 toplankton: Analytic solutions for daily rates per unit area of water surface.
3127 *Proceedings of the Royal Society of London Series B: Biological Sciences* 241,
3128 101–111.

3129 Platt, T., Sathyendranath, S., Ulloa, O., Harrison, W.G., Hoepffner, N., Goes,
3130 J., 1992. Nutrient control of phytoplankton photosynthesis in the Western
3131 North Atlantic. *Nature* 356, 229–231. URL: <https://doi.org/10.1038/356229a0>,
3132 doi:10.1038/356229a0.

3133 Platt, T., White III, G.N., Zhai, L., Sathyendranath, S., Roy, S., 2009. The phe-
3134 nology of phytoplankton blooms: Ecosystem indicators from remote sensing.
3135 *Ecological Modelling* 220, 3057–3069. doi:10.1016/j.ecolmodel.2008.
3136 11.022.

- 3137 Poulet, S.A., Ianora, A., Laabir, M., Klein Breteler, W.C.M., 1995. Towards the
3138 measurement of secondary production and recruitment in copepods. ICES Jour-
3139 nal of Marine Science 52, 359–368. doi:10.1016/1054-3139(95)80051-4.
- 3140 Powell, J.R., Ohman, M.D., 2012. Use of glider-class acoustic Doppler profilers
3141 for estimating zooplankton biomass. Journal of Plankton Research 34, 563–568.
3142 doi:10.1093/plankt/fbs023.
- 3143 Pradhan, H.K., Völker, C., Losa, S.N., Bracher, A., Nerger, L., 2019. Assimi-
3144 lation of global total chlorophyll OC-CCI data and its impact on individual
3145 phytoplankton fields. Journal of Geophysical Research: Oceans 124, 470–490.
3146 doi:10.1029/2018JC014329.
- 3147 Quirantes, A., Bernard, S., 2004. Light scattering by marine algae: two-layer
3148 spherical and nonspherical models. Journal of Quantitative Spectroscopy and
3149 Radiative Transfer 89, 311–321. doi:10.1016/j.jqsrt.2004.05.031.
- 3150 Racault, M.F., 2009. Climate influence on phytoplankton phenology in the global
3151 ocean, PhD Thesis, University of East Anglia. URL: [https://ueaeprints.uea.ac.
3152 uk/id/eprint/10572/1/Thesis_racault_m_2009.pdf](https://ueaeprints.uea.ac.uk/id/eprint/10572/1/Thesis_racault_m_2009.pdf).
- 3153 Racault, M.F., Abdulaziz, A., George, G., Menon, N., Jasmin, C., Punathil, M.,
3154 McConville, K., Loveday, B., Platt, T., Sathyendranath, S., Vijayan, V., 2019.
3155 Environmental reservoirs of *Vibrio cholerae*: Challenges and opportunities
3156 for ocean-color remote sensing. Remote Sensing 11, 2763. URL: [https:
3157 //doi.org/10.3390/rs11232763](https://doi.org/10.3390/rs11232763), doi:10.3390/rs11232763.
- 3158 Racault, M.F., Le Quéré, C., Buitenhuis, E., Sathyendranath, S., Platt, 2012.
3159 Phytoplankton phenology in the global ocean. Ecological Indicators 14, 152–
3160 163. doi:10.1016/j.ecolind.2011.07.010.
- 3161 Racault, M.F., Sathyendranath, S., Brewin, R.J.W., Raitsos, D., Jackson, T., Platt,
3162 T., 2017. Impact of El Niño variability on oceanic phytoplankton. Frontiers
3163 in Marine Science 4, 133. URL: [https://www.frontiersin.org/article/10.3389/
3164 fmars.2017.00133](https://www.frontiersin.org/article/10.3389/fmars.2017.00133), doi:10.3389/fmars.2017.00133.
- 3165 Raitsos, D.E., Lavender, S.J., Maravelias, C.D., Haralambous, J., Richardson,
3166 A.J., Reid, P.C., 2008. Identifying four phytoplankton functional types from
3167 space: An ecological approach. Limnology and Oceanography 53, 605–613.

- 3168 Rasse, R., Dall’Olmo, G., Graff, J., Westberry, T.K., van Dongen-Vogels, V.,
3169 Behrenfeld, M.J., 2017. Evaluating optical proxies of particulate organic
3170 carbon across the surface Atlantic ocean. *Frontiers in Marine Science* doi:10.
3171 3389/fmars.2017.00367.
- 3172 Regnier, P., Friedlingstein, P., Ciais, P., Mackenzie, F.T., Gruber, N., Janssens,
3173 I.A., Laruelle, G.G., Lauerwald, R., Luysaert, S., Andersson, A.J., Arndt,
3174 S., Arnosti, C., Borges, A.V., Dale, A.W., Gallego-Sala, A., Godd ris, Y.,
3175 Goossens, N., Hartmann, J., Heinze, C., Ilyina, T., Joos, F., LaRowe, D.E.,
3176 Leifeld, J., Meysman, F.J.R., Munhoven, G., Raymond, P.A., Spahni, R.,
3177 Suntharalingam, P., Thullner, M., 2013. Anthropogenic perturbation of the
3178 carbon fluxes from land to ocean. *Nature Geoscience* 6, 597–607. doi:10.
3179 1038/ngeo1830.
- 3180 Remer, L.A., Davis, A.B., Mattoo, S., Levy, R.C., Kalashnikova, O.V., Coddington,
3181 O., Chowdhary, J., Knobelspiesse, K., Xu, X., Ahmad, Z., Boss, E., Cairns,
3182 B., Dierssen, H.M., Diner, D.J., Franz, B., Frouin, R., Gao, B.C., Ibrahim, A.,
3183 Martins, J.V., Omar, A.H., Torres, O., Xu, F., Zhai, P.W., 2019. Retrieving
3184 aerosol characteristics from the PACE mission, part 1: Ocean color instrument.
3185 *Frontiers in Earth Science* 7, 152. URL: [https://www.frontiersin.org/article/10.](https://www.frontiersin.org/article/10.3389/feart.2019.00152)
3186 [3389/feart.2019.00152](https://www.frontiersin.org/article/10.3389/feart.2019.00152), doi:10.3389/feart.2019.00152.
- 3187 Resplandy, L., Keeling, R.F., R denbeck, C., Stephens, B.B., Khatiwala, S.,
3188 Rodgers, K.B., Long, M.C., Bopp, L., Tans, P.P., 2018. Revision of global
3189 carbon fluxes based on a reassessment of oceanic and riverine carbon transport.
3190 *Nature Geoscience* 11, 504–509. doi:10.1038/s41561-018-0151-3.
- 3191 Resplandy, L., L vy, M., McGillicuddy Jr, D.J., 2019. Effects of eddy-driven
3192 subduction on ocean biological carbon pump. *Global Biogeochemical Cycles*
3193 33, 1071–1084. doi:10.1029/2018GB006125.
- 3194 Reygondeau, G., Longhurst, A., Martinez, E., Beaugrand, G., Antoine, D., Maury,
3195 O., 2013. Dynamic biogeochemical provinces in the global ocean. *Global*
3196 *Biogeochemical Cycles* 27, 1046–1058. doi:10.1002/gbc.20089.
- 3197 Richardson, K., Bendtsen, J., 2019. The vertical distribution of phytoplankton and
3198 primary production in relation to nutricline depth in the open ocean. *Marine*

- 3199 Ecology Progress Series 620, 33–46. doi:10.3354/meps12960.
- 3200 Richardson, K., Bendtsen, J., Kragh, T., Mousing, E.A., 2016. Constraining
3201 the distribution of photosynthetic parameters in the Global Ocean. *Frontiers*
3202 *in Marine Science* 3, 269. URL: <https://doi.org/10.3389/fmars.2016.00269>,
3203 doi:10.3389/fmars.2016.00269.
- 3204 Riebesell, U., Zondervan, I., Rost, B., Tortell, P.D., Zeebe, R.E., Morel, F.M.,
3205 2000. Reduced calcification of marine plankton in response to increased
3206 atmospheric CO₂. *Nature* 407, 364–367. doi:10.1038/35030078.
- 3207 Riley, G.A., 1963. Organic aggregates in seawater and the dynamics of their
3208 formation and utilization. *Limnology and Oceanography* 8, 372–381. doi:10.
3209 4319/10.1963.8.4.0372.
- 3210 Robertson Lain, L., Bernard, S., Evers-King, H., 2014. Biophysical modelling
3211 of phytoplankton communities from first principles using two-layered spheres:
3212 Equivalent Algal Populations (EAP) model. *Optics Express* 22, 16745–16758.
3213 URL: <https://doi.org/10.1364/OE.22.016745>, doi:10.1364/OE.22.016745.
- 3214 Robinson, C., Williams, P.L.B., 2005. Respiration and its measurement in surface
3215 marine waters, in: del Giorgio, P.A., Williams, P.L.B. (Eds.), *Respiration in*
3216 *aquatic ecosystems*. Oxford University Press, pp. 147–180.
- 3217 Robinson, I., 1983. Satellite observations of ocean colour. *Philosophical Trans-*
3218 *actions of the Royal Society of London. Series A, Mathematical and Phys-*
3219 *ical Sciences* 309, 415–432. URL: <https://doi.org/10.1098/rsta.1983.0052>,
3220 doi:10.1098/rsta.1983.0052.
- 3221 Roesler, C.S., Boss, E., 2003. Spectral beam attenuation coefficient retrieved
3222 from ocean color inversion. *Geophysical Research Letters* 30, 1468. doi:10.
3223 1029/2002GL016185.
- 3224 Roshan, S., DeVries, T., 2017. Efficient dissolved organic carbon production and
3225 export in the oligotrophic ocean. *Nature Communications* , 2036 URL: [https://](https://doi.org/10.1038/s41467-017-02227-3)
3226 doi.org/10.1038/s41467-017-02227-3, doi:10.1038/s41467-017-02227-3.
- 3227 Rost, R., Riebesell, U., 2004. Coccolithophores and the biological pump: re-
3228 sponses to environmental changes. in (pp. 99-125). *springer, berlin, heidelberg.*,
3229 in: Thierstein, H.R., Young, J.R. (Eds.), *Coccolithophores: from molecular*

3230 processes to global impact, Springer. pp. 99–125.

3231 Rousseaux, C.S., Gregg, W.W., 2015. Recent decadal trends in global phy-
3232 toplankton composition. *Global Biogeochemical Cycles* 29, 1674–1688.
3233 doi:10.1002/2015GB005139.

3234 Roy, S., Broomhead, D.S., Platt, T., Sathyendranath, S., Ciavatta, S., 2012.
3235 Sequential variations of phytoplankton growth and mortality in an NPZ model:
3236 A remote-sensing-based assessment. *Journal of Marine Systems* 92, 16–29.
3237 doi:10.1016/j.jmarsys.2011.10.001.

3238 Roy, S., Sathyendranath, S., Platt, T., 2017. Size-partitioned phytoplankton carbon
3239 and carbon-to-chlorophyll ratio from ocean colour by an absorption-based bio-
3240 optical algorithm. *Remote Sensing of Environment* 194, 177–189. URL: <https://doi.org/10.1016/j.rse.2017.02.015>, doi:10.1016/j.rse.2017.02.015.

3242 Rudnick, D.L., 2016. Ocean research enabled by underwater glid-
3243 ers. *Annual Review of Marine Science* 8, 519–541. URL:
3244 <https://doi.org/10.1146/annurev-marine-122414-033913>, doi:10.1146/
3245 annurev-marine-122414-033913.

3246 Rudnick, D.L., Cole, S.T., 2011. On sampling the ocean using underwater
3247 gliders. *Journal of Geophysical Research: Oceans* 116, C8. doi:10.1029/
3248 2010JC006849.

3249 Saba, V.S., Friedrichs, M.A.M., Antoine, D., Armstrong, R.A., Asanuma, I.,
3250 Behrenfeld, M.J., Ciotti, A.M., Dowell, M., Hoepffner, N., Hyde, K.J.W.,
3251 Ishizaka, J., Kameda, T., Marra, J., Mélin, F., Morel, A., O'Reilly, J., Scardi, M.,
3252 Smith Jr, W.O., Smyth, T.J., Tang, S., Uitz, J., Waters, K., Westberry, T.K., 2011.
3253 An evaluation of ocean color model estimates of marine primary productivity
3254 in coastal and pelagic regions across the globe. *Biogeosciences* 8, 489–503.
3255 URL: <https://doi.org/10.5194/bg-8-489-2011>, doi:10.5194/bg-8-489-2011.

3256 Saba, V.S., Friedrichs, M.A.M., Carr, M.E., Antoine, D., Armstrong, R.A.,
3257 Asanuma, I., Aumont, O., Bates, N.R., Behrenfeld, M.J., Bennington, V.,
3258 Bopp, L., Bruggeman, J., Buitenhuis, E.T., Church, M.J., Ciotti, A.M., Doney,
3259 S.C., Dowell, M., Dunne, J., Dutkiewicz, S., Gregg, W., Hoepffner, N., Hyde,
3260 K.J.W., Ishizaka, J., Kameda, T., Karl, D.M., Lima, I., Lomas, M.W., Marra,

3261 J., McKinley, G.A., Mélin, F., Moore, J.K., Morel, A., O'Reilly, J., Salihoglu,
3262 B., Scardi, M., Smyth, T.J., Tang, S., Tjiputra, J., Uitz, J., Vichi, M., Waters,
3263 K., Westberry, T.K., Yool, A., 2010. Challenges of modeling depth-integrated
3264 marine primary productivity over multiple decades: A case study at BATS and
3265 HOT. *Global Biogeochemical Cycles* 24. URL: <https://agupubs.onlinelibrary.wiley.com/doi/abs/10.1029/2009GB003655>, doi:10.1029/2009GB003655.
3266
3267 Sadeghi, A., Dinter, T., Vountas, M., Taylor, B., Altenburg-Soppa, M., Bracher,
3268 A., 2012. Remote sensing of coccolithophore blooms in selected oceanic
3269 regions using the PhytoDOAS method applied to hyper-spectral satellite data.
3270 *Biogeosciences* 9, 2127–2143. URL: <https://doi.org/10.5194/bg-9-2127-2012>,
3271 doi:10.5194/bg-9-2127-2012.
3272 Sanders, R., Henson, S.A., Koski, M., Christina, L., Painter, S.C., Poulton, A.J.,
3273 Riley, J., Salihoglu, B., Visser, A., Yool, A., Bellerby, R., 2014. The biological
3274 carbon pump in the North Atlantic. *Progress in Oceanography* 129, 200–218.
3275 doi:10.1016/j.pocean.2014.05.005.
3276 Sarma, V.V.S.S., 2003. Monthly variability in surface pCO₂ and net air-sea CO₂
3277 flux in the Arabian Sea. *Journal of Geophysical Research: Oceans* 108, C8.
3278 doi:10.1029/2001JC001062.
3279 Sarma, V.V.S.S., Saino, T., Sasaoka, K., Nojiri, Y., Ono, T., Ishii, M., Inoue,
3280 H.Y., Matsumoto, K., 2006. Basin-scale pCO₂ distribution using satellite sea
3281 surface temperature, Chl a, and climatological salinity in the North Pacific
3282 in spring and summer. *Global Biogeochemical Cycles* 20, GB3005. doi:10.
3283 1029/2005GB002594.
3284 Sarmiento, J.L., Gruber, N., 2006. *Ocean Biogeochemical Dynamics*. Princeton
3285 University Press, Princeton, Woodstock.
3286 Sathyendranath, S., Abdulaziz, A., Menon, N., George, G., Evers-King, H.,
3287 Kulk, G., Colwell, R., Jutla, A., Platt, T., 2020a. Building capacity and
3288 resilience against diseases transmitted via water under climate perturbations
3289 and extreme weather stress, in: Ferretti, S. (Ed.), *Space Capacity Building*
3290 *in the XXI Century*. *Studies in Space Policy*, Springer, Cham. doi:10.1007/
3291 978-3-030-21938-3_24.

- 3292 Sathyendranath, S., Brewin, R.J.W., Brockmann, C., Brotas, V., Calton, B.,
3293 Chuprin, A., Cipollini, P., Couto, A.B., Dingle, J., Doerffer, R., Donlon, C.,
3294 Dowell, M., Farman, A., Grant, M., Groom, S., Horseman, A., Jackson, T.,
3295 Krasemann, H., Lavender, S., Martinez-Vicente, V., Mazeran, C., Mélin, F.,
3296 Moore, T.S., Müller, D., Regner, P., Roy, S., Steele, C.J., Steinmetz, F., Swinton,
3297 J., Taberner, M., Thompson, A., Valente, A., Zühlke, M., Brando, V.E., Feng,
3298 H., Feldman, G., Franz, B.A., Frouin, R., Gould, R.W., Hooker, S.B., Kahru,
3299 M., Kratzer, S., Mitchell, B.G., Muller-Karger, F.E., Sosik, H.M., Voss, K.,
3300 Werdell, J., Platt, T., 2019a. An ocean-colour time series for use in climate
3301 studies: The experience of the Ocean-Colour Climate Change Initiative (OC-
3302 CCI). *Sensors* 19, 4285.
- 3303 Sathyendranath, S., Brewin, R.J.W., Jackson, T., Mélin, F., Platt, T., 2017. Ocean-
3304 colour Products for Climate-Change Studies: What are their ideal character-
3305 istics? *Remote Sensing of Environment* 203, 125–138. doi:10.1016/j.rse.
3306 2017.04.017.
- 3307 Sathyendranath, S., Longhurst, A., Caverhill, C.M., Platt, T., 1995. Regionally
3308 and seasonally differentiated primary production in the North Atlantic. *Deep*
3309 *Sea Research I* 42, 1773–1802.
- 3310 Sathyendranath, S., Platt, T., 1989. Computation of aquatic primary production:
3311 extended formalism to include effect of angular and spectral distribution of
3312 light. *Limnology and Oceanography* 34, 188–198.
- 3313 Sathyendranath, S., Platt, T., 2007. Spectral effects in bio-optical control on the
3314 ocean system. *Oceanologia* 49, 5–39.
- 3315 Sathyendranath, S., Platt, T., Brewin, R.J.W., Jackson, T., 2019b. Primary pro-
3316 duction distribution, in: Cochran, J.K., Bokuniewicz, J.H., Yager, L.P. (Eds.),
3317 *Encyclopedia of Ocean Sciences*, 3rd Edition. Elsevier. volume 1, pp. 635–640.
- 3318 Sathyendranath, S., Platt, T., Caverhill, C.M., Warnock, R.E., Lewis, M.R.,
3319 1989. Remote sensing of oceanic primary production: computations using a
3320 spectral model. *Deep Sea Research Part A. Oceanographic Research Papers* 36,
3321 431–453. URL: [https://doi.org/10.1016/0198-0149\(89\)90046-0](https://doi.org/10.1016/0198-0149(89)90046-0), doi:10.1016/
3322 0198-0149(89)90046-0.

- 3323 Sathyendranath, S., Platt, T., Horne, E.P.W., Harrison, W. G. Ulloa, O., Out-
3324 erbridge, R., Hoepffner, N., 1991. Estimation of new production in the
3325 ocean by compound remote sensing. *Nature* 353, 129–133. URL: <https://doi.org/10.1038/353129a0>, doi:10.1038/353129a0.
3326
- 3327 Sathyendranath, S., Platt, T., Kovač, Ž., Dingle, J., Jackson, T., Brewin, R.J.W.,
3328 Franks, P., Marañón, E., Kulk, G., Bouman, H., 2020b. Reconciling models
3329 of primary production and photoacclimation. *Applied Optics* 59, C100–C114.
3330 doi:10.1364/AO.386252.
- 3331 Sathyendranath, S., Stuart, V., Nair, A., Oka, K., Nakane, T., Bouman, H., Forget,
3332 H.M., Maass, H., Platt, T., 2009. Carbon-to-chlorophyll ratio and growth rate
3333 of phytoplankton in the sea. *Marine Ecological Progress Series* 383, 73–84.
3334 doi:10.3354/meps07998.
- 3335 Saux Picart, S., Sathyendranath, S., Dowell, M., Moore, T., Platt, T., 2014.
3336 Remote sensing of assimilation number for marine phytoplankton. *Remote*
3337 *Sensing Environment* 146, 87–96. doi:10.1016/j.rse.2013.10.032.
- 3338 Schiebel, R., 2002. Planktic foraminiferal sedimentation and the marine
3339 calcite budget. *Global Biogeochemical Cycles* 16, 1065. doi:10.1029/
3340 2001GB001459.
- 3341 Schueler, C., Holmes, A., 2016. SeaHawk CubeSat system engineering, in:
3342 Ardanuy, P.E., Puschell, J.J. (Eds.), *Remote Sensing System Engineering*
3343 *VI*, International Society for Optics and Photonics. SPIE. pp. 38–43. URL:
3344 <https://doi.org/10.1117/12.2242298>, doi:10.1117/12.2242298.
- 3345 Scott, J.P., Crooke, S., Cetinić, I., Del Castillo, C.E., Gentemann, C.L., 2020. Cor-
3346 recting non-photochemical quenching of saildrone chlorophyll-a fluorescence
3347 for evaluation of satellite ocean color retrievals. *Optics Express* 28, 4274–4285.
3348 URL: <https://doi.org/10.1364/OE.382029>, doi:10.1364/OE.382029.
- 3349 Seegers, B.N., Stumpf, R.P., Schaeffer, B.A., Loftin, K.A., Werdell, P.J., 2018. Per-
3350 formance metrics for the assessment of satellite data products: an ocean color
3351 case study. *Optics Express* 26, 7404–7422. doi:10.1364/OE.26.007404.
- 3352 Seitzinger, S.P., Mayorga, E., Bouwman, A.F., Kroeze, C., Beusen, A.H.W.,
3353 Billen, G., Van Drecht, G., Dumont, E., Fekete, B.M., Garnier, J., Harrison,

3354 J.A., 2010. Global river nutrient export: A scenario analysis of past and future
3355 trends. *Global Biogeochemical Cycles* 24. doi:10.1029/2009GB003587.

3356 Sharp, J., 1974. Improved analysis for particulate organic carbon and nitrogen
3357 from seawater. *Limnology and Oceanography* 19, 984–989.

3358 Sharp, J.H., 1979. Excretion of organic matter by marine phytoplankton: Do
3359 healthy cells do it? *Limnology and Oceanography* 22, 381–399. doi:10.4319/
3360 lo.1977.22.3.0381.

3361 Sharp, J.H., 2002. Analytical methods for total DOM pools, in: Hansell, D.A.,
3362 Carlson, C.A. (Eds.), *Biogeochemistry of marine dissolved organic matter*.
3363 Academic Press, pp. 35–58.

3364 Shutler, J.D., Grant, M.G., Miller, P.I., Rushton, E., Anderson, K., 2010. Coccolithophore bloom detection in the north east Atlantic using SeaWiFS: Algorithm
3365 description, application and sensitivity analysis. *Remote Sensing of Environment* 114, 1008–1016. URL: <https://doi.org/10.1016/j.rse.2009.12.024>,
3366 doi:10.1016/j.rse.2009.12.024.

3367
3368

3369 Shutler, J.D., Land, P.E., Brown, C.W., Findlay, H.S., Donlon, C.J., Medland, M.,
3370 Snooke, R., Blackford, J.C., 2013. Coccolithophore surface distributions in the
3371 North Atlantic and their modulation of the air-sea flux of CO₂ from 10 years
3372 of satellite Earth Observation data. *Biogeosciences* 10, 2699–2709. URL:
3373 <https://doi.org/10.5194/bg-10-2699-2013>, doi:10.5194/bg-10-2699-2013.

3374 Shutler, J.D., Wanninkhof, R., Nightingale, P.D., Woolf, D.K., Bakker, D.C.E.,
3375 Watson, A., Ashton, I., Holding, T., Chapron, B., Quilfen, Y., Fairall, C.,
3376 Schuster, U., Nakajima, M., Donlon, C.J., 2019. Satellites will address critical
3377 science priorities for quantifying ocean carbon. *Frontiers in Ecology and the*
3378 *Environment* 18, 27–35. doi:10.1002/fee.2129.

3379 Siegel, D.A., Behrenfeld, M.J., Maritorena, S., McClain, C.R., Antoine, D., Bailey,
3380 S.W., Bontempi, P.S., Boss, E.S., Dierssen, H.M., Doney, S.C., Eplee Jr, R.E.,
3381 Evans, R.H., Feldman, G.C., Fields, E., Franz, B.A., Kuring, N.A., Mengelt, C.,
3382 Nelson, N.B., Patt, F.S., Robinson, W.D., Sarmiento, J.L., Swan, C.M., Werdell,
3383 P.J., Westberry, T.K., Wilding, J.G., Yoder, J.A., 2013. Regional to global
3384 assessments of phytoplankton dynamics from the SeaWiFS mission. *Remote*

3385 Sensing of Environment 135, 77–91. doi:10.1016/j.rse.2013.03.025.

3386 Siegel, D.A., Buesseler, K.O., Behrenfeld, M.J., Benitez-Nelson, C.R., Boss, E.,
3387 Brzezinski, M.A., Burd, A., Carlson, C.A., D’Asaro, E.A., Doney, S.C., Perry,
3388 M.J., Stanley, R.H.R., Steinberg, D.K., 2016. Prediction of the export and fate
3389 of global ocean net primary production: The EXPORTS science plan. *Frontiers*
3390 *in Marine Science* 3. doi:10.3389/fmars.2016.00022.

3391 Siegel, D.A., Buesseler, K.O., Doney, S.C., Sailley, S.F., Behrenfeld, M.J., Boyd,
3392 P.W., 2014. Global assessment of ocean carbon export by combining satellite
3393 observations and food-web models. *Global Biogeochemical Cycles* 28, 181–
3394 196. doi:10.1002/2013gb004743.

3395 Sigman, D.M., Hain, M.P., 2012. The biological productivity of the ocean. *Nature*
3396 *Education Knowledge* 3, 21.

3397 Silió-Calzada, A., Bricaud, A., Uitz, J., Gentili, B., 2008. Estimation of new
3398 primary production in the Benguela upwelling area, using ENVISAT satellite
3399 data and a model dependent on the phytoplankton community size structure.
3400 *Journal of Geophysical Research* 113, C11023. doi:10.1029/2007JC004588.

3401 Simis, S.G.H., Olsson, J., 2013. Unattended processing of shipborne hyperspectral
3402 reflectance measurements. *Remote Sensing of Environment* 135, 202–212.
3403 doi:10.1016/j.rse.2013.04.001.

3404 Sinha, E., Michalak, A.M., Balaji, V., 2017. Eutrophication will increase during
3405 the 21st century as a result of precipitation changes. *Science* 357, 405–408.
3406 doi:10.1126/science.aan2409.

3407 Skákala, J., Ford, D., Brewin, R.J.W., McEwan, R., Kay, S., Taylor, B., de Mora,
3408 L., Ciavatta, S., 2018. The assimilation of phytoplankton functional types for
3409 operational forecasting in the northwest European shelf. *Journal of Geophysical*
3410 *Research: Oceans* 123, 5230–5247.

3411 Slade, W.H., Boss, E., Dall’Olmo, G., Langner, M.R., Loftin, J., Behrenfeld,
3412 M.J., Roesler, C., Westberry, T.K., 2010. Underway and moored methods
3413 for improving accuracy in measurement of spectral particulate absorption and
3414 attenuation. *Journal of Atmospheric and Oceanic Technology* 27, 1733–1746.
3415 doi:10.1175/2010JTECH0755.1.

- 3416 Smith, R.C., Eppley, R.W., Baker, K.S., 1982. Correlation of primary production
3417 as measured aboard ship in southern california coastal waters and as estimated
3418 from satellite chlorophyll images. *Marine Biology* 66, 281–288. URL: <https://doi.org/10.1007/BF00397033>, doi:10.1007/BF00397033.
3419
- 3420 Smyth, T.J., Tilstone, G.H., Groom, S.B., 2005. Integration of radiative transfer
3421 into satellite models of ocean primary production. *Journal of Geophysical*
3422 *Research: Oceans* 110, C10014. URL: <https://doi.org/10.1029/2004JC002784>,
3423 doi:10.1029/2004JC002784.
- 3424 Smyth, T.J., Tyrrell, T., Tarrant, B., 2004. Time series of coccolithophore activ-
3425 ity in the Barents Sea, from twenty years of satellite imagery. *Geophysical*
3426 *Research Letters* 31.
- 3427 Solanki, H.U., Chauhan, R., George, L.B., Dwivedi, R.M., 2015. Development of
3428 bio-physical model for the estimation of zooplankton biomass production in
3429 the Arabian Sea using remotely sensed oceanographic variables. *Indian Journal*
3430 *of Marine Science* 44, 348–353.
- 3431 Spencer, R.G.M., Stubbins, A., Hernes, P.J., Baker, A., Mopper, K., Aufdenkampe,
3432 A.K., Dyda, R.Y., Mwamba, V.L., Mangangu, A.M., Wabakanghanzi, J.N.,
3433 Six, J., 2009. Photochemical degradation of dissolved organic matter and dis-
3434 solved lignin phenols from the Congo River. *Journal of Geophysical Research:*
3435 *Biogeosciences* 114, G03010. doi:10.1029/2009JG000968.
- 3436 Steinberg, D.K., Landry, M.R., 2017. Zooplankton and the ocean carbon
3437 cycle. *Annual Review of Marine Science* 9, 413–444. doi:10.1146/
3438 annurev-marine-010814-015924.
- 3439 Stommel, H., 1989. The Slocum mission. *Oceanography* 2, 22–25.
- 3440 Stomp, M., Huisman, J., Stal, L.J., Matthijs, H.C., 2007. Colorful niches of
3441 phototrophic microorganisms shaped by vibrations of the water molecule. *The*
3442 *ISME journal* 1, 271–282. doi:10.1038/ismej.2007.59.
- 3443 Stramska, M., 2010. The diffusive component of particulate organic carbon export
3444 in the North Atlantic estimated from SeaWiFS ocean color. *Deep Sea Research*
3445 *Part I: Oceanographic Research Papers* 57, 284–296. doi:10.1016/j.dsr.
3446 2009.11.007.

- 3447 Stramska, M., Cieszyńska, A., 2015. Ocean colour estimates of particulate
3448 organic carbon reservoirs in the global ocean – revisited. *International Journal*
3449 *of Remote Sensing* 36, 3675–3700. doi:10.1080/01431161.2015.1049380.
- 3450 Stramska, M., Stramski, D., 2005. Variability of particulate organic carbon
3451 concentration in the north polar Atlantic based on ocean color observations with
3452 Sea-viewing Wide Field-of-view Sensor (SeaWiFS). *Journal of Geophysical*
3453 *Research: Oceans* 110, C10018. doi:10.1029/2004JC002762.
- 3454 Stramski, D., Boss, E., Bogucki, D., Voss, K.J., 2004. The role of seawater
3455 constituents in light backscattering in the ocean. *Progress in Oceanography* 61,
3456 27–56. URL: <https://doi.org/10.1016/j.pocean.2004.07.001>, doi:10.1016/j.
3457 pocean.2004.07.001.
- 3458 Stramski, D., Kiefer, D.A., 1991. Light scattering by microorganisms in the open
3459 ocean. *Progress in Oceanography* 28, 343–383. doi:10.1016/0079-6611(91)
3460 90032-H.
- 3461 Stramski, D., Reynolds, R.A., Babin, M., Kaczmarek, S., Lewis, M.R., Röttgers,
3462 R., Sciandra, A., Stramska, M., Twardowski, M.S., Franz, B.A., Claustre, H.,
3463 2008. Relationships between the surface concentration of particulate organic
3464 carbon and optical properties in the eastern South Pacific and eastern Atlantic
3465 Oceans. *Biogeosciences* 5, 171–201. doi:10.5194/bg-5-171-2008.
- 3466 Stramski, D., Reynolds, R.A., Kahru, M., Mitchell, B.G., 1999. Estimation of
3467 particulate organic carbon in the ocean from satellite remote sensing. *Science*
3468 285, 239–242. doi:10.1126/science.285.5425.239.
- 3469 Strömberg, K.H.P., Smyth, T.J., Allen, J.I., Pitois, S., O’Brien, T.D., 2009. Estima-
3470 tion of global zooplankton biomass from satellite ocean colour. *Journal of Ma-
3471 rine Systems* 78, 18–27. URL: <https://doi.org/10.1016/j.jmarsys.2009.02.004>,
3472 doi:10.1016/j.jmarsys.2009.02.004.
- 3473 Stukel, M.R., Kahru, M., Benitez-Nelson, C.R., Décima, M., Goericke, R., Landry,
3474 M.R., Ohman, M.D., 2015. Using Lagrangian-based process studies to test
3475 satellite algorithms of vertical carbon flux in the eastern North Pacific Ocean.
3476 *Journal of Geophysical Research: Oceans* 120, 7208–7222. doi:10.1002/
3477 2015jc011264.

3478 Su, T.C., 2017. A study of a matching pixel by pixel (MPP) algorithm to establish
3479 an empirical model of waterquality mapping, as based on unmanned aerial
3480 vehicle (UAV) images. *International Journal of Applied Earth Observation and*
3481 *Geoinformation* 58:, 213–224. URL: <https://doi.org/10.1016/j.jag.2017.02.011>,
3482 doi:10.1016/j.jag.2017.02.011.

3483 Suess, E., 1980. Particulate organic carbon flux in the oceans–Surface productivity
3484 and oxygen utilization. *Nature* 288, 260–263. doi:10.1038/288260a0.

3485 Sun, X., Shen, F., Brewin, R.J.W., Liu, D., Tang, R., 2019. Twenty-year variations
3486 in satellite-derived chlorophyll-a and phytoplankton size in the Bohai Sea and
3487 Yellow Sea. *Journal of Geophysical Research: Oceans* 124, 8887–8912. URL:
3488 <https://doi.org/10.1029/2019JC015552>, doi:10.1029/2019JC015552.

3489 Suzuki, N., Kato, K., 1953. Studies on suspended materials. Marine snow in the
3490 sea. I. sources of marine snow. *Bull. Fac. Fish. Hokkaido Univ.* 4, 132–35.

3491 Świrgoń, M., Stramska, M., 2015. Comparison of in situ and satellite ocean color
3492 determinations of particulate organic carbon concentration in the global ocean.
3493 *Oceanologia* 57, 25–31. URL: <https://doi.org/10.1016/j.oceano.2014.09.002>,
3494 doi:10.1016/j.oceano.2014.09.002.

3495 Taboada, F.G., Barton, A.D., Stock, C.A., Dunne, J., John, J.G., 2019. Seasonal
3496 to interannual predictability of oceanic net primary production inferred from
3497 satellite observations. *Progress in Oceanography* 170, 28–39. URL: <https://doi.org/10.1016/j.pocean.2018.10.010>, doi:10.1016/j.pocean.2018.10.010.

3498 Takahashi, T., Sutherland, S.C., Kozyr, A., 2019. Global ocean surface wa-
3499 ter partial pressure of CO₂ database: Measurements performed during 1957-
3500 2018 (LDEO database version 2018) (ncei accession 0160492). version 7.7.
3501 NOAA National Centers for Environmental Information. Dataset. URL:
3502 [https://doi.org/10.3334/CDIAC/OTG.NDP088\(V2015\)](https://doi.org/10.3334/CDIAC/OTG.NDP088(V2015)), doi:10.3334/CDIAC/
3503 OTG.NDP088(V2015).

3504 Takahashi, T., Sutherland, S.C., Sweeney, C., Poisson, A., Metzl, N., Tilbrook,
3505 B., Bates, N., Wanninkhof, R., Feely, R.A., Sabine, C. Olafsson, J., Nojiri, Y.,
3506 2002. Global sea–air CO₂ flux based on climatological surface ocean pCO₂, and
3507 seasonal biological and temperature effects. *Deep Sea Research Part II: Topical*
3508

- 3509 Studies in Oceanography 49, 1601–1622. doi:10.1016/S0967-0645(02)
3510 00003-6.
- 3511 Tang, K.W., Gladyshev, M.I., Dubovskaya, O.P., Kirillin, G., Grossart, H.P., 2014.
3512 Zooplankton carcasses and non-predatory mortality in freshwater and inland
3513 sea environments. *Journal of Plankton Research* 36, 597–612. doi:10.1093/
3514 plankt/fbu014.
- 3515 Tehrani, N.C., D'Sa, E.J., Osburn, C.L., Bianchi, T.S., Schaeffer, B.A., 2013.
3516 Chromophoric Dissolved Organic Matter and Dissolved Organic Carbon from
3517 Sea-Viewing Wide Field-of-view Sensor (SeaWiFS), Moderate Resolution
3518 Imaging Spectroradiometer (MODIS) and MERIS Sensors: Case study for
3519 the northern Gulf of Mexico. *Remote Sensing* 5, 1439–1464. doi:10.3390/
3520 rs5031439.
- 3521 Terada, A., Morita, Y., Hashimoto, T., Mori, T., Ohba, T., Yaguchi, M., Kanda, W.,
3522 2018. Water sampling using a drone at Yugama crater lake, Kusatsu-Shirane
3523 volcano, Japan. *Earth Planets Space* 70, 64. URL: [https://doi.org/10.1186/
3524 s40623-018-0835-3](https://doi.org/10.1186/s40623-018-0835-3), doi:10.1186/s40623-018-0835-3.
- 3525 Thomalla, S.J., Ogunkoya, A.G., Vichi, M., Swart, S., 2017. Using optical sensors
3526 on gliders to estimate phytoplankton carbon concentrations and chlorophyll-to-
3527 carbon ratios in the southern ocean. *Frontiers in Marine Science* 4, 133–119.
3528 doi:10.3389/fmars.2017.00034.
- 3529 Thomson, J., Girton, J., 2017. Sustained measurements of Southern Ocean air-sea
3530 coupling from a wave glider autonomous surface vehicle. *Oceanography* 30,
3531 104–109. URL: <https://www.jstor.org/stable/26201855>.
- 3532 Tilstone, G., Lange, P.K., Misra, A., Brewin, R.J.W., Cain, T., 2017. Micro-
3533 phytoplankton photosynthesis, primary production and potential export produc-
3534 tion in the Atlantic Ocean. *Progress in Oceanography* 158, 109–129. URL:
3535 <https://doi.org/10.1016/j.pocean.2017.01.006>, doi:10.1016/j.pocean.2017.
3536 01.006.
- 3537 Tilstone, G., Smyth, T., Poulton, A., Hutson, R., 2009. Measured and remotely
3538 sensed estimates of primary production in the Atlantic Ocean from 1998 to 2005.
3539 *Deep Sea Research II* 56, 918–930. doi:10.1016/j.dsr2.2008.10.034.

- 3540 Tilstone, G.H., Taylor, B.H., Blondeau-Patissier, D., Powell, T., Groom, S.B.,
3541 Rees, A.P., Lucas, M.I., 2015. Comparison of new and primary production
3542 models using SeaWiFS data in contrasting hydrographic zones of the northern
3543 North Atlantic. *Remote Sensing of Environment* 156, 473–489. doi:10.1016/
3544 j.rse.2014.10.013.
- 3545 Todd, R.E., Rudnick, D.L., Sherman, J.T., Owens, W.B., George, L., 2017.
3546 Absolute velocity estimates from autonomous underwater gliders equipped with
3547 Doppler current profilers. *Journal of Atmospheric and Oceanic Technology* 34,
3548 309–333. URL: <https://doi.org/10.1175/JTECH-D-16-0156.1>, doi:10.1175/
3549 JTECH-D-16-0156.1.
- 3550 Toole, D.A., Siegel, D.A., 2001. Modes and mechanisms of ocean color variability
3551 in the Santa Barbara Channel. *Journal of Geophysical Research: Oceans* 106,
3552 26985–27000. doi:10.1029/2000JC000371.
- 3553 Tran, T.K., Duforêt-Gaurier, L., Vantrepotte, V., Jorge, D.S.F., Mériaux, X.,
3554 Cauvin, A., Fanton d'Andon, O., Loisel, H., 2019. Deriving particulate organic
3555 carbon in coastal waters from remote sensing: Inter-comparison exercise and
3556 development of a maximum band-ratio approach. *Remote Sensing* 11, 2849.
3557 URL: <https://doi.org/10.3390/rs11232849>, doi:10.3390/rs11232849.
- 3558 Tranvik, L.J., Downing, J.A., Cotner, J.B., Loisel, S.A., Striegl, R.G., Ballatore,
3559 T.J., Dillon, P., Finlay, K., Fortino, K., Knoll, L.B., Kortelainen, P.L., Kutser,
3560 T., Larsen, S., Laurion, I., Leech, D.M., McCallister, S.L., McKnight, D.M.,
3561 Melack, J.M., Overholt, E., Porter, J.A., Prairie, Y., Renwick, W.H., Roland,
3562 F., Sherman, B.S., Schindler, D.W., Sobek, S., Tremblay, A., Vanni, M.J.,
3563 Verschoor, A.M., von Wachenfeldt, E., Weyhenmeyer, G.A., 2009. Lakes and
3564 reservoirs as regulators of carbon cycling and climate. *Limnology and Oceanog-*
3565 *raphy* 54, 2298–2314. doi:10.4319/lo.2009.54.6_part_2.2298.
- 3566 Tremblay, J., Klein, B., Legendre, L., Rivkin, R.B., Therriault, J., 1997. Estima-
3567 tion of f-ratios in oceans based on phytoplankton size structure. *Limnology*
3568 *and Oceanography* 42, 595–601. doi:10.4319/lo.1997.42.3.0595.
- 3569 Uitz, J., Claustre, H., Brian Griffiths, F., Ras, J., Garcia, N., Sandroni, V., 2009.
3570 A phytoplankton class-specific primary production model applied to the Ker-

- 3571 guelen Islands region (Southern Ocean). *Deep-Sea Research I* 56, 541–560.
3572 doi:10.1016/j.dsr.2008.11.006.
- 3573 Uitz, J., Claustre, H., Gentili, B., Stramski, D., 2010. Phytoplankton class-
3574 specific primary production in the world’s oceans: Seasonal and interannual
3575 variability from satellite observations. *Global Biogeochemical Cycles* 24,
3576 GB3016. doi:10.1029/2009GB003680.
- 3577 Uitz, J., Huot, Y., Bruyant, F., Babin, M., Claustre, H., 2008. Relating phyto-
3578 plankton photophysiological properties to community structure on large scales.
3579 *Limnology and Oceanography* 53, 614–630.
- 3580 Uitz, J., Stramski, D., Gentili, B., D’Ortenzio, F., Claustre, H., 2012. Estimates of
3581 phytoplankton class-specific and total primary production in the Mediterranean
3582 Sea from satellite ocean color observations. *Global Biogeochemical Cycles* 26,
3583 GB2024. doi:1029/2011GB004055.
- 3584 Ulloa, O., Sathyendranath, S., Platt, T., 1994. Effect of the particle-size distribu-
3585 tion on the backscattering ratio in seawater. *Applied Optics* 33, 7070–7077.
3586 doi:10.1364/AO.33.007070.
- 3587 Valente, A., Sathyendranath, S., Brotas, V., Groom, S., Grant, M., Taberner, M.,
3588 Antoine, D., Arnone, R., Balch, W.M., Barker, K., Barlow, R., Bélanger, S.,
3589 Berthon, J.F., Beşiktepe, c., Borsheim, Y., Bracher, A., Brando, V., Canuti, E.,
3590 Chavez, F., Cianca, A., Claustre, H., Clementson, L., Crout, R., Frouin, R.,
3591 García-Soto, C., Gibb, S.W., Gould, R., Hooker, S.B., Kahru, M., Kampel, M.,
3592 Klein, H., Kratzer, S., Kudela, R., Ledesma, J., Loisel, H., Matrai, P., McKee,
3593 D., Mitchell, B.G., Moisan, T., Muller-Karger, F., O’Dowd, L., Ondrusek, M.,
3594 Platt, T., Poulton, A.J., Repecaud, M., Schroeder, T., Smyth, T., Smythe-Wright,
3595 D., Sosik, H.M., Twardowski, M., Vellucci, V., Voss, K., Werdell, J., Wernand,
3596 M., Wright, S., Zibordi, G., 2019a. A compilation of global bio-optical in situ
3597 data for ocean-colour satellite applications – version two. *Earth System Science*
3598 *Data* 11, 1037–1068. URL: <https://www.earth-syst-sci-data.net/11/1037/2019/>,
3599 doi:10.5194/essd-11-1037-2019.
- 3600 Valente, A., Sathyendranath, S., Brotas, V., Groom, S., Grant, M., Taberner, M.,
3601 Antoine, D., Arnone, R., Balch, W.M., Barker, K., Barlow, R.G., Bélanger, S.,

- 3602 Berthon, J.F., Besiktepe, S., Borsheim, K.Y., Bracher, A., Brando, V.E., Canuti,
3603 E., Chavez, F.P., Cianca, A., Claustre, H., Clementson, L., Crout, R., Frouin,
3604 R., García-Soto, C., Gibb, S.W., Gould, R., Hooker, S.B., Kahru, M., Kampel,
3605 M., Klein, H., Kratzer, S., Kudela, R.M., Ledesma, S., Loisel, H., Matrai,
3606 P.A., McKee, D., Mitchell, B.G., Moisan, T., Muller-Karger, F.E., O’Dowd,
3607 L., Ondrusek, M., Platt, T., Poulton, A.J., Repecaud, M., Schroeder, T., Smyth,
3608 T.J., Smythe-Wright, D., Sosik, H., Twardowski, M.S., Vellucci, V., Voss, K.,
3609 Werdell, P.J., Wernand, M.R., Wright, S., Zibordi, G., 2019b. A compilation of
3610 global bio-optical in situ data for ocean-colour satellite applications - version
3611 two. PANGAEA. URL: <https://doi.org/10.1594/PANGAEA.898188>, doi:10.
3612 1594/PANGAEA.898188.
- 3613 Vanhellefont, Q., 2019. Daily metre-scale mapping of water turbidity using
3614 CubeSat imagery. *Optics Express* 27, A1372–A1399. doi:10.1364/OE.27.
3615 0A1372.
- 3616 Vazquez-Cuervo, J., Gomez-Valdes, J., Bouali, M., Miranda, L.E., Van der
3617 Stocken, T., Tang, W., Gentemann, C., 2019. Using saildrones to validate
3618 satellite-derived sea surface salinity and sea surface temperature along the
3619 California/Baja Coast. *Remote Sensing* 11, 1964. URL: [https://doi.org/10.](https://doi.org/10.3390/rs11171964)
3620 [3390/rs11171964](https://doi.org/10.3390/rs11171964), doi:10.3390/rs11171964.
- 3621 Veldhuis, M.J.W., Kraay, G.W., 2002. Application of flow cytometry in marine
3622 phytoplankton research: current applications and future perspectives. *Scientia*
3623 *Marina* 64, 121–134.
- 3624 Villareal, T.A., Wilson, C., 2014. A comparison of the pac-X trans-pacific wave
3625 glider data and satellite data (MODIS, aquarius, TRMM and VIIRS). *PLoS*
3626 *One* 9, e92280. doi:10.1371/journal.pone.0092280.
- 3627 Vincent, A.G., Pascal, R.W., Beaton, A.D., Walk, J., Hopkins, J.E., Woodward,
3628 E.M.S., Mowlem, M., Lohan, M.C., 2018. Nitrate drawdown during a shelf
3629 sea spring bloom revealed using a novel microfluidic in situ chemical sensor
3630 deployed within an autonomous underwater glider. *Marine Chemistry* 205,
3631 29–36.
- 3632 Vinogradova, N., Lee, T., Boutin, J., Drushka, K., Fournier, S., Sabia, R., Stammer,

- 3633 D., Bayler, E., Reul, N., Gordon, A., Melnichenko, O., Li, L., Hackert, E.,
3634 Martin, M., Kolodziejczyk, N., Hasson, A., Brown, S., Misra, S., Lindstrom,
3635 E., 2019. Satellite salinity observing system: Recent discoveries and the way
3636 forward. *Frontiers in Marine Science* 6, 243. URL: [https://www.frontiersin.](https://www.frontiersin.org/article/10.3389/fmars.2019.00243)
3637 [org/article/10.3389/fmars.2019.00243](https://www.frontiersin.org/article/10.3389/fmars.2019.00243), doi:10.3389/fmars.2019.00243.
- 3638 Vodacek, A., Blough, N.V., DeGrandpre, M.D., Peltzer, E.T., Nelson, R.K.,
3639 1997. Seasonal variations of CDOM and DOC in the Middle Atlantic Bight:
3640 Terrestrial inputs and photooxydation. *Limnology and Oceanography* 42,
3641 674–686.
- 3642 Volk, T., Hoffert, M.I., 1985. Ocean carbon pumps: Analysis of relative strengths
3643 and efficiencies in ocean-driven atmospheric CO₂ changes, in: Sundquist, E.T.,
3644 Broecker, W.S. (Eds.), *Geophysical Monograph Series*, American Geophysical
3645 Union, Washington, DC. pp. 99–110.
- 3646 Wadham, J.L., Hawkings, J.R., Tarasov, L., Gregoire, L.J., Spencer, R.G.M.,
3647 Gutjahr, M., Ridgwell, A., Kohfeld, K.E., 2019. Ice sheets matter for the
3648 global carbon cycle. *Nature Communications* 10, 3567. doi:10.1038/
3649 s41467-019-11394-4.
- 3650 Waite, A., Gallager, S., Dam, H.G., 1997. New measurements of phytoplankton
3651 aggregation in a flocculator using videography and image analysis. *Marine*
3652 *Ecology Progress Series* 155, 77–88.
- 3653 Van der Wal, P., Kempers, R.S., Veldhuis, M.J.W., 1995. Production and down-
3654 ward flux of organic matter and calcite in a North Sea bloom of the coccol-
3655 ithophore *Emiliana huxleyi*. *Marine Ecological Progress Series* 126, 247–265.
3656 doi:10.3354/meps126247.
- 3657 Wanninkhof, R., Park, G.H., Takahashi, T., Sweeney, C., Feely, R., Nojiri, Y.,
3658 Gruber, N., Doney, S.C., McKinley, G.A., Lenton, A., Le Quéré, C., Heinze,
3659 C., Schwinger, J., Graven, H., Khatiwala, S., 2013. Global ocean carbon
3660 uptake: magnitude, variability and trends. *Biogeosciences* 10, 1983–2000.
3661 doi:10.5194/bg-10-1983-2013.
- 3662 Ward, B.A., 2015. Temperature-Correlated Changes in Phytoplankton Community
3663 Structure Are Restricted to Polar Waters. *PLoS ONE* 10, e0135581. doi:10.

3664 1371/journal.pone.0135581.

3665 Ward, B.A., Dutkiewicz, S., Jahn, O., Follows, M.J., 2012. A size-structured food-
3666 web model for the global ocean. *Limnology and Oceanography* 57, 1877–1891.
3667 doi:10.4319/lo.2012.57.6.1877.

3668 Wassman, P., 1990. Relationship between primary and export production in the
3669 boreal coastal zone of the North Atlantic. *Limnology and Oceanography* 35,
3670 464–471. doi:10.4319/lo.1990.35.2.0464.

3671 Watson, A.J., Schuster, U., Bakker, D.C.E., Bates, N.R., Corbière, A., González-
3672 Dávila, M., Friedrich, T., Hauck, J., Heinze, C., Johannessen, T., Körtzinger,
3673 A., Metzl, N., Olafsson, J., Olsen, A., Oschlies, A., Padin, X.A., Pfeil, B.,
3674 Santana-Casiano, J.M., Steinhoff, T., Telszewski, M., Rios, A.F., Wallace,
3675 D.W.R., Wanninkhof, R., 2009. Tracking the variable North Atlantic sink for
3676 atmospheric CO₂. *Science* 326, 1391–1393. doi:10.1126/science.1177394.

3677 Watt, W.D., Fogg, G.E., 1966. Release of dissolved organic material from the
3678 cells of phytoplankton populations. *Proc. R. Soc. Lond. B.* , 521–551doi:10.
3679 1098/rspb.1966.0047.

3680 Wei, X., Shen, F., Pan, Y., Chen, S., Sun, X., Wang, Y., 2019. Satellite observa-
3681 tions of the diurnal dynamics of particulate organic carbon in optically complex
3682 coastal oceans: The continental shelf seas of China. *Journal of Geophysical*
3683 *Research: Oceans* 124, 4710–4726. doi:10.1029/2018JC014715.

3684 Weiss, R., 1974. Carbon dioxide in water and seawater: the solubility of a
3685 non-ideal gas. *Marine Chemistry* 2, 203–215. doi:10.1016/0304-4203(74)
3686 90015-2.

3687 Werdell, P.J., Bailey, S.W., 2005. An improved in-situ bio-optical data set for
3688 ocean colour algorithm development and satellite data production validation.
3689 *Remote Sensing Environment* 98, 122–140. doi:10.1016/j.rse.2005.07.
3690 001.

3691 Westberry, T., Behrenfeld, M.J., Siegel, D.A., Boss, E., 2008. Carbon-based pri-
3692 mary productivity modeling with vertically resolved photoacclimation. *Global*
3693 *Biogeochemical Cycles* 22. URL: <https://doi.org/10.1029/2007GB003078>,
3694 doi:10.1029/2007GB003078.

- 3695 White, J.R., Roman, M.R., 1991. Measurement of zooplankton grazing using par-
3696 ticles labelled in light and dark with [methyl-³H] methylamine hydrochloride.
3697 Marine Ecological Progress Series 71, 45–52. doi:10.3354/meps071045.
- 3698 Wiebe, W.J., Smith, D.F., 1977. Direct measurement of dissolved organic carbon
3699 release by phytoplankton and incorporation by microheterotrophs. Marine
3700 Biology 42, 213–223. doi:10.1007/BF00397745.
- 3701 Williams, N.L., Juranek, L.W., Feely, R.A., Johnson, K.S., Sarmiento, J.L.,
3702 Talley, L.D., Dickson, A.G., Gray, A.R., Wanninkhof, R., Russell, J.L., Riser,
3703 S.C., 2017. Calculating surface ocean pCO₂ from biogeochemical Argo floats
3704 equipped with pH: An uncertainty analysis. Global Biogeochemical Cycles
3705 31, 591–604. URL: [https://doi.org/10.1002/](https://doi.org/10.1002/2016GB005541)
3706 [2016GB005541](https://doi.org/10.1002/2016GB005541).
- 3707 Williams, P.M., Druel, E.R.M., 1987. Radiocarbon in dissolved organic matter in
3708 the central north Pacific Ocean. Nature 330, 246–248.
- 3709 Woolf, D.K., Land, P.E., Shutler, J.D., Goddijn-Murphy, L.M., Donlon, C.J., 2016.
3710 On the calculation of air-sea fluxes of CO₂ in the presence of temperature and
3711 salinity gradients. Journal of Geophysical Research: Oceans 121, 1229–1248.
3712 doi:10.1002/2015JC011427.
- 3713 Wright, S., Hull, T., Sivyer, D.B., Pearce, D., Pinnegar, J.K., Sayer, M.D.J., Mogg,
3714 A.O.M., Azzopardi, E., Gontarek, S., Hyder, K., 2016. SCUBA divers as
3715 oceanographic samplers: The potential of dive computers to augment aquatic
3716 temperature monitoring. Scientific Reports 6, 1–8. doi:10.1038/srep30164.
- 3717 Xavier, J.C., Cherel, Y., Ceia, F.R., Queirós, J.P., Guimarães, B., Rosa, R.,
3718 Cunningham, D.M., Moors, P.J., Thompson, D.R., 2018. Eastern rock-
3719 hopper penguins *Eudyptes filholi* as biological samplers of juvenile and
3720 sub-adult cephalopods around Campbell Island, New Zealand. Polar Bi-
3721 ology 41, 1937–1949. URL: <https://doi.org/10.1007/s00300-018-2333-2>,
3722 doi:10.1007/s00300-018-2333-2.
- 3723 Xing, X., Briggs, N., Boss, E., Claustre, H., 2018. Improved correction for
3724 non-photochemical quenching of in situ chlorophyll fluorescence based on
3725 the synchronous irradiance profile. Optics Express 26, 24734–24751. doi:10.

- 3726 1364/OE.26.024734.
- 3727 Xing, X., Morel, A., Claustre, H., Antoine, D., D'Ortenzio, F., Poteau, A.,
3728 Mignot, A., 2011. Combined processing and mutual interpretation of ra-
3729 diometry and fluorimetry from autonomous profiling Bio-Argo floats. The
3730 retrieval of Chlorophyll a. *Journal of Geophysical Research* 116, C06020.
3731 doi:10.1029/2010JC006899.
- 3732 Xing, X., Morel, A., Claustre, H., D'Orenzio, F., A., P., 2012. Combined
3733 processing and mutual interpretation of radiometry and fluorometry from
3734 autonomous profiling bio-argo floats: 2. colored dissolved organic mat-
3735 ter absorption retrieval. *Journal of Geophysical Research* 117, C04022.
3736 doi:10.1029/2011JC007632.
- 3737 Xu, F., Gao, Z., Jiang, X., Shang, W., Ning, J., Song, D., Ai, J., 2018. A UAV and
3738 S2A data-based estimation of the initial biomass of green algae in the South
3739 Yellow Sea. *Marine Pollution Bulletin* 128, 408–414. URL: [https://doi.org/10.](https://doi.org/10.1016/j.marpolbul.2018.01.061)
3740 [1016/j.marpolbul.2018.01.061](https://doi.org/10.1016/j.marpolbul.2018.01.061), doi:10.1016/j.marpolbul.2018.01.061.
- 3741 Yoda, K., Shiomi, K., Sato, K., 2014. Foraging spots of streaked shearwaters
3742 in relation to ocean surface currents as identified using their drift movements.
3743 *Progress in Oceanography* 122, 54–64. doi:10.1016/j.pocean.2013.12.
3744 002.
- 3745 Yonehara, Y., Goto, Y., Yoda, K., Watanuki, Y., Young, L.C., Weimerskirch, H.,
3746 Bost, C.A., Sato, S., 2016. Flight paths of seabirds soaring over the ocean
3747 surface enable measurement of fine-scale wind speed and direction. *Proc. Natl.*
3748 *Acad. Sci.* 113, 9039–9044. doi:10.1073/pnas.1523853113.
- 3749 Zaneveld, J.R.V., Barnard, A.H., Boss, E., 2005. Theoretical derivation of the
3750 depth average of remotely sensed optical parameters. *Optics Express* 13,
3751 9052–9061. doi:10.1364/OPEX.13.009052.
- 3752 Zeebe, R.E., 2012. History of seawater carbonate chemistry, atmospheric CO₂,
3753 and ocean acidification. *Annual Review of Earth and Planetary Sciences* 40,
3754 141–165. doi:10.1146/annurev-earth-042711-105521.
- 3755 Zeebe, R.E., Wolf-Gladrow, D., 2001. CO₂ in seawater: equilibrium, kinetics,
3756 isotopes. 65, Gulf Professional Publishing.

3757 Zhai, L., Platt, T., Tang, C., Dowd, M., Sathyendranath, S., Forget, M.H., 2008.
3758 Estimation of phytoplankton loss rate by remote sensing. *Geophysical Research*
3759 *Letters* 35, L23606. doi:10.1029/2008GL035666.